공학박사학위논문

A study on the optical property, thermal stability, and dispersion characteristics of phthalocyanine dyes and their application on color filters

컬러필터용 프탈로시아닌 염료의 광학적 특성, 열 안정성 및 분산특성에 관한 연구

2020년 02월

서울대학교 대학원

재료공학부

남 궁 진 웅

Abstract

A study on the optical property, thermal stability, and dispersion characteristics of phthalocyanine dyes and their application on color filters

Jin Woong Namgoong

Department of Material Science and Engineering

The Graduated School

Seoul National University

In contemporary times, the world is moving beyond the information age to a new technological era. In this high-tech period, information acquisition and disclosure have become considerably easier, which necessitates the incremental development and performance of cameras and display devices. In line with this trend, since a color filter is still considered an indispensable component.in those

devices, the demand for technological development of color filters used in CMOS sensors and display devices is also increasing. Although pigments have inferior color properties owing to its aggregate-behavior, they are still used for color filters due to its superior durability. However, it is necessary to introduce a dye to improve the color characteristics of color filters. Dyes show excellent color properties such as a sharp absorption band and high tinctorial strength, but their low durability is an obstacle to the application of dyes to color filters. Thus, this study is conducted to investigate phthalocyanine dyes that can improve optical properties and the durability and of green color filters. For this purpose, phthalocyanine derivatives containing bulky functional groups are synthesized, and their optimized structures, optical properties, and thermal stability were characterized. Furthermore, their dispersions are prepared to obtain highly durable dye inks for color filters. The dye-based color filter is manufactured using the prepared dyes and the dispersions.

Tetrasubstituted- and octasubstituted- phthalocyanine dyes, and chlorine-rich phthalocyanine dyes with bulky benzoate group were synthesized for a soluble-dye-based color filter, and the dyes were characterized by computational method, UV-Vis spectrometer, thermogravimetric analysis. The chromatic properties, heat fastness, and thickness of the color filters were analyzed by spectrophotometer, surface profiler, and electron microscopy. It is examined whether the dye could

enable the decrease in the thickness of the filter and provide a superior color property.

Phthalocyanine derivatives with different substituents such as primary amine, tertiary amine, ester, and carboxylic acid were also prepared to investigate a dispersion synergist dye. The dyes were mixed with C.I pigment green 7, and mixtures then dispersed with a paint shaker. The dispersion properties of their dispersion were determined by dynamic light scattering. The contrast ratio and surface properties of color filters with dispersions was tested to characterize their particle distribution in films. In this work, it is explored that an appropriate functional group for a dispersion anchoring group, applicable to phthalocyanine.

In addition, to improve the color property and thermal stability of a dye-based color filter, phthalocyanine dyes bearing bulky benzoic acid groups and chlorine were synthesized and dispersed. It is intended to improve the durability of a dye-based color filter by formation well dispersed fine particles of dyes. Their optimized molecular structures, electrostatic potential surfaces, optical properties, thermal stability, and dispersion properties were determined using computational modeling, UV-Vis spectrometry, thermogravimetric analysis. The dyes were dispersed with a probe sonicator, and the dispersion properties were analyzed using dynamic light scattering. The dispersed-dye-based color filter was then developed using dye dispersions. In this investigation, it is attempted to confirm

a suitable phthalocyanine structure for dispersion, and whether the dispersed-dye-based color filter with fine dye particles exhibits superior stability compared with the dye-based color filter, without compromising color properties.

Asymmetric phthalocyanines were also synthesized and dispersed for the dispersed-dye-based color filter. Mono-substituted, di-substituted, and tetra-substituted polychloro zinc phthalocyanine with a benzoic acid substituent were prepared. In this work, it is tried to finely adjust the bulkiness and spectral characteristics of the dye by controlling the number of substituents. The dyes with polymeric dispersant were dispersed by a probe sonicator. The dyes and dye dispersions were characterized by computational methods, UV-Vis spectrometry, thermogravimetric analysis, and dynamic light scattering. The properties of the dyes and dye dispersions were also compared with those of C.I pigment green 7. It is examined if the decrease in the number of bulky substituents can increase the durability of dyes and their color filter.

It is determined that the thickness of the film can be reduced because of the exclusive properties of the dye, while the carboxylic acid group can be effective for dye dispersion. Further, the durability and color characteristics of the color filter can be improved upon by introducing the disperse dyes as colorants. In addition, it is ascertained that among the asymmetric polychloro phthalocyanine, disubstituted phthalocyanine can be an appropriate structure that is applied to the

dispersed-dye-based color filter with high durability. In summary, this study develops phthalocyanine dyes for green color filters and proposes the dispersed-dye-based color filter over the pigment-based color filter because of the superior durability and color properties of the former.

KEYWORDS: Color filter, Phthalocyanine, Image sensor, Liquid crystal display, Dispersion, Dispersion synergist, Aggregation

Student Number: 2011-20635

Contents

List of Tables

List of Figures

Figure 5.8. Transmittance spectra of the prepared color filters.

Figure 5.9. SEM images of the color filters. (a) C.I pigment green 7; (b) di-substituted Pc; (c) tetra-substituted Pc; (d) a mixture of di-substituted Pc and tetra-substituted Pc (7:3).

List of Schemes

Chapter 1

Introduction

1.1 Introduction to the color filter

Although the color components of visible light are numerous, they can be largely divided into red, green, and blue. These are called the primary colors of light. By combining these three fundamental hues, many other colors can be produced. The component that divides white light into these three primary colors in devices is called a color filter. In addition to the basic types, there are also filters that produce four primary colors (red, green, blue, and yellow) using white light [1]. Color filters are used in CMOS sensors as well as in the display devices of LCDs and white OLEDs [2-5]. Fig. 1.1 shows color filters for CMOS sensors and display devices. These filters perform functions including separation of the light injected from outside into red, green, and blue light in CMOS sensors such that the energy of the lights is measured by photodiodes, and recorded as an image. Furthermore, the white light generated in the display device passes through the color filter, is divided into individual colors, and then the device

reproduces the image by mixing the split colors. Hence, it can be said that the performance of these devices is determined by the ability of the color filter to decompose light. It is therefore essential to improve the performance of color filters to develop high performance display devices and CMOS sensors. Consequently, this study was conducted for improving the features of the color filter.

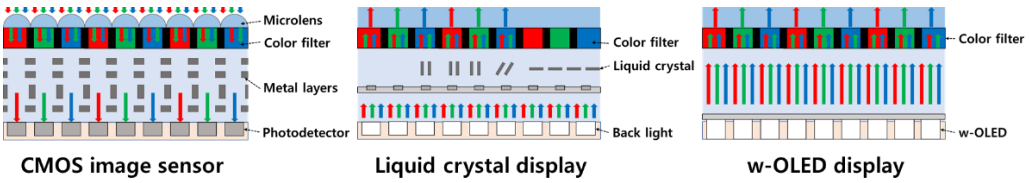

Figure 1.1. Conventional structure of CMOS image sensor, liquid crystal display, and w-OLED display.

The color filter comprises three parts, namely, substrate, black matrix, and sub-pixel (R, G, B). The fundamental structure of a color filter is illustrated in Fig. 1.2. While glass is mainly used as the substrate for color filters, transparent polyimide (PI) films can also be used depending on the application [6]. The black matrix serves as a framework for composing the pixels of the color filter. Representative methods of manufacturing color filters include electrodeposition, inkjet printing, and photolithography. Currently, the latter method is predominantly used. Photolithography has the advantages of easy formation of

nano-sized fine patterns, short processing time, and excellent reliability [7]. However, the associated disadvantage entails the large amount of material that is discarded during the development process.

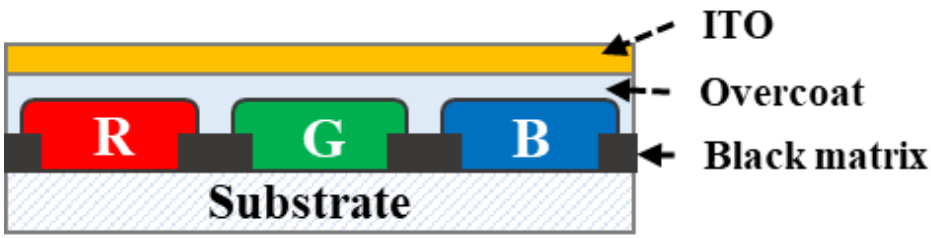

Figure 1.2. Structure of color filter.

The color filter material for photolithography is called color photoresist or color resist, which consists of the solvent, binder resin, multifunctional monomer, photoinitiator, additives, and colorant. From the abovementioned, it is evident that the color resist is a composite material of various chemicals, which presupposes that all the constituents of the color resist should have high miscibility with one another. Among these components, the optical property of the colorant is the main factor that determines the color property of the color filter. Therefore, it can be inferred that developing high-quality colorants is important for improving device performance.

Organic pigments and dyes can be applied as colorants, although both materials have their unique advantages and disadvantages for use in color filters [8]. For instance, pigments exhibit weaknesses of low absorbance and wide absorption bands, while demonstrating excellent stability. Dyes on the other hand however, possess inferior durability, while exhibiting superior spectral properties, such as high absorbance and sharp absorption [9].

To produce a clear image, the color filter needs colorants that have excellent transmittance for each of the primary colors of light. Thus, if the excellent color characteristics of the color filter are solely considered, dyes can be suitable colorants. Nevertheless, because the color filter requires high heat, light, and chemical resistances for its manufacturing process and operation procedure, the color filter is currently produced by using pigments with high durability [10].

However, efforts geared toward improving the color characteristics of the pigment-based color filter though have reached their limit. To advance the color characteristics of the color filter, it is essential to concentrate on the dye. Therefore, it is imperative to conduct ample research aimed at developing dyes with improved durability.

1.2 Manufacturing process for the color filter

As mentioned above, photolithography is the most popular used in the manufacture of the color filter. Though the order and shape of sub-pixels varies from one manufacturer to another, the fundamental process is the same. The general manufacturing process, which is also illustrated in Figures 1.3, is as follows [2].

(1) Coating of black matrix: a black color resist is coated on a substrate.

(2) Heat treatment of black matrix (pre-bake): the black color resist is baked at 80 - 100 °C to evaporate the solvent.

(3) UV curing of black matrix: to make a pattern, the black color resist is cured by exposure to UV light through a photomask.

(4) Development of black matrix: any uncured black color resist is removed by the developing solution (aqueous KOH solution.)

(5) Baking of black matrix (post-bake): the black color resist is further cured, and the residual solvent is removed by baking at 230 °C.

(6) Formation of black matrix: a framework of black matrix is formed to inhibit leakage of backlight as well as mixing of the RGB color resist.

(7) Coating of red color resist: same as process 1.

(8) Heat treatment of red color resist: same as process 2.

(9) UV curing of red color resist: to make a red sub-pixel, the red color resist is exposed to UV light through photomask.

(10) Development of red color resist: same as process 4.

(11) Baking of red color resist (post-bake): same as process 5.

(12) Repetition of processes 6 - 10 for green and blue color resists.

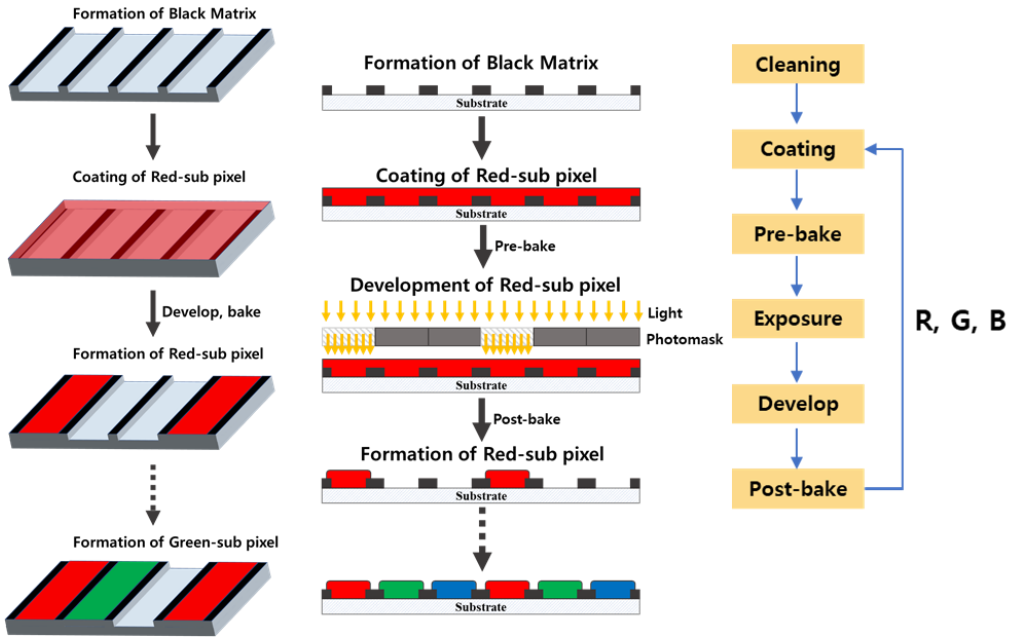

Figure 1.3. Manufacturing process of color filter.
(Reproduced from Wang et al. Appl. Sci. 2019; 9(9): 1893 [11].)

1.3 General requirements for colorants for the color filter

Colorants for the color filter should have high transmittance in each color area. They should be able to strongly transmit the light regions corresponding to blue, green, and red. Figures 1.4 show the basic transmittance spectra of colorants for color filters.

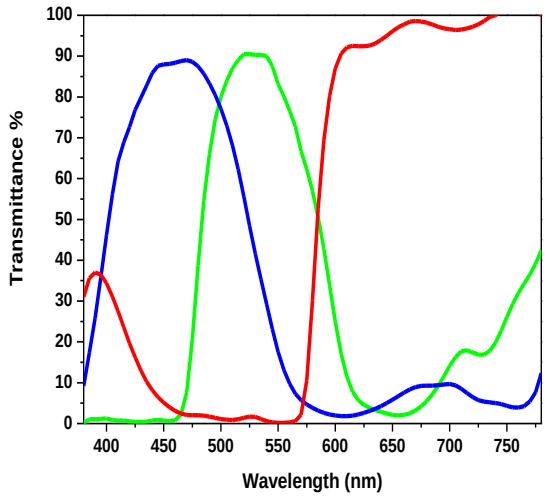

Figure 1.4. Transmittance spectra of a color filter for display devices.

Since the color filter is manufactured using a photolithography process, it is washed with basic and organic solvents in the process. In addition, the color filter is cured at a significantly high temperature, and the color filter is exposed to

excess light while the device is running. In this environment, the color filter is expected to maintain its color characteristics, while colorants should show excellent durability with respect to resistance to light, heat and chemicals. As noted earlier, although each condition may slightly change depending on the device and manufacturer, the general requirements for colorants for the color filter are as follows.

(1) Transmittance: the colorant should generally have sharp and robust transmittance in the blue (440 nm - 480 nm), green (500 nm - 540 nm), and red (600 nm -700 nm) ranges.

(2) Light resistance: to confirm the light resistance, the color filter is exposed 24 h - 48 h under a xenon lamp (300 - 400 W). The chromaticity coordinates of the color filter are then measured and compared with the values before exposure. The difference in chromaticity coordinates is called the color differential (Δ Eab), which should be less than 3.

(3) Heat resistance: to determine the heat resistance, the color filter is baked for an additional 30 min - 90 min at 230°C, following the post-bake process. The color difference is calculated by comparing the chromaticity coordinates of the color filters before and after further baking.

(4) Chemical resistance: after developing the color filter, the colorants should not be dissolved in the developing solution nor in the process solvents, such as PGMEA and PGME after post-baking. To test the elution of the colorants, the color filter is soaked in a solvent for 5 min. The degree of dissolution is determined by measuring the absorbance of solvent-dipping the color filter using a UV-Vis spectrometer.

1.4 Phthalocyanine pigments for the color filter

A representative aromatic and macrocyclic compound, phthalocyanine, is an artificial organic colorant with a structure similar to porphyrin. The phthalocyanine is composed of four isoindole rings connected by nitrogen, which has a plane structure with 18 localized π-electrons. This material exhibits excellent electrical, chemical, thermal, and optical stability due to its structural properties, particularly metal phthalocyanine, which have very high durability [12]. The phthalocyanine strongly absorbs the Q-band region owing to its π-π* transition. As a result, the phthalocyanine shows excellent color characteristics in the blue-green region [13].

The phthalocyanine is synthesized through cyclotetramerization of precursors. Typical precursors are phthalic acid, phthalic anhydride, phthalimide, o-

cyanobenzamide, o-dibromonenzene, and phthalonitrile [14]. The synthesis method for this is shown in Figures 1.5.

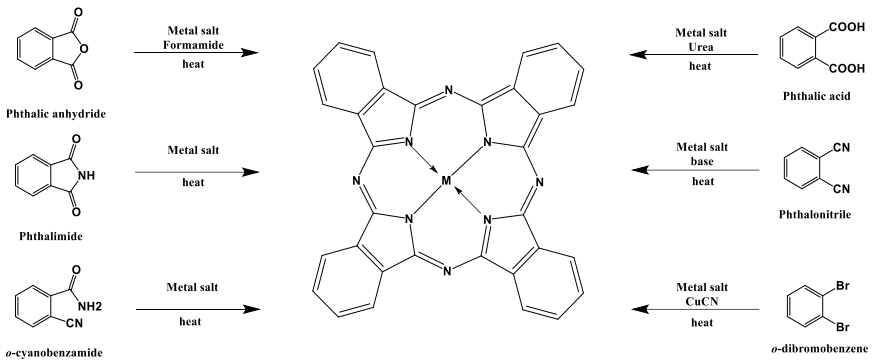

Figure 1.5. Fundamental synthesis method for phthalocyanine.

Phthalocyanine pigments are used in blue and green pixels of the color filter because of their excellent durability and color characteristics [13]. Table 1.1 lists the colorants for the color filter.

The α-form of the phthalocyanine pigment is metastable, resulting in low thermodynamic stability, while the β-form is more stable, although the latter appears greenish-blue, which is unsuitable for a colorant for the color filter. For this reason, phthalocyanine blue 15:6 of ε-form was developed and is currently used as the blue colorant for the color filter [15]. On the other hand, halogenated phthalocyanine is used as an alpha-polymorph modification because substituted halogen stabilizes α-form. However, since its Q-band undergoes bathochromic

shifts due to the introduction of halogen, it is used as the green colorant for the color filter. A representative example is C.I. pigment green 7.

Table 1.1. Common colorants (R, G, B) for color filters

Colorants	Molecular structure	Sub-pixel
C.I pigment blue 15:6	Phthalocyanine	Blue
C.I pigment green 7	Phthalocyanine	Green
C.I pigment green 36	Phthalocyanine	Green
C.I pigment green 58	Phthalocyanine	Green
C.I pigment red 254	Diketopyrrolopyrrole	Red
C.I pigment red 177	Anthraquinone	Red

1.5 Drawbacks of the pigment-based color filter

Generally, pigments have large particle sizes. The particle size of a colorant is closely related to its physical features, such as transmittance, absorption wavelength, and layer thickness. The particle size is inversely proportional to the advantages inherent in these properties [16-18].

In addition, the fineness of a pigment particle largely depends on its crystalline morphology [19]. For this reason, with respect to pigments, it is important to control the synthesis conditions and complex processes to produce

a stable crystal form with suitable color characteristics, as well as pretreatment and particle stabilization, respectively [20]. As mentioned above, pigments have relatively inferior optical properties to dyes, which hinder the improvement of the color filter's performance.

1.6 Previous studies and the present study research objectives

Various studies have been conducted to develop the dye-based color filter to compensate for these drawbacks. Early researches have been performed to test various dye chromophores as colorants for the color filter [21-25]. Previous studies have reported azo, triphenylmethane, cyanine, xanthene, and dioxazine dyes. However, the durability of most dyes was unsatisfactory for the color filter. Nonetheless, studies have also been conducted to modify organic pigment chromophores to develop highly durable dyes. In these studies, anthraquinone, perylene, quinophthalone, and phthalocyanine derivatives have been reported [26-40]. These dyes showed significantly improved durability. These investigations have demonstrated that pigment-modified dyes have potentials to be used as colorants for color filters, and that the prepared dye-based color filters can exhibit better optical properties than pigment-based variants. These studies

have significant implications for proposing industrial solvent-soluble dyes and validating the potentials of dye-based color filters.

Thus far, however, research has been conducted to develop soluble-coloring materials considering solution-state, such as solubility improvement in process solvents and control of absorption bands. Limited research has been conducted for appraising solid-state features of colorants such as film thickness and behavior in the color filter.

In addition, the developed dyes in previous studies have required further improvement as regards their durability. Problems relating to change of color characteristics of color filters due to the migration of dyes in post-baking in the soluble dye-based color filter have also been reported [38, 41].

Furthermore, fewer studies have been carried out on green dyes in contrast to red, yellow, and violet dyes for the color filter. Although phthalocyanine has excellent durability and color characteristics as green dyes, only a handful of studies have been conducted on phthalocyanine dyes. Hence, further research on the phthalocyanine dye for green color filters is essential.

This study aims to develop highly stable phthalocyanine dyes for the color filter, as well as a color filter to ameliorate the challenges associated with the soluble dye-based color filter. For this purpose, tetrasubstituted metal phthalocyanine, octasubstituted metal phthalocyanine, and hexadecasubstituted

polychloro-metal phthalocyanine derivatives were designed and synthesized. A benzoate moiety was adopted as a large functional group, and a benzoic acid moiety was incorporated as a bulky dispersant anchoring group. Furthermore, the dispersions of phthalocyanine dyes were prepared to improve the durability and optical properties of the color filter. The current study proposed a highly durable dye-based color filter and some phthalocyanine dyes for the green color filter.

1.7 References

[1] Sugiura T. A History of CFs Development for Color LCD. Journal of Printing Science and Technology. 1996;33(6):356-68.

[2] Sabnis RW. Color filter technology for liquid crystal displays. Displays. 1999;20(3):119-29.

[3] Helber MJ, Alessi PJ, Burberry M, Evans S, Brick MC, Diehl DR, et al. 19.2: Color Filter Formulations for Full-Color OLED Displays: High Color Gamut Plus Improved Efficiency and Lifetime. SID Symposium Digest of Technical Papers. 2007;38(1):1022-5.

[4] Taguchi H, Enokido M. Technology of color filter materials for image sensor. Proc Proc Int Image Sensor Workshop2011. p. 8-11.

[5] Lee MT, Wang CL, Chan CS, Fu CC, Shih CY, Chen CC. Achieving a

foldable and durable OLED display with BT.2020 color space using innovative color filter structure. Journal of the Society for Information Display. 2017;25(4):229-39.

[6] Tsuda K. Colour filters for LCDs. Displays. 1993;14(2):115-24.

[7] Kudo T, Nanjo Y, Nozaki Y, Yamaguchi H, Kang WB, Pawlowski G. Polymer optimization of pigmented photoresists for color filter production. Jpn J Appl Phys Part 1 - Regul Pap Short Notes Rev Pap. 1998;37(3A):1010-6.

[8] Freeman HS, Peters AT. Colorants for Non-Textile Applications: Elsevier Science, 2000.

[9] Sugiura T. Dyed color filters for liquid-crystal displays. Journal of the Society for Information Display. 1993;1(2):177.

[10] Jhun CG, Gwag JS. Size Effect of Light Scattering on the Nano-Sized Color Filter Pigment in Liquid Crystal Display. Journal of the Optical Society of Korea. 2014;18(2):184-7.

[11] Wang CN, Chiu PC, Cheng I, Huang YF. Contamination Improvement of Touch Panel and Color Filter Production Processes of Lean Six Sigma. Applied Sciences. 2019;9(9):1893 (CC BY 4.0).

[12] Löbbert G. Phthalocyanines. Ullmann's Encyclopedia of Industrial Chemistry: Wiley-VCH Verlag GmbH & Co. KGaA; 2012. p. 181-213.

[13] Gregory P. Industrial applications of phthalocyanines. Journal of Porphyrins

and Phthalocyanines. 2000;04(04):432-7.

[14] Sakamoto K, Ohno-Okumura E. Syntheses and Functional Properties of Phthalocyanines. Materials. 2009;2(3):1127-79.

[15] Kim JH, Kim SH, Kim SJ, Hong SS, Lee GD, Park SS. Synthesis and Characteristic of ε-type Copper Phthalocyanine Used as Color Filter in LCD Panel. Appl Chem Eng. 2012;23(2):138-42.

[16] Gueli AM, Bonfiglio G, Pasquale S, Troja SO. Effect of particle size on pigments colour. Color Research & Application. 2017;42(2):236-43.

[17] Athanasiu AA, Marian D, Crudu M, Doncea S, Stoica R, Oproiu L, et al. Synthesis and characterization of nanosized copper(II)-phthalocyanine pigment (P BI 15:3) with the modified surface. i. Revista de Chimie. 2017;68:343-9.

[18] Jones FN, Nichols ME, Pappas SP. Effect of Pigments on Coating Properties. Organic Coatings: John Wiley & Sons, Inc.; 2017. p. 323-30.

[19] Müller M, Dinnebier RE, Jansen M, Wiedemann S, Plüg C. The influence of temperature, additives and polymorphic form on the kinetics of the phase transformations of copper phthalocyanine. Dyes and Pigments. 2010;85(3):152-61.

[20] Jung I-B, Ahn S-C, Nam S-Y. A study on the millbase dispersion for LCD color filters. Clean Technology. 2008;14(1):21-8.

[21] Kim YD, Kim JP, Kwon OS, Cho IH. The synthesis and application of

thermally stable dyes for ink-jet printed LCD color filters. Dyes and Pigments. 2009;81(1):45-52.

[22] Kim YD, Cho JH, Park CR, Choi J-H, Yoon C, Kim JP. Synthesis, application and investigation of structure–thermal stability relationships of thermally stable water-soluble azo naphthalene dyes for LCD red color filters. Dyes and Pigments. 2011;89(1):1-8.

[23] Kong NS, Jung H, Kim B, Lee CK, Kong H, Jun K, et al. Development of dimeric triarylmethine derivatives with improved thermal and photo stability for color filters. Dyes and Pigments. 2017;144:242-8.

[24] Lee J-Y, Kim J-H, Bae J-H, Yoon C, Kim J-P, Choi J-H. The Synthesis and Characterizations of Thermally-Stable Yellow Metal Complex Dyes for LCD Color Filters. Molecular Crystals and Liquid Crystals. 2013;583(1):60-9.

[25] Tatsumi Y, Inoue M. 40-4: Development of Color Resists Containing Novel Dyes for Liquid Crystal Displays. SID Symposium Digest of Technical Papers. 2016;47(1):521-3.

[26] Yuk SB, Lee JM, Namgoong JW, Sakong C, Hwang TG, Kim SH, et al. Synthesis of bay-linked perylene dimers with enhanced solubility for high optical density black matrix material. Dyes and Pigments. 2019;171:107695.

[27] Yuk SB, Lee W, Kim SH, Namgoong JW, Lee JM, Kim JP. Application of perylene dyes for low dielectric hybrid-type black matrices. Journal of Industrial

and Engineering Chemistry. 2018;64:237-44.

[28] Namgoong JW, Kim SH, Chung S-W, Kim YH, Kwak MS, Kim JP. Aryloxy- and chloro-substituted zinc(II) phthalocyanine dyes: Synthesis, characterization, and application for reducing the thickness of color filters. Dyes and Pigments. 2018;154:128-36.

[29] Kim JY, Woo SW, Namgoong JW, Kim JP. A study on the fluorescence property of the perylene derivatives with methoxy groups. Dyes and Pigments. 2018;148:196-205.

[30] Kim JY, Hwang TG, Kim SH, Namgoong JW, Kim JE, Sakong C, et al. Synthesis of high-soluble and non-fluorescent perylene derivatives and their effect on the contrast ratio of LCD color filters. Dyes and Pigments. 2017;136:836-45.

[31] Yoon C, Kwon H-S, Yoo J-S, Lee H-Y, Bae J-H, Choi J-H. Preparation of thermally stable dyes derived from diketopyrrolopyrrole pigment by polymerisation with polyisocyanate binder. Coloration Technology. 2015;131(1):2-8.

[32] Kim SH, Namgoong JW, Yuk SB, Kim JY, Lee W, Yoon C, et al. Synthesis and characteristics of metal-phthalocyanines tetra-substituted at non-peripheral (α) or peripheral (β) positions, and their applications in LCD color filters. Journal of Inclusion Phenomena and Macrocyclic Chemistry. 2015;82(1):195-202.

[33] Kim JY, Choi J, Namgoong JW, Kim SH, Sakong C, Yuk SB, et al. Synthesis and characterization of novel perylene dyes with new substituents at terminal-position as colorants for LCD color filter. Journal of Inclusion Phenomena and Macrocyclic Chemistry. 2015;82(1):203-12.

[34] Lee H-Y, Kim J-H, Yoo J-S, Bae J-H, Yoon C, Choi J-H. Synthesis and Thermal Stability of Solvent Soluble Dyes Based on Dimerized Diketo-pyrrolo-pyrrole Pigment. Bulletin of the Korean Chemical Society. 2014;35(2):659-62.

[35] Lee W, Yuk SB, Choi J, Jung DH, Choi S-H, Park J, et al. Synthesis and characterization of solubility enhanced metal-free phthalocyanines for liquid crystal display black matrix of low dielectric constant. Dyes and Pigments. 2012;92(3):942-8.

[36] Choi J, Lee W, Sakong C, Yuk SB, Park JS, Kim JP. Facile synthesis and characterization of novel coronene chromophores and their application to LCD color filters. Dyes and Pigments. 2012;94(1):34-9.

[37] Choi J, Kim SH, Lee W, Yoon C, Kim JP. Synthesis and characterization of thermally stable dyes with improved optical properties for dye-based LCD color filters. New Journal of Chemistry. 2012;36(3):812.

[38] Choi J, Kim SH, Lee W, Chang JB, Namgoong JW, Kim YH, et al. The influence of aggregation behavior of novel quinophthalone dyes on optical and thermal properties of LCD color filters. Dyes and Pigments. 2014;101:186-95.

[39] Muthukumar P, Kim H-S, Jeong JW, Son Y-A. Synthesis and characterization of tetra phenoxy-substituted halogen-rich metallophthalocyanine derivatives: A study on their LCD color filter requirements. Journal of Molecular Structure. 2016;1119:325-31.

[40] Jeong J, Kumar RS, Kim IJ, Son Y-A. Synthesis, characterization of symmetrical and unsymmetrical naphthoxy substituted metallophthalocyanines. Molecular Crystals and Liquid Crystals. 2017;644(1):249-56.

[41] Kalugasalam P, Ganesan S. Surface morphology of annealed lead phthalocyanine thin films. International journal of engineering science and technology. 2010;2(6):1773-9.

Chapter 2

Synthesis and characterization of aryloxy- and chloro- substituted zinc(II) phthalocyanine dyes and their application for reducing the thickness of color filters

2.1 Introduction

A color filter is one of the most important components in a display panel because it significantly influences the image quality of display devices. The color filter is employed not only in liquid crystal displays (LCDs) but also in OLED displays. [1-3] In an LCD, the color filter separates the white light from the backlight unit into red, green, and blue; images of LCD are produced by controlling these R, G, and B light. This color filter method is also adopted in the White-OLED display [2]. Furthermore, an R, G, B-type OLED display requires a color filter to suppress the ambient light reflection and enhance the optical

performance, including color saturation and color gamut.[3] Therefore, the color filter is expected to play a key role in the display industry, as in the past.

There are four conventional methods for manufacturing a color filter for display, *viz*., dyeing, printing, electrodeposition, and pigment dispersion methods [4]. The pigment dispersion method has been widely utilized owing to its high durability and reliability. This method uses pigments as coloring materials. Pigments have large particle sizes and broad absorption bands, features that are advantageous for light fastness, heat resistance, and blocking a wide range of light. These advantages, however, may also be the drawbacks of the pigments in a color filter [5]. Absorption over a wide spectral range means a diminution of the transmittance. Hence, it may deteriorate the image quality by reducing the brightness of the display panel. Further, pigments typically exist as large particles, and they should be dispersed fine to achieve chromatic features required for use in a color filter [6]. Since the spectral properties of the dispersed pigments are highly dependent on their dispersity and particle size, the image quality of the display also relies on the conditions of the pigment dispersion. However, it is hard to modify the spectral properties of pigments and the dispersion properties of their dispersions. Thus, two or more types of pigment are blended to satisfy the current demands of improved image quality and color gamut in the pigment dispersion method. Consequently, an additional optimization procedure is

required for achieving a thorough dispersion and color adjusting of the pigments. Moreover, their mixing can lead to issues such as increased thickness, decreased brightness, and rise in costs.

Incorporation of dyes in color filters has been studied because the pigment dispersion method presents the aforementioned drawbacks [7-13]. In case of dyes, the particle size is smaller and the absorption band is narrower than those of the pigments [5]. The dyes also show higher transmittances. Further, the spectral properties of the dyes can be altered by modifying their molecular structures, and no additional dispersing processes are required because of their high solubility in common solvents. Although inferior durability has been deemed a disadvantage of dyes to be used in color filters, it has demonstrated in previous studies that this limitation could be overcome, using perylene and phthalocyanine (PC) derivatives that have good thermal and light stabilities [7-11].

Currently, the development of thin display panels with superior color properties is one of the most important issues in the field of LCD and OLED displays. Therefore, a reduction in the thickness of the color filter is also desired. However, decreasing the thickness of a color filter leads to a diminution of the color strength [5], whereas increasing the quantity of the colorants to enhance the color strength leads to increased thickness. Thus, it is hard to lower the thickness of a color filter with no decline in the color property by adopting the pigments

currently in use. Under these circumstances, dyes can be good alternatives to pigments, provided that the dyes have appropriate spectral properties. Dyes are characterized by high absorbance and sharp absorption bands, which are effective for high transmittance, and provide better color purity than pigments [14]. This may be beneficial for reducing the thickness of a color filter.

In a previous study, the feasibility of some green dyes for use in a color filter on LCD was shown [9, 11]. However, the color properties of those dyes are not suitable for the color features required at present, and the thicknesses of the dye-based color filters are also similar to those of the pigment-based color filters.

In this article, the effect of dyes on reducing the thickness of a color filter is presented. In addition, it was investigated the ability of the dye-based color filters to provide superior color properties such as the brightness and color strength. For this study, four green dyes, with high solubility and absorbance, were synthesized by introducing chlorine atoms and bulky substituents into the phthalocyanine moiety. the spectral properties, solubilities, and thermal stabilities of the newly synthesized dyes were analyzed and compared with those of the pigments in use. Color filters based on these dyes were then fabricated and their characteristics, including the chromatic properties and heat fastness were examined. Finally, color values according to the variation of the thickness were measured to evaluate the decrease in the thickness of the color filters.

2.2 Experimental

2.2.1. Materials

1,8-diazabicyclo-7-undecene (DBU), 4-nitrophthalonitrile, 4,5-dichlorophthalonitrile, 3,4,5,6-tetrachlorophthalonithrile, and ethyl 4-hydroxy-3-methoxybenzoate were purchased from TCI, and $ZnCl_2$, potassium carbonate anhydrous, and 1-pentanol were purchased from Sigma-Aldrich. All the other reagents and solvents were of reagent-grade and obtained from commercial suppliers. Transparent glass substrates were provided by NTP, Inc., and the acrylic polymer binder (Mw 16,000 g/mol) was supplied by NDM, Inc [12].

2.2.2. Characterization and instruments

^1H NMR spectra were measured on a Bruker Avance 500 spectrometer (National Center for Inter-University Research Facilities at Seoul National University) at 500MHz using dimethyl sulfoxide-d6 and chloroform-d as the solvent. Tetramethylsilane (TMS) was used as an internal standard. Elemental analysis was conducted with a Thermo Scientific Flash EA 1112 elemental analyzer. Matrix-Assisted Laser Desorption/Ionization-Time of Flight (MALDI-TOF) mass spectra were collected on a Voyager-DE STR Biospectrometry Workstation (National Center for Inter-University Research Facilities at Seoul

National University) with α-cyano-4-hydroxy-cynamic acid (CHCA) as the matrix. UV-Vis absorption spectra were recorded using a PerkinElmer Lambda 25 spectrophotometer. Thermogravimetric analysis (TGA) was performed in nitrogen atmosphere at a heating rate of 10°C/min using a TA Instruments Thermogravimetric Analyzer 2050. The thickness of the spin-coated color filter was measured using a KLA-TENCOR Nanospec AFT/200 alpha step. The optical properties of the color filters were measured on a Scinco color spectrophotometer.

2.2.3. Synthesis

2.2.3.1. Preparation of compound 1a (ethyl 4-(3,4-dicyanophenoxy)-3-methoxybenzoate)

4-Nitrophthalonitrile (1 g, 5.77 mmol) and ethyl 4-hydroxy-3-methoxybenzoate (1.18 g, 6.00 mmol) were dissolved in dry DMF (30 ml) and anhydrous K_2CO_3 (1.24 g, 9.00 mmol) was added portion wise during 2 h. The mixture was stirred at 80 °C for 12 h under nitrogen atmosphere. The solution was then poured into ice water (100 mL) with vigorous stirring. The resulting suspension filtered to give a white-yellowish powder. Pure product was collected by column chromatography on silica gel using MC as an eluent. Yield 87%; ^{1}H NMR (d6-DMSO, 500 MHz, 25 °C): δ 8.07 (d, J=8 Hz, 1H, Ar-H), 7.75 (d, J=2.5 Hz, 1H, Ar-H), 7.70(d, J=2 Hz, 1H, Ar-H), 7.66 (dd, J=8, 2 Hz, 1H, Ar-H), 7.34

(m, 2H, Ar-H), 4.35 (q, J=7 Hz, 2H, CH2CH3), 3.80 (s, 3H, OCH3), 1.34 (t, J=7, 3H, CH_2CH_3). Elemental analysis: Calcd for $C_{18}H_{14}N_2O_4$: C, 67.08; H, 4.38; N, 8.69; O, 19.85 %. Found: C, 66.99; H, 4.30; N, 8.62; O, 20.05.

2.2.3.2. Preparation of compound 2a (ethyl 4-(2-chloro-4,5-dicyanophenoxy)-3-methoxybenzoate)

2a was synthesized following the same procedure for 1a using ethyl 4-hydroxy-3-methoxybenzoate (0.99 g, 5.07 mmol), 4,5-dichlorophthalonitrile (1 g, 5.07 mmol), DMF (30 ml), and anhydrous K_2CO_3 (1.06 g, 7.66 mmol). Yield 66%; ^{1}H NMR ($CDCl_3$, 500 MHz, 25 °C, TMS): δ 7.87 (s, 1H, Ar-H), 7.77 (d, J=10 Hz, 2H, Ar-H), 7.20 (d, J = 8.5 Hz, 1H, Ar-H), 6.88 (s, 1H, Ar-H), 4.43 (q, J = 7 Hz, 2H, CH2CH3), 3.85 (s, 3H, OCH3), 1.43 (t, J=7.5 Hz, 3H, CH2CH3). Elemental analysis: Calcd for $C_{18}H_{13}ClN_2O_4$: C, 60.60; H, 3.67; N, 7.85; O, 17.94 %. Found: C, 61.07; H, 3.74; N, 7.75; O, 17.81.

2.2.3.3. Preparation of compound 3a (ethyl 3-methoxy-4-(2,3,6-trichloro-4,5-dicyanophenoxy)benzoate)

3a was synthesized following the same procedure for 1a using ethyl 4-hydroxy-3-methoxybenzoate (0.74 g, 3.76 mmol), 3,4,5,6-tetrachlorophthalonitrile (1 g, 3.76 mmol), DMF (30 ml), and anhydrous K_2CO_3 (0.78 g, 5.64 mmol). Yield 75%; ^{1}H NMR (d6-DMSO, 500 MHz, 25 °C): δ 7.67 (d, J=2 Hz, 1H, Ar-H), 7.47 (dd, J=8.5, 2 Hz, 1H, Ar-H), 6.87 (d, J = 8.5 Hz, 1H,

Ar-H), 4.31 (q, J = 6.5 Hz, 2H, CH_2CH_3), 3.93 (s, 3H, OCH_3), 1.31 (t, J=7 Hz, 3H, CH_2CH_3). Elemental analysis: Calcd for $C_{18}H_{11}Cl_3N_2O_4$: C, 50.79; H, 2.60; N, 6.58; O, 15.04 %. Found: C, 51.18; H, 2.84; N, 6.43; O, 16.41.

2.2.3.4. Preparation of compound 4a (diethyl 4,4'-((4,5-dicyano-1,2-phenylene)bis(oxy))bis(3-methoxybenzoate))

4a was synthesized following the same procedure for 1a using ethyl 4-hydroxy-3-methoxybenzoate (2.09 g, 10.65 mmol), 4,5-dichlorophthalonitrile (1 g, 5.07 mmol), DMF (30 ml), and anhydrous K_2CO_3 (2.12 g, 15.32 mmol). Yield 82%; ^{1}H NMR ($CDCl_3$, 500 MHz, 25 °C, TMS): δ 7.74 (d, J=9 Hz, 2H, Ar-H), 7.73 (s, 2H, Ar-H), 7.16 (d, J = 9 Hz, 2H, Ar-H), 7.02 (s, 2H, Ar-H), 4.41 (q, J = 7 Hz, 4H, CH_2CH_3), 3.88 (s, 6H, OCH_3), 1.42 (t, J=7.5 Hz, 6H, CH_2CH_3). Elemental analysis: Calcd for $C_{28}H_{24}N_2O_8$: C, 65.11; H, 4.68; N, 5.42; O, 24.78 %. Found: C, 64.98; H, 4.59; N, 5.35; O, 25.01.

2.2.3.5. Preparation of compound 1b (2,9(10),16(17),23(24)-tetra(4-(ethoxycarbonyl)-2-methoxyphenoxy)phthalocyaninato zinc(II))

A mixture of 1a (1.61 g, 5.00 mmol), $ZnCl_2$ (0.22 g, 1.65 mmol) and DBU (0.50 g, 3.30 mmol), in 1-pentanol (50mL) was heated to 150 °C and stirred for 12h under nitrogen atmosphere. The crude product was precipitated by pouring the reaction solution into methanol (100mL). After filtering the mixture, the

collected solid was dried under vacuum. The solid was loaded onto a silica gel column with a 10:1 mixture of methylene chloride/MeOH eluent. As the crude product elutes from the column, the green band was collected and dried to afford product 1b as a green solid. Yield 82%; MALDI-TOF MS: m/z 1354.4 (100%, $[M + H]^+$). Elemental analysis: Calcd for $C_{72}H_{56}N_8O_{16}Zn$: C, 63.84; H, 4.17; N, 8.27; O, 18.90 %. Found: C, 63.50; H, 4.05; N, 8.41; O, 18.85.

2.2.3.6. Preparation of compound 2b (2,9(10),16(17),23(24)-tetrachloro-3,9(10),16(17),23(24)-tetra(4-(ethoxycarbonyl)-2-methoxyphenoxy)phthalocyaninato zinc(II))

2b was synthesized following the same procedure for 1b using 2a (1.78 g, 5.00 mmol), $ZnCl_2$ (0.22 g, 1.65 mmol) and DBU (0.50 g, 3.30 mmol), in 1-pentanol (50mL). Column chromatography with an 80:1 mixture of chloroform/MeOH eluent was performed to obtain the product as a green solid. Yield 76%; MALDI-TOF MS: m/z 1492.1 (100%, $[M + H]^+$). Elemental analysis: Calcd for $C_{72}H_{52}Cl_4N_8O_{16}Zn$: C, 57.95; H, 3.51; N, 7.51; O, 17.15 %. Found: C, 58.21; H, 3.57; N, 7.60; O, 17.05.

2.2.3.7. Preparation of compound 3b (1, 2, 4, 8, 9(10), 11, 15, 16(17), 18, 22, 23(24), 25-dodecachloro-3,9(10),16(17),23(24)-tetra(4-(ethoxycarbonyl)-2-methoxyphenoxy)phthalocyaninato

zinc(II))

3b was synthesized following the same procedure for 1b using 3a (2.58 g, 5.00 mmol), $ZnCl_2$ (0.22 g, 1.65 mmol) and DBU (0.50 g, 3.30 mmol), in 1-pentanol (50mL). Column chromatography with an 80:1 mixture of chloroform/MeOH eluent was performed to obtain the product as a green solid. Yield 64%; MALDI-TOF MS: m/z 1786.9 (100%, $[M + Na]^+$). Calcd for $C_{72}H_{44}Cl_{12}N_8O_{16}Zn$: C, 48.91; H, 2.51; N, 6.34; O, 14.48 %. Found: C, 48.55; H, 2.48; N, 6.46; O, 14.24 %.

2.2.3.8. Preparation of compound 4b (2, 3, 9, 10, 16, 17, 23, 24-octa(4-(ethoxycarbonyl)-2-methoxyphenoxy)phthalocyaninato zinc(II))

4b was synthesized following the same procedure for 1b using 2a (2.13 g, 5.00 mmol), $ZnCl_2$ (0.22 g, 1.65 mmol) and DBU (0.50 g, 3.30 mmol), in 1-pentanol (50mL). Column chromatography with an 80:1 mixture of chloroform/MeOH eluent was performed to obtain the product as a green solid. Yield 77%; MALDI-TOF MS: m/z 2130.4 (100%, $[M + H]^+$). Calcd for $C_{112}H_{96}N_8O_{32}Zn$: C, 63.11; H, 4.54; N, 5.26; O, 24.02%. Found: C, 63.53; H, 4.62; N, 5.11; O, 24.35%.

2.2.4. Preparation of color inks and spin-coated films

Commercial pigment green 58 dispersion was purchased from DIC Corporation, and pigment green 7 and yellow 138 dispersions were purchased

from BASF. Pigment green 58 and 7 were blended in a ratio of 1: 1.5 to prepare a green pigment mixture.

A dye ink and pigment ink for a color filter was comprised of the propylene glycol methyl ether acetate (PGMEA) (2.10 g), acrylic binder (2.74 g), dye (0.15 g), and pigment mixture (0.15 g). The prepared inks were coated on a transparent glass substrate using a MIDAS System SPIN-1200D spin coater. The ink-coated glasses were then pre-baked at 100°C for 100 secs and post-baked at 230°C for 30 min. After post-baking, the coordinate values of the pigment-coated glasses were measured.

2.2.5. Solubility Measurement

The prepared dyes were dissolved in the propylene glycol methyl ether acetate (PGMEA) at different concentrations, and the solutions were sonicated for 5 min on an ultrasonic cleaner ME6500E. After the solutions were left to stand for 24 h at room temperature, precipitation was checked to determine the solubility of the dyes.

2.2.6. Measurement of spectral and chromatic properties

Absorption spectra of the prepared dyes and transmittance spectra of dye-based color filters and pigment-based color filters were measured using a

PerkinElmer Lambda 25 UV-vis spectrophotometer. Chromatic values were examined by a Scinco colormate color spectrophotometer.

2.2.7. Measurement of thermal stability

Thermal stability of the synthesized dyes was evaluated by TGA. The prepared dyes were heated to 230°C and held at the temperature for 30 min to simulate the color filter manufacturing thermal condition. The dyes were finally heated to 350°C to determine their degradation temperature. The temperature was raised at the rate of 10 °C/ min under nitrogen atmosphere. To confirm the thermal stability of the dye-based color filters and pigment-based color filters, the spin-coated color filter was heated to 230°C and held at the temperature for 30 min. The color difference values (ΔEab) before and after heating were measured using Scinco colormate color spectrophotometer in CIE L'a'b' mode.

2.3 Results and discussion

2.3.1. Synthesis of the dyes

Four zinc phthalocyanine (PC) dyes containing phenyl derivatives on the peripheral positions were designed and synthesized, as shown in Scheme 2.1. Each precursor (**1a**, **2a**, **3a**, and **4a**) was prepared by the nucleophilic aromatic

substitution reaction between phthalonitrile (4-nitrophthalonitrile, 3,4,5,6-tetrachlorophthalonitrile, and 4,5-dichlorophthalonitrile) and ethyl vanillate. The zinc PCs (**1b**, **2b**, **3b**, and **4b**) were then synthesized *via* cyclotetramerization of the precursors [15].

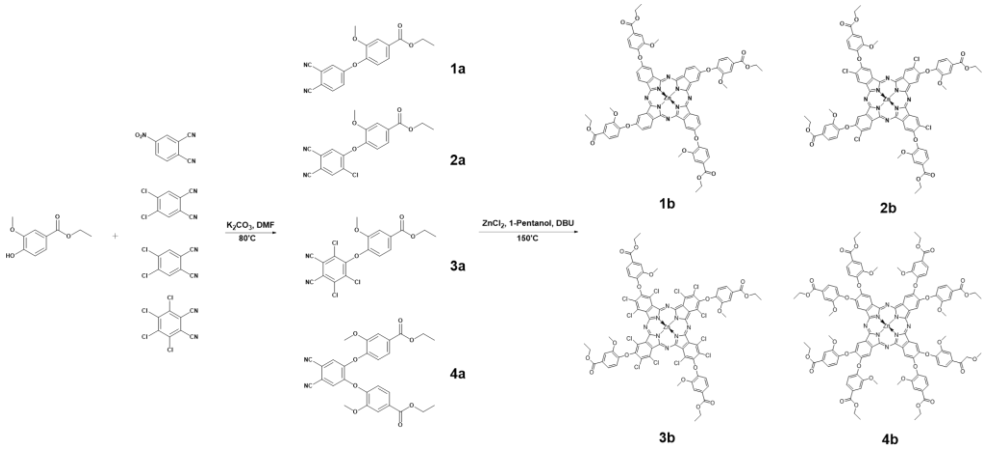

Scheme 2.1. Synthesis of the prepared dyes.

All the products were purified by column chromatography and a yield of 50–90% was obtained depending on the substituent. The structures of the precursors were analyzed by NMR and elemental analysis, and those of PCs were confirmed by MALDI-TOF mass spectroscopy and elemental analysis. In principle, all PCs except **4b** which was synthesized from disubstituted phthalonitrile have constitutional isomers [16]. However, in this study, their properties were examined without separating the isomers.

2.3.2. Geometry optimization and TD-DFT calculations

For the geometry optimization and prediction of the optical absorption spectrum, density functional theory (DFT) and time-dependent (TD) DFT calculations were performed using the B3LYP functional of the Gaussian09 software packages with 6-311G (d) basis sets [17].

Fig. 2.1 shows the optimized geometry of the synthesized dyes. The methoxy group of the phenyl substituents causes steric strain, so that the plane of phenyl was almost perpendicular to that of PC, as intended; the twisted angles of dyes **1b**, **2b**, **3b**, and **4b** are 72, 80, 83, and 84 degrees, respectively. The angles are higher for dyes **2b**, **3b**, and **4b** containing chlorine at the other peripheral positions, than that in dye **1b** carrying hydrogen. This can be considered as an indication of an increase in the steric strain because the size of the other substituent besides phenyl groups increased. Meanwhile, although dyes **1b**, **2b**, and **4b** had a planar phthalocyanine structure, dye **3b** possessed a saddle core structure. This can be attributed to the presence of chlorine at the non-peripheral (α) positions in dye **3b**. The PC core structure can be deformed by large atoms, such as chlorine, at the non-peripheral (α) positions, because of their steric interactions, and the distortion of the molecule can lead to the saddle structure [18]. Furthermore, the vertical axial bulkiness was the highest in dye **3b** because

of the distortion of the structure: dye **1b** (10.164 Å), dye **2b** (17.438 Å), dye **3b** (23.436 Å), dye **4b** (18.640 Å). This enhancement in bulkiness can inhibit intermolecular interactions such as the π-π stacking of the phthalocyanine molecules. A dye with a deformed structure is expected to have increased solubility because of its increased bulkiness.

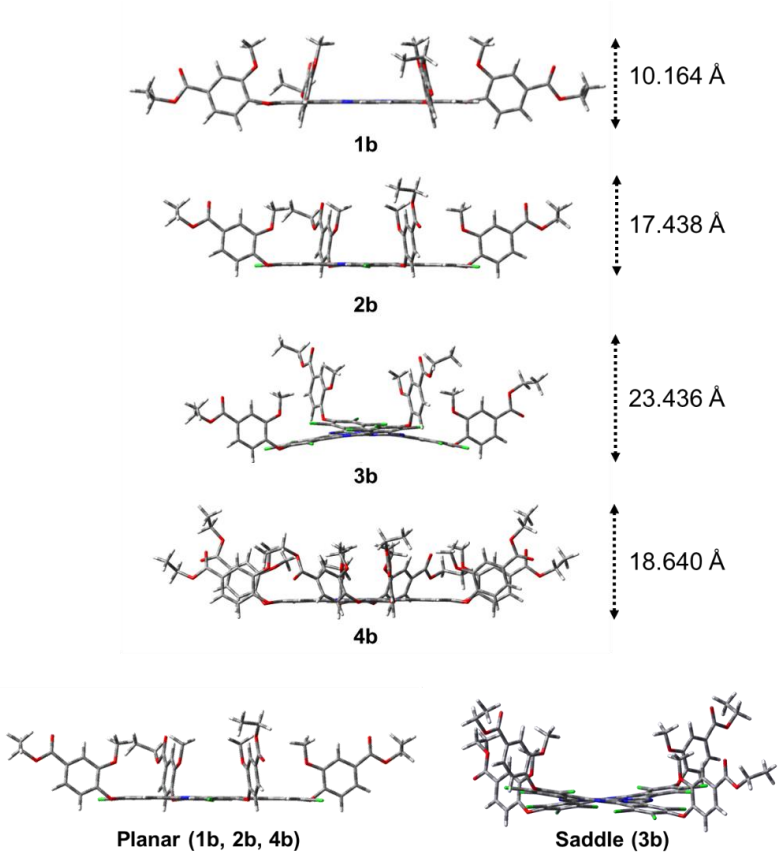

Figure 2.1. Geometry-optimized structures of the prepared dyes.

Table 2.1. Experimental and calculated spectral properties of the prepared dyes

Dye	Experimental		TD-DFT	
	λ_{max}[a]	ε_{max}[b]	λ_{max}	Transition
1b	678 nm	198,700	616 nm	HOMO → LUMO
			616 nm	HOMO → LUMO+1
2b	678 nm	190,710	617 nm	HOMO → LUMO
			617 nm	HOMO → LUMO+1
3b	697 nm	137,710	654 nm	HOMO → LUMO
			654 nm	HOMO → LUMO+1
4b	678 nm	199,510	621 nm	HOMO → LUMO
			621 nm	HOMO → LUMO+1

[a]Absorption maximum wavelength of Q-band of dyes
[b]Molar extinction coefficient (L mol-1 cm-1)

The vertical transitions calculated by TD-DFT are displayed in Table 2.1. All the transitions corresponding to Q-band showed HOMO → LUMO and LUMO + 1. Dyes **1b** and **2b** had similar maximum absorption wavelengths (616 and 617 nm), whereas dye **4b** has a slightly bathochromically shifted absorption maximum at 621 nm. However, the absorption maximum of dye **3b** is at 654 nm, with a red shift of over 30 nm. Substituted PCs are known to absorb longer wavelengths because of the increased electron density in the isoindole ring. Therefore, it can generally be deemed that the greater the number of substituents is and the larger their electron donating power is, the longer the absorption wavelength is [16]. However, the results indicate that a considerable shift of the maximum absorption wavelength is observed only for dye **3b**, which uniquely

has a deformed core structure in the form of a saddle structure. Hence, it appears that not only the substituent type and the electron donating power, but also the geometrical structure of PCs has a significant influence on the spectral characteristics, and the distortion of the PC core structure can cause a shift in the optical absorption band. These findings correspond well with the results of the earlier study [18].

2.3.3. Spectral properties of the dyes

All the synthesized PC dyes were dissolved in propylene glycol monomethyl ether acetate (PGMEA); their absorption spectra were measured by a UV-Vis spectrometer and compared. The relevant data are presented in Fig. 2.2 and Table 2.1. The dyes exhibit the typical Q-band (600–700 nm) and B-band (300–400 nm) absorption spectrum of PC. The Q- and B-bands are attributed to the π–π* transition of the heteroaromatic 18–π electron system of PC. The transition from the HOMO to LUMO level is represented by the Q-band, and the transition from deeper π levels to the LUMO is expressed as the B-band [16]. These transitions could be confirmed by the calculated vertical transitions discussed above. The Q-band transitions are indicated as HOMO to LUMO or LUMO + 1.

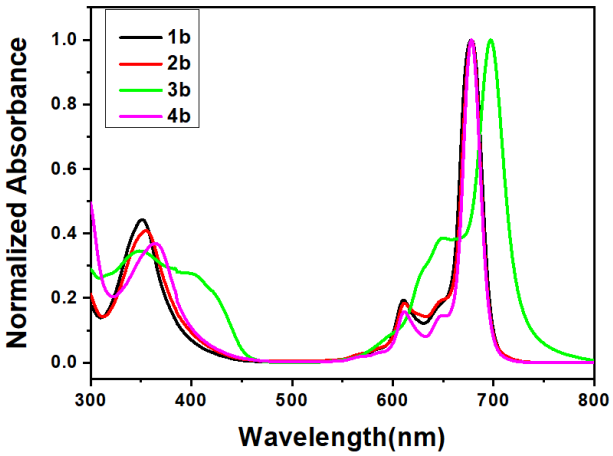

Figure 2.2. Normalized absorption spectra of the synthesized dye solutions dissolved in PGMEA. (1×10^{-6}M)

All the prepared dyes present maximum absorption in the 675–700 nm range and provide colors from cyan to green. In dyes **1b**, **2b**, and **4b**, an identical maximum absorption was observed at 678 nm; this trend is consistent with the TD-DFT calculation results. Compared to dye **1b**, the number of substituents at the peripheral positions is doubled from 4 to 8 in **2b** and **4b**. However, the maximum absorption wavelength remains the same. This is also observed between dye **2b** and **4b**, which contain different substituents at the peripheral positions; in dye **4b**, eight phenoxy groups are substituted, whereas in dye **2b**, four chlorines and four phenoxy groups are substituted, and these have different electron donating powers. Therefore, presumably, the difference in the electron

donating powers of the chlorine and phenoxy groups substituted at the peripheral positions does not affect the optical absorption wavelength.

However, in the case of dye **3b**, the Q-band appears at 697 nm, which is 20 nm longer wavelengths than those of dyes **1b**, **2b**, and **4b**. This propensity is also consistent with the TD-DFT calculation results. Furthermore, the molar extinction coefficient of dye **3b** is slightly smaller than those of the other dyes. Substituents at the non-peripheral positions are postulated to be the cause of these differences in dye **3b**. In other words, owing to the introduction of a substituent at the non-peripheral position of PC, the molecular geometry is twisted into a saddle shape, and the electron density distribution of the isoindole ring of PC is influenced; thus, the molecular absorption coefficient is lowered, and the Q-band is shifted to a longer wavelength.

As for the color property, dyes **1b**, **2b,** and **4b** show a strong absorption at 678 nm and appear cyan, while dye **3b** has a maximum absorbance at 697 nm and appears green. As the absorption band tends to be a slightly hypsochromically shifted and gets broadened when a dye is coated, the dye for the color filter should absorb light in the 690–700 nm range in order to uniformly transmit light in the green region of 500–550 nm [9]. Thus, dye **3b** is considered to possess the appropriate color property for the green color filter.

2.3.4. Solubility of the dyes

Table 2.2. Solubility of the synthesized dyes at 20°C.

Dye	Solubility (g / 100 ml)
1b	7.0
2b	7.1
3b	9.1
4b	4.5

A dye for the color filter must be soluble in an industrial solvent like PGMEA. However, PC is easily packed by intermolecular interactions such as the strong π-π and van der Waals interactions as a result of its planar molecule structure, and hence has low solubility in common solvents [19]. Therefore, to suppress the π-π stacking, a methoxy-substituted phenol derivative was introduced, and the twist between the planes of the phenyl and PC moieties was induced by their steric strain. This is confirmed by the results of geometry optimization. In addition, an ester group was adopted on the para position of the phenyl substituent of the dyes to improve compatibility with PGMEA. Accordingly, enhanced solubility of the dyes in PGMEA was intended by the introduction of these functional groups. Solubilities of the dyes are listed in Table 2.2.

Dye **4b** exhibited the lowest solubility among the prepared dyes, dissolving at less than 5 wt% in PGMEA. This is due to a higher degree of order in the solid state of octa-substituted PC. The octa-substituted PC exists as a single isomer,

because of its symmetrical structure [20]. This leads to an improved degree of molecular ordering compared to that of unsymmetrically substituted PC. In contrast to dye **4b**, the other dyes present high solubilities of 7 wt% or more because of the constitutional isomers. It should be especially noted that dye **3b** shows the highest solubility, which is attributed to its geometry. The geometry optimization results reveal that dyes **1b**, **2b**, and **4b** have planar core structures, whereas dye **3b** has a saddle core structure, which results in its lower planarity and larger vertical axial bulkiness. As a result of the decreased planarity, the packing of the PC molecules could be hindered, thereby increasing the degree of disorder. Thus, the solubility can be increased by suppressing the π-π stacking between the dye molecules.

Although dye **4b** showed a relatively low solubility, it appears that the introduced functional groups are effective in increasing the solubility in PGMEA. Furthermore, dyes **1b**, **2b**, and **3b**, which have a higher solubility of 7% or more, can be adequately applied as colorants in a color filter.

2.3.5. Thermal properties of the dyes

The PC cores of the molecules are strongly stacked, leading to poor solubility in common solvents. On the other hand, the packing of molecules provides excellent durability such as the heat resistance and lightfastness. However, in PCs

containing substituents, a bulky one causes steric hindrance and inhibits the molecular ordering; the solubility is improved, but the durability is decreased. Therefore, it is important to introduce a substituent with appropriate bulkiness for sustaining high heat resistance. It was reasoned that the substituted phenol derivative induces appropriate steric hindrance, and ensures high durability along with good solubility.

The color filter manufacturing temperature is 230℃, and the dyes should be able to withstand this condition without decomposition. Therefore, to determine the thermal stability of the synthesized dye, a thermal gravimetric analysis (TGA) was performed under isothermal conditions at 230℃ for 30 min. Fig. 2.3 shows that the mass reduction of the dyes up to 300 °C is within 5%. Table 2.3 summarizes the decrease in mass in the isothermal region.

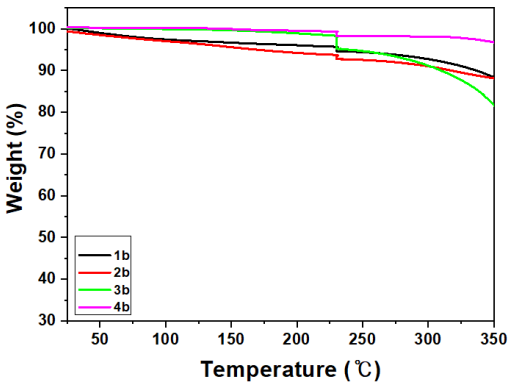

Figure 2.3. TGA analysis of the synthesized dyes. Dyes were heated to 230°C and held at the temperature for 30 min, and then further heated to 350°C.

Dye **3b** showed a relatively low thermal stability compared to other dyes. This is due to its bulky structure. The high bulkiness of molecule structure hinders intermolecular interactions, leading to low crystallinity. As a result, the improvement of molecular bulkiness could weaken the stability to thermal degradation. As presented in Fig. 2.1, dye 3b has the highest vertical bulkiness owing to its twisted structure among prepared dyes. Thus, this property can decrease the thermal stability because of its low crystallinity.

However, all the prepared dyes exhibit mass decline of less than 5% that is sufficient to be applied in color filters. This can be confirmed by the color difference value of the color filter fabricated using dye 3b in Table 2.6. These results indicate that the introduced of substituents do not significantly decrease the heat resistance of the dyes.

Table 2.3. Weight loss (%) of prepared dyes at 230℃

Dye	Weight loss at 230℃
1b	1.7%
2b	1.7%
3b	3.0%
4b	1.1%

2.3.6. Characterization of the spin-coated films

2.3.6.1. Spectral and chromatic properties of the spin-coated films

Among the prepared dyes, dye **3b** showed the most suitable spectral property and solubility to be applied in a green color filter. Therefore, a dye-based color filter was fabricated using dye **3b**. The color filter was fabricated by spin coating at different rpm, and a pigment-based color filter was also prepared under the same conditions. The transmittance of the color filters is displayed in Fig. 2.4 and Table 2.4, and their color features are indicated in Fig. 2.6 and Table 2.6.

To produce the green required for the currently used color filter, a high transmittance in the 500–540 nm range is required. Therefore, a green colorant for the color filter should present a maximum transmittance at approximately 520 nm and absorb from 600 nm or more. At present, the pigment dispersion for the color filter consists of a mixture of two or more green pigments to satisfy these conditions.

However, in the pigment-based color filter, the transmittance is decreased owing to the large particle size of the pigment and the broad absorption band. Furthermore, because the spectral characteristics and dispersities of the respective pigments in a pigment mixture are different, a loss of transmittance

can occur due to a pigment with a lower transmittance. This can cause a decline in the brightness of the color filter.

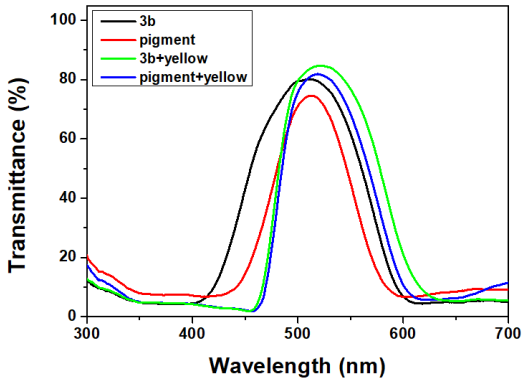

Figure 2.4. Transmittance spectra of color filter fabricated using pigment ink and dye (3b) ink. The inks were prepared by mixing colorant, binder in PGMEA. Those inks were then spin-coated on a glass.

A dye-based color filter can overcome these issues. In this study, it was evaluated that the spectral properties of a dye-based color filter using dye **3b** and compared to those of a pigment-based color filter with the currently used pigment mixture. This is given in Fig. 2.4 and Table 2.4.

The color filter with dye **3b** shows strong absorption above 600 nm and strong transmission near 500–530 nm. In addition, compared to the pigment-based color filter, the dye-based one has a similar transmission spectrum, higher transmittance, and higher brightness, as shown in Fig. 2.4, Tables 2.4 and 2.6.

This can be attributed to the sharp absorption band and the higher absorbance of the dye compared to the pigment. In general, the absorption of a dye is narrower and higher than that of a pigment [5]. The PC dyes have particularly excellent absorption properties among various dyes. Therefore, the desired range of light can be absorbed solely, and the remaining can be strongly transmitted. In contrast, pigments exist in the form of particles and have a broad absorption bands and a low absorbance [5]. Therefore, light is absorbed over a large wavelength range, thereby reducing the transmittance in the targeted region.

Table 2.4. Transmittance of the pigment-based and dye-based color filters.

Spin-coated colorfilter	Wavelength of T_{max}[a]	Transmittance
3b	512 nm	80.11%
Pigment	512 nm	74.59%
3b+Y138	520 nm	84.73%
Pigment+Y138	520 nm	81.83%

[a]Wavelength of maximum transmittance

The absorption characteristics of the pigment ink and dye **3b** ink at the same concentrations (wt%) indicated in Fig. 2.5 and Table 2.5 clearly support this assumption. The pigment ink somewhat absorbs light in the 500–530 nm range of the green region and has a moderate absorption between 600–700 nm, leading to a broad absorption in the overall region, whereas dye **3b** exhibits an excellent

transmittance of approximately 100% in the 500–530 nm range, a sharp absorption between 600–700 nm, and 53% higher absorbance at the maximum absorption wavelength than that of the pigment mixture. Hence, this superior spectral property of the dye **3b** compared to that of the pigment mixture is reflected in the dye-based color filter, and an excellent brightness is achieved.

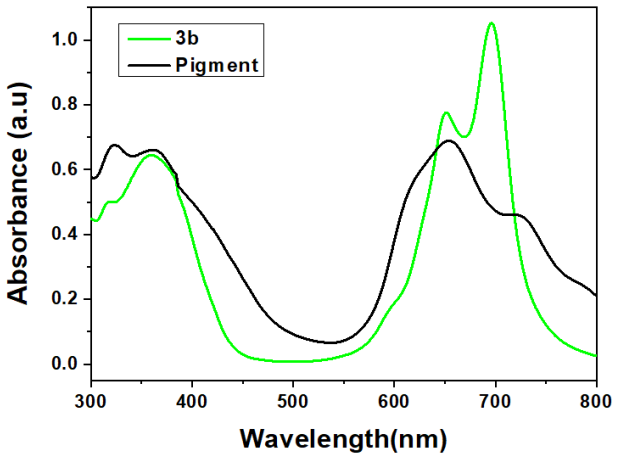

Figure 2.5. Absorption spectra of dye (3b) ink and pigment ink, blended with binder and PGMEA. The prepared inks were diluted to a 4×10^{-3} wt%.

Table 2.5. Absorption spectra and absorbance (a.u) of dye (3b) and pigment ink.

Dye	Absorption (nm)	Absorbance (a.u)
3b	651, 696	0.78, 1.05
Pigment	654	0.69

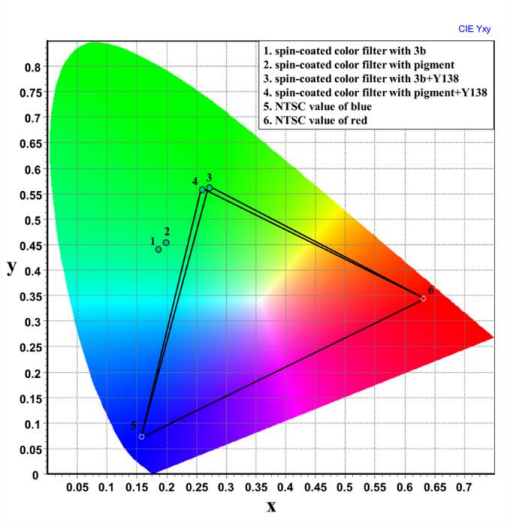

Figure 2.6. CIE 1931 chromaticity diagram of the pigment-based and dye-based color filters.

As shown in Fig. 2.6 and Table 2.6, the dye-based color filter without compensation had a smaller *x* value than that of the pigment-based one in the chromatic property. This is due to the additional blue light before 500 nm, which is transmitted much more than that for a pigment mixture. However, because a yellow compensating colorant is introduced to remove the light before 500 nm in the green color filter, the *x* value before the compensation matters little. This can be confirmed from the color characteristic of the color filter using an ink with the yellow compensating colorant, shown in Fig. 2.6 and 2.7 and Table 2.6. The dye-based color filter with pigment Y138, used as a compensating pigment, exhibits color coordinate values (*x*, *y*) similar to those of the pigment-based one with the

same compensating colorant. Furthermore, the dye-based filter yields higher brightness because of its higher transmittance in the green region. Thus, the color filters with dye 3b demonstrate excellent spectral characteristics compared to that of the pigment mixture, indicating that dye 3b can be adequately applied in a green color filter.

Table 2.6. The coordinate values corresponding to the CIE 1931 chromaticity diagram and the color difference values of the pigment-based and dye-based color filters.

Spin-coated color filter	Y	x	y	Thermal stability (ΔEab)	Thickness (μm)
3b	47.60	0.185	0.438	2.53	2.91
Pigment	38.84	0.199	0.452	1.97	3.44
3b+Y138	55.66	0.269	0.560	2.41	3.18
Pigment+Y138	53.76	0.260	0.558	1.90	3.62

The color difference (ΔE_{ab}) measured to evaluate the heat resistance of the color filter is provided in Table 2.6. After baking at 230℃, an additional baking was carried out at the same temperature for 30 min, and the change in the color coordinate values before and after the additional baking was measured. For commercial purpose, a color difference value of less than 3 is required. The ΔE_{ab} of the pigment- and dye-based color filters are 1.9 and 2.5, respectively. Thus,

the dye-based color filter is confirmed to fulfill the required heat fastness. This result is consistent with that of the TGA measurement.

The study demonstrates that the dye shows a satisfactory color property for the color filter. Furthermore, the dye-based color filter can provide a superior transmittance than that of the pigment-based one. This is due to the advantages of the dyes, such as the excellent spectral properties, *viz.*, the high absorbance and narrow absorption band. Moreover, the ΔE_{ab} value of the color filter of dye **3b** satisfies the commercial requirement, and the PCs are inferred to be a suitable moiety for providing heat resistance to the dye-based color filter.

2.3.6.2. Thickness of the spin-coated films

For improving the color gamut of the color filter, it is crucial that a colorant produces a deep color. The method for presenting a deeper color is to have a higher absorbance of the colorant at the same thickness or to increase the thickness of the colorant layer [5]. In the latter case, however, there is a commercially available thickness limit for the color filter. Moreover, reducing the thickness of each component is demanded owing to the recent trend of slim display technology. Thus, a deep color with a thin layer is necessary. For this, the higher absorbance and the smaller particle size of the applied colorant is advantageous.

In this respect, it is postulated that the synthesized dyes could be an adequate alternative to the pigment. Hence, in order to test the effect of the dye on the thickness of the color filter, the dye ink and the pigment ink with similar color properties (*x*, *y* value) were prepared by blending with Y138, and color filters using the inks were fabricated with various thicknesses using a spin-coating method at different rpm (150, 250, 300, 350, 400, 450 rpm). Eventually, the thickness and the color chromatic feature of the prepared color filters were measured. A correlation between those properties was subsequently examined and compared. In Fig. 2.7, *x* and *y* values of the color filters with various thickness are plotted. The relationship between the *y* value and thickness is shown in Fig. 2.8.

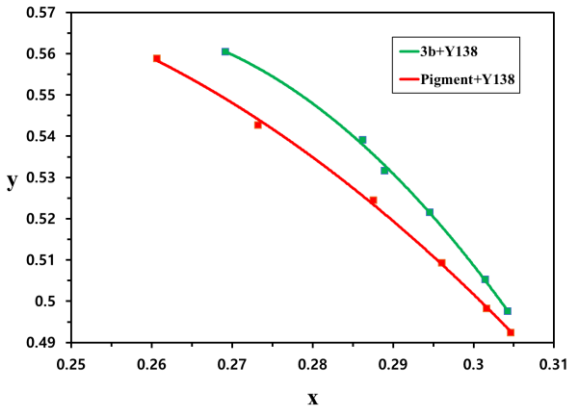

Figure 2.7. The coordinate values (x, y) on different thickness of dye-based and pigment-based color filters with yellow compensation.

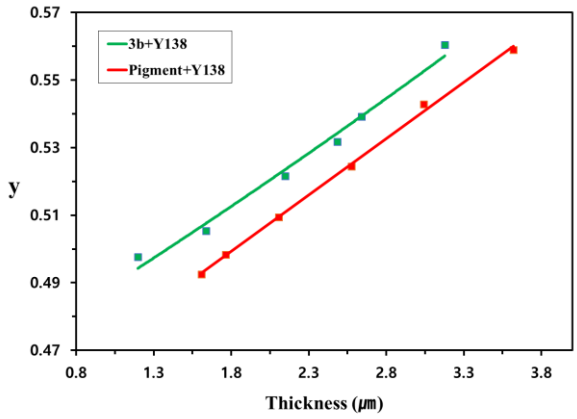

Figure 2.8. The coordinate values (y) of various thickness of dye-based and pigment-based color filters with yellow compensation.

The correlation shows that the dye-based color filter has larger *x* and *y* values, implying higher color strength than those of the pigment-based one at the same thickness. Furthermore, the thickness is reduced by 20% compared to that of the pigment-based one for the same color coordinate value (*x*, *y* value). This is attributed to the higher absorbance in the 600–700 nm range and the larger transmittance between 500–550 nm of the dye-ink at the same concentration, as indicated in Fig. 2.5. The sharp and strong absorption can lead to a high color strength and color purity, and these chromatic features are intimately related to the quantity of the colorant in the color filter; the larger the color strength and the color purity, the smaller is the amount of a colorant needed for the same chromatic feature. Thus, because the dye-based color filter shows superior color

strength, it is possible to achieve the similar color for lower thickness. A deeper color can be produced likewise for the same thickness.

According to these findings, because of its outstanding spectral property, the prepared dye is proven effective for reducing the thickness of a color filter. Additionally, it presents the advantage of producing a deep color.

2.4 Conclusion

In order to reduce the thickness of the color filter and to replace the pigments used in the green color filter, four phthalocyanine dyes were synthesized, in which, chlorine and bulky phenyl derivatives were substituted at the peripheral and non-peripheral positions. A dye-based color filter was then fabricated by applying the prepared dye and compared its characteristics with that of a pigment-based color filter.

Dye **3b** showed the longest wavelength maximum absorbance and the highest solubility in PGMEA among the prepared dyes. This is attributed to the distorted geometry of the dye. Substitution at the non-peripheral position is suggested to cause deformation of the PC's planar structure, and this distortion induces a bathochromic shift of absorption band and enhances the solubility in industrial solvents. The dye conclusively demonstrates appropriate features for the color filter.

The dye-based color filter exhibits superior brightness and lower thickness than those of the pigment-based color filter. This is attributed to the sharp and higher absorbance of the dye, which are the advantages of dyes compared to pigments. Owing to the superior spectral property of dye **3b,** a higher transmittance and a better color strength of the dye-based color filter was achieved. Thus, a higher brightness with a similar color property is obtained at a reduced thickness than that of the pigment-based one.

In conclusion, it has demonstrated that the prepared PC dye can replace pigments in color filters, provided that the dye presents appropriate thermal stability and spectral properties, and that the thickness of the color filter can be reduced using the dye without diminishing the chromatic feature. Furthermore, it is confirmed that the dye-based color filter can show a better color property at a thickness similar to that of a pigment-based one.

2.5 References

[1] Tsuda K. Colour filters for LCDs. Displays. 1993;14(2):115-24.

[2] Helber MJ, Alessi PJ, Burberry M, Evans S, Brick MC, Diehl DR, et al. 19.2: Color Filter Formulations for Full-Color OLED Displays: High Color Gamut Plus Improved Efficiency and Lifetime. SID Symposium Digest of Technical Papers. 2007;38(1):1022-5.

[3] Lee M-T, Wang C-L, Chan C-S, Fu C-C, Shih C-Y, Chen C-C, et al. Achieving a foldable and durable OLED display with BT.2020 color space using innovative color filter structure. Journal of the Society for Information Display. 2017;25(4):229-39.

[4] Sabnis RW. Color filter technology for liquid crystal displays. Displays. 1999;20(3):119-29.

[5] Freeman HS, Peters AT. Colorants for Non-Textile Applications: Elsevier Science, 2000.

[6] Herbst W, Hunger K. Industrial Organic Pigments: Production, Properties, Applications: Wiley, 2006.

[7] Choi J, Sakong C, Choi J-H, Yoon C, Kim JP. Synthesis and characterization of some perylene dyes for dye-based LCD color filters. Dyes and Pigments. 2011;90(1):82-8.

[8] Sakong C, Kim YD, Choi J-H, Yoon C, Kim JP. The synthesis of thermally-stable red dyes for LCD color filters and analysis of their aggregation and spectral properties. Dyes and Pigments. 2011;88(2):166-73.

[9] Choi J, Kim SH, Lee W, Yoon C, Kim JP. Synthesis and characterization of thermally stable dyes with improved optical properties for dye-based LCD color filters. New Journal of Chemistry. 2012;36(3):812.

[10] Choi J, Lee W, Sakong C, Yuk SB, Park JS, Kim JP. Facile synthesis and

characterization of novel coronene chromophores and their application to LCD color filters. Dyes and Pigments. 2012;94(1):34-9.

[11] Kim SH, Namgoong JW, Yuk SB, Kim JY, Lee W, Yoon C, et al. Synthesis and characteristics of metal-phthalocyanines tetra-substituted at non-peripheral (α) or peripheral (β) positions, and their applications in LCD color filters. Journal of Inclusion Phenomena and Macrocyclic Chemistry. 2015;82(1-2):195-202.

[12] Yoon C, Kwon H-S, Yoo J-S, Lee H-Y, Bae J-H, Choi J-H. Preparation of thermally stable dyes derived from diketopyrrolopyrrole pigment by polymerisation with polyisocyanate binder. Coloration Technology. 2015;131(1):2-8.

[13] Muthukumar P, Kim H-S, Jeong JW, Son Y-A. Synthesis and characterization of tetra phenoxy-substituted halogen-rich metallophthalocyanine derivatives: A study on their LCD color filter requirements. Journal of Molecular Structure. 2016;1119:325-31.

[14] Tatsumi Y, Inoue M. 40-4: Development of Color Resists Containing Novel Dyes for Liquid Crystal Displays. SID Symposium Digest of Technical Papers. 2016;47(1):521-3.

[15] Nemykin VN, Lukyanets EA. Synthesis of substituted phthalocyanines. Arkivoc. 2010:136-208.

[16] Mack J, Kobayashi N. Low Symmetry Phthalocyanines and Their

Analogues. Chem Rev. 2011;111(2):281-321.

[17] Frisch MJ, Trucks GW, Schlegel HB, Scuseria GE, Robb MA, Cheeseman JR, et al. Gaussian 09, Revision E.01. Wallingford CT2009.

[18] Lee SU, Kim JC, Mizuseki H, Kawazoe Y. The origin of the halogen effect on the phthalocyanine green pigments. Chem Asian J. 2010;5(6):1341-6.

[19] Ghani F, Kristen J, Riegler H. Solubility Properties of Unsubstituted Metal Phthalocyanines in Different Types of Solvents. Journal of Chemical & Engineering Data. 2012;57(2):439-49.

[20] Tau P, Nyokong T. Synthesis, electrochemical and photophysical properties of phthalocyaninato oxotitanium(IV) complexes tetra-substituted at the alpha and beta positions with arylthio groups. Dalton Trans. 2006(37):4482-90.

Chapter 3

Synthesis of phthalocyanine derivatives as dispersion synergist for improving nanoparticle dispersions of pigment and its application to a color filter

3.1 Introduction

In display devices using a backlight unit such as an LCD, especially, the particle size of the pigments affects not only chromatic properties such as brightness and color but also contrast ratio related to light scattering [1]. The large pigment particles in the color filter scatter the transmitted light. The polarization of the light is changed and becomes uncontrollable, resulting in a transmission of additional light and a decrease in the contrast ratio. Light scattering is related to the particle size, ratio of the refractive indices between the particle and surrounding medium, and particle shape. Among these factors, the particle size exerts a profound influence on the scattering of incident light [2]. Theoretically, larger particles cause more scattering than smaller particles, provided that the refractive index of the particles is the same [3].

For this reason, the solvent-based wet dispersion method with polymer dispersant is used to obtain fine particles, incorporated into an LCD color filter. To obtain a well-dispersed system, preventing the coagulation of the colloidal pigment is very important. This stabilization mainly occurs *via* electrostatic and steric stabilization. However, the former is induced in highly polar systems such as aqueous inks, while the latter is the primary factor in solvent-based systems [4]. Therefore, additives like a polymeric surfactant and synergists are added to obtain stabilized particles in a non-polar solvent, and these additives play a crucial role in producing fine particles. In the wet-dispersion process, the ground pigment powder is stabilized by a dispersing agent. The dispersing agent is adhered to the surface of the pigments after the wetting and grinding stage, and this adsorption of the dispersing agent leads to repulsion between the particles, thereby preventing the flocculation of the particles. The interaction between the dispersant and pigment particles could be induced by different types of force (*e.g.,* ionic, hydrogen-bonding, and electrostatic) [4].

However, in some organic pigments such as phthalocyanine and dioxazine derivatives, the pigment molecules are not responsive to any of the dispersants, owing to their large planar structures. Thus, dispersions of these pigments easily flocculate after grinding. This issue could be resolved by enhancing the interaction between the pigment and dispersant. The synergist can play this role

by adsorbing on the pigment surface and then anchoring the dispersant. When the pigments are dispersed by using only the dispersant without a synergist, the dispersion performance including particle size is inferior, and the stability is also considerably reduced. In contrast, when synergists are introduced, the particle size and dispersion stability can then be improved, resulting in better chromatic characteristics [5].

The synergist has a structure capable of interacting with pigments and contains a functional group indicating high affinity with a dispersant, thus increasing the dispersion performance in the dispersion matrix [6]. Because chromatic features and transmittance are crucial to image quality, the spectral characteristics of the synergist must be contemplated for the ink of the color filter. Therefore, it is necessary to adopt a synergist, which has similar spectral characteristics to the pigment for the color filter.

Several studies have been carried out to introduce synergists to improve the dispersion of pigments applied to the color filter [5, 7-9]. Those studies focused on a blue, a red, and a yellow pigment. To the best of our knowledge, the investigation of a new synergist for green pigments has not been reported. The present study was performed to propose new green synergists that can retain the color properties and increase the dispersion performance of a green pigment used in the color filter. Ultimately, the contrast ratio of the LCD color filter was

enhanced by reducing the pigment particle size.

Synergists were synthesized to enhance the dispersion of pigment green 7, which is widely used as a green colorant for the color filter and exhibits inferior dispersion properties. The synergists are designed to ensure the color characteristics of the color filter by showing appropriate spectral characteristics for green. The phthalocyanine was modified to indicate a high intermolecular interaction between the synergist and the pigment. Furthermore, the bathochromic shift of the absorption wavelength was intended by chlorination, and various substituents were added as a dispersant-affinic group to interact with the dispersant: ester, carboxylic acid, primary amine, and tertiary amine. The dispersion characteristics and color properties were investigated by average particle size, polydispersed index (PDI), and UV-Vis spectrometer. The interaction between the synergists and a dispersant was demonstrated by using FT-IR spectrometer. The contrast ratio of the green color filter with the pigment dispersion was then examined. Finally, a suitable synergist that can improve the dispersion of pigment green 7 was proposed. The results were used to increase the contrast ratio of a green color filter for LCDs.

3.2 Experimental

3.2.1. Materials

1,8-diazabicyclo-7-undecene (DBU), 4,5-dichlorophthalonitrile, ethyl 4-hydroxy-3-methoxybenzoate, N, N-dimethyl-3-aminophenol, and 3-aminophenol were purchased from TCI, and $ZnCl_2$, potassium carbonate anhydrous, lithium hydroxide monohydrate, and 1-pentanol were purchased from Sigma-Aldrich. The other reagents and solvents were obtained from commercial suppliers. All chemicals were reagent-grade. Transparent glass substrates were provided by NTP, Inc., and acrylic polymer binder [9] was supplied by NDM, Inc.

3.2.2. Characterization and instruments

^1H NMR spectra were recorded on a Bruker Avance 500 spectrometer (National Center for Inter-University Research Facilities at Seoul National University) at 500MHz using dimethyl sulfoxide-d6, chloroform-d with tetramethylsilane (TMS) Elemental analysis was performed with a Thermo Scientific Flash EA 1112 elemental analyzer. Matrix-Assisted Laser Desorption/Ionization-Time of Flight (MALDI-TOF) mass spectra were collected on a Voyager-DE STR Biospectrometry Workstation (National Center

for Inter-University Research Facilities at Seoul National University). UV-Vis absorption spectra were measured using a PerkinElmer Lambda 25 spectrophotometer, and Fourier transform infrared spectroscopy (FT-IR) was conducted using a Thermo Scientific Nicolet 6700. The particle size analysis was performed using a Photal Otsuka Electronics ELSZ-1000, samples were prepared by diluting the dispersion with PGMEA (0.1 wt.%). The thickness of the spin-coated color filter was measured using a KLA-TENCOR Nanospec AFT/200 alpha step. Transmission electron microscopy (TEM) was performed on an FEI Tecnai F20 with an acceleration voltage of 200 kV; samples were prepared according to the literature procedures [7]. Field-emission scanning electronic microscopy (FE-SEM) images were acquired on a Zeiss MERLIN Compact; Pt was coated on the samples using JEOL MSC-101 for 40 secs at a current strength of 40 mA to avoid charging of the surface. Atomic Force Microscopy (AFM) was undertaken using a Park Systems NX-10. The color properties and transmittance spectra of the color filters were measured on a Scinco color spectrophotometer. The contrast ratio was analyzed using Tsubosaka Electric CT-1 BSLE.

3.2.3. Synthesis

3.2.3.1. Synthesis of compound 1 (ethyl 4-(2-chloro-4,5-dicyanophenoxy)-3-methoxybenzoate)

4,5-Dichlorophthalonitrile (1 g, 5.10 mmol) and ethyl 4-hydroxy-3-

methoxybenzoate (1.10 g, 5.61 mmol) were dissolved in dry DMF (50 ml) and anhydrous K_2CO_3 (3.52 g,25.5 mmol) was added portion wise for 3h. The mixture was stirred at 80 °C for 12 h under nitrogen atmosphere. The solution was then poured into ice water (100mL) with vigorous stirring to precipitate the product. The resulting suspension filtered to give a white-yellowish powder. Pure product was collected by column chromatography on silica gel using MC/hexane (3:1) mixture as an eluent. Yield 66%; ^{1}H NMR ($CDCl_3$, 500MHz, 25 °C, TMS): δ 7.87 (s, 1H, Ar-H), 7.77 (d, J=10 Hz, 2H, Ar-H), 7.20 (d, J = 8.5 Hz, 1H, Ar-H), 6.88 (s, 1H, Ar-H), 4.43 (q, J = 7 Hz, 2H, ester-CH2), 3.85 (s, 3H, OCH3), 1.43 (t, J=7.5 Hz, 3H, CH3); ^{13}C NMR ($CDCl_3$, 500MHz, 25 °C, TMS): δ 165.36, 157.24, 150.71, 144.76, 135.41, 130.27, 128.83, 123.38, 122.13, 119.54, 115.35, 114.38, 114.28, 109.83, 61.54, 56.24, 14.32.

3.2.3.2. Synthesis of compound 2 (4-chloro-5-(3-(dimethylamino)phenoxy)benzene-1,2-dicarbonitrile)

The product was synthesized following the same procedure for ethyl 4-(2-chloro-4,5-dicyanophenoxy)-3-methoxybenzoate using 4,5-dichlorophthalonitrile (1 g, 5.10 mmol), 3-(dimethylamino)phenol (0.77 g, 5.61 mmol), DMF (50 ml), and anhydrous K_2CO_3 (3.52 g, 25.5 mmol). The crude product was purified by column chromatography on silica gel using EA/hexane (1:4) mixture as the eluent. Yield 73%; ^{1}H NMR (d6-DMSO, 500MHz, 25 °C):

δ 8.51 (s, 1H, Ar-H), 7.50 (s, 1H, Ar-H), 7.26 (t, J = 8.5 Hz, 1H, Ar-H), 6.64 (dd, J = 8.5, 2.5 Hz, 1H, Ar-H), 6.48 (t, J = 2.5 Hz, 1H, Ar-H), 6.36 (dd, J = 8.0, 2.5 Hz,1H, Ar-H), 2.91 (s, 6H, amine-CH3); ^{13}C NMR (d6-DMSO, 500MHz, 25 °C): δ 157.07, 154.69, 152.25, 136.00, 130.66, 128.53, 121.93, 115.14, 114.98, 109.70, 109.16, 106.28, 103.27, 39.92.

3.2.3.3. Synthesis of compound 3 (4-(3-aminophenoxy)-5-chlorobenzene-1,2-dicarbonitrile)

The product was synthesized following the same procedure for ethyl 4-(2-chloro-4,5-dicyanophenoxy)-3-methoxybenzoate using 4,5-dichlorophthalonitrile (1 g, 5.10 mmol), 3-aminophenol (0.61 g, 5.61 mmol), DMF (50 ml), and anhydrous K_2CO_3 (3.52 g,25.5 mmol). The white yellowish solid was obtained that was purified by column chromatography on silica gel using MC/hexane (10:1) mixture as the eluent. Yield 78%; ^{1}H NMR (d6-DMSO, 500MHz, 25 °C): δ 8.51 (s, 1H, Ar-H), 7.56 (s, 1H, Ar-H), 7.09 (t, J = 8 Hz, 1H, Ar-H), 6.49 (d, J = 8 Hz, 1H, Ar-H), 6.28 (t, J = 2.5 Hz, 1H, Ar-H), 6.23 (dd, J = 8, 2.5 Hz, 1H, Ar-H), 5.41 (s, 2H, amine-H); ^{13}C NMR (d6-DMSO, 500MHz, 25 °C): δ 156.82, 154.85, 151.06, 136.08, 130.70, 128.91, 122.49, 115.14, 114.96, 111.38, 109.39, 105.92, 104.12.

3.2.3.4. Synthesis of compound GS-1 (2,9(10),16(17),23(24)-tetrachloro-3,9(10),16(17),23(24)-tetra(4-(ethoxycarbonyl)-2-

methoxyphenoxy)phthalocyaninato zinc (II))

A mixture of 4-(2-chloro-4,5-dicyanophenoxy)-3-methoxybenzoate (1.70 g, 4.80 mmol), $ZnCl_2$ (0.20 g, 1.44 mmol) and DBU (0.44 g, 2.88 mmol), in 1-pentanol (50mL) was heated to 150 °C and stirred for 12h under nitrogen atmosphere. The crude product was precipitated by pouring the reaction solution into methanol (100mL). After filtering the mixture, the collected solid was dried under vacuum. The solid was loaded onto a silica gel column with a 10:1 mixture of methylene chloride/MeOH eluent. As the crude product elutes from the column, the green band was collected and dried to afford GS-1 as a green solid. Yield 78%; MALDI-TOF MS: m/z 1492.1 (100%, [M + H]). Elemental analysis: Calcd for $C_{72}H_{52}Cl_4N_8O_{16}Zn$: C, 57.95; H, 3.51; N, 7.51; O, 17.15. Found: C, 58.50; H, 3.55; N, 7.57; O, 17.28.

3.2.3.5. Synthesis of compound GS-2 (2,9(10),16(17),23(24)-tetrachloro-3,9(10),16(17),23(24)-tetra(4-carboxy-2-methoxyphenoxy)phthalocyaninato zinc (II))

GS-2 was synthesized according to the literature procedures[10] using GS-1 (0.89 g, 0.59 mmol), LiOH•H2O (1.57 g, 36.6 mmol) in 70% aqueous methanol (100 ml), and THF (30 ml). The product was dried under vacuum to give GS-2. Yield 79%; MALDI-TOF MS: m/z 1380.9 (100%, [M + H]). Elemental analysis: Calcd for $C_{64}H_{36}Cl_4N_8O_{16}Zn$: C, 55.69; H, 2.63; N, 8.12; O, 18.55. Found: C,

54.58; H, 2.66; N, 8.18; O, 18.84%.

3.2.3.6. Synthesis of compound GS-3 (2,9(10),16(17),23(24)-tetrachloro-3,9(10),16(17),23(24)-tetra(3-(dimethylamino)phenoxy)phthalocyaninato zinc (II))

GS-3 was synthesized following the same procedure for GS-1 using 4-chloro-5-(3-(dimethylamino)phenoxy)benzene-1,2-dicarbonitrile (1.52 g, 5.10 mmol). ZnCl2 (0.21 g, 1.53 mmol) and DBU (0.47 g, 3.06 mmol), in 1-pentanol (50mL). Column chromatography with an 80:1 mixture of chloroform/MeOH eluent was performed to obtain GS-3 as a green solid. Yield 71%; MALDI-TOF MS: m/z 1257.1 (100%, [M + H]). Elemental analysis: Calcd for $C_{64}H_{48}Cl_4N_{12}O_4Zn$: C, 61.19; H, 3.85; N, 13.38; O, 5.09. Found: C, 60.56; H, 3.90; N, 13.64; O, 5.19.

3.2.3.7. Synthesis of compound GS-4 (2,9(10),16(17),23(24)-tetrachloro-3,9(10),16(17),23(24)-tetra(3-aminophenoxy)phthalocyaninato zinc (II))

The cyclotetramerization of 4-(3-aminophenoxy)-5-chlorobenzene-1,2-dicarbonitrile was carried out following the same procedure for GS-1 using 4-(3-aminophenoxy)-5-chlorobenzene-1,2-dicarbonitrile (1.38 g, 5.10 mmol), $ZnCl_2$ (0.21 g, 1.53 mmol) and DBU (0.47 g, 3.06 mmol), in 1-pentanol (50mL). The reaction solution was dried at 80 °C under vacuum to remove 1-pentanol and DBU. The crude solid was dissolved in DMF and water was added dropwise to the solution with continuous stirring. The mixture solution was then cooled to 0-

5 °C and kept 24h to precipitate the product. The solid was then filtered out and dried under vacuum. The suspension of the product in MeOH was heated under reflux for 1h to dissolve impurities. At the end of reflux, the mixture was cooled to room temperature. The green solid was collected by vacuum filtration and chromatographed on silica with THF as an eluent, followed by recrystallization in ethanol. Yield 46%; MALDI-TOF MS: m/z 1444.9 (100%, [M + H]). Elemental analysis: Calcd for $C_{56}H_{32}Cl_4N_{12}O_4Zn$: C, 58.79; H, 2.82; N, 14.69; O, 5.59. Found: C, 59.28; H, 2.79; N, 14.93; O, 5.70.

3.2.4. Preparation of pigment dispersion

Pigment green 7 was mixed with the prepared synergist, a dispersant polymer, and acrylic polymer binder in propylene glycol methyl ether acetate (PGMEA). Zr beads were then introduced into the mixture. After mixing, a pre-milling (60 min) was performed using a paint shaker, followed by main-milling (120 min) with 550 times/min. The pigment dispersion was isolated by vacuum filtering.

3.2.5. Preparation of color inks and spin-coated films

Pigment ink for a color filter was comprised of PGMEA (2.10 g), acrylic polymer binder (2.74 g), pigment dispersion (0.15 g). The acrylic polymer binder (Mw 16,000 g/mol) [9] was dissolved in PGMEA, followed by adding pigment

dispersion, and then the mixture was stirred vigorously for 120min at room temperature. The prepared inks were coated on a transparent glass substrate using a MIDAS System SPIN-1200D spin coater. The ink-coated glasses were then pre-baked at 100 °C for 100 secs and post-baked at 230 °C for 30 min. After post-baking, the coordinate values of the pigment-coated glasses were measured.

3.3 Results and discussion

3.3.1. Design and synthesis of the synergists

A synergist should interact intimately with the target pigment to function effectively in the dispersion process, and this can be mediated by different types of forces like ionic, hydrogen-bonding, and van der Waals interactions [4]. For phthalocyanine, two parts, *viz.*, the hydrophilic metal cation in the center of the macrocycle and the hydrophobic isoindole rings at the periphery of the macrocycle [11], could be used to react with the synergist. However, the phthalocyanine-based pigment, like pigment green 7, has a strong tendency to aggregate because of its planar structure, and this attractive interaction hinders the reaction between both these sites and the synergist [4]. Therefore, large planar structures could be effective for adsorbing on such aromatic macrocyclic compounds. Therefore, phthalocyanine moieties were employed and the π-π

stacking interaction that readily occurs between large planar molecules was induced. The functional groups (ester, carboxylic acid, tertiary amine, and primary amine) were adopted for the phthalocyanine derivatives to interact with pigment-affinic groups of a dispersant such as aminic and carbonyl groups. In addition, chlorine and phenoxy groups, which are electron-donating groups, were introduced at the peripheral position of the phthalocyanine to provoke the bathochromic shift of the Q-band, causing spectral characteristics corresponding to green [12].

The phenyl derivatives with each functional group were substituted by one equivalent of 4,5-dichloro phthalonitrile through the SN reaction. The zinc (II) phthalocyanine was then prepared by cyclotetramerization of the phthalonitriles with zinc chloride. This is displayed in Scheme 3.1. The synthesis of the precursors was carried out using DMF as a solvent and a base of K_2CO_3. 1-pentanol, and DBU was used as a nucleophile and a non-nucleophilic base catalyst for the cyclotetramerization of the phthalonitriles [12]. The synthesized phthalonitriles and phthalocyanines were purified by column chromatography. GS-4 was further purified by recrystallization using ethanol. Theoretically, all synergists can have constitutional isomers. Because the isomers hardly influence the dispersion of the pigment, the test in this study was conducted without separation of the isomers. The prepared materials were obtained with a yield of

30–80% depending on the substituent. Their structure was confirmed by NMR, MALDI-TOF-MS, and the elemental analyzer.

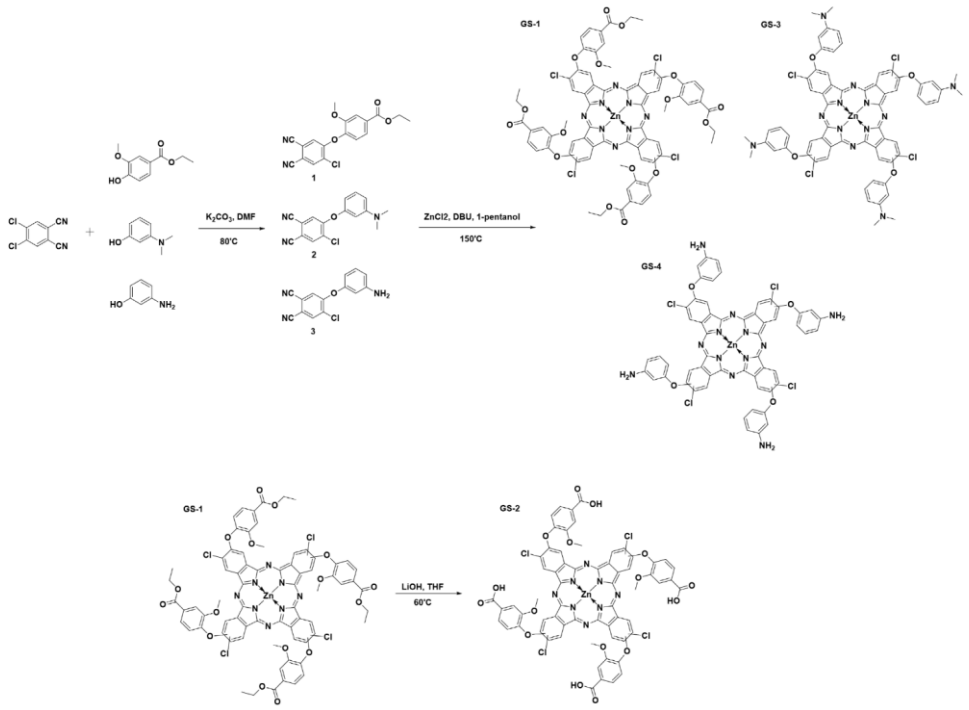

Scheme 3.1. Synthetic route of the prepared synergists.

3.3.2. Spectral properties of the synergists

The prepared synergists should transmit the region of 500–550 nm for the green color filter. To confirm the absorption and transmission of the synergists, the optical properties were evaluated by UV-vis spectroscopy. The results are

shown in Fig. 3.1.

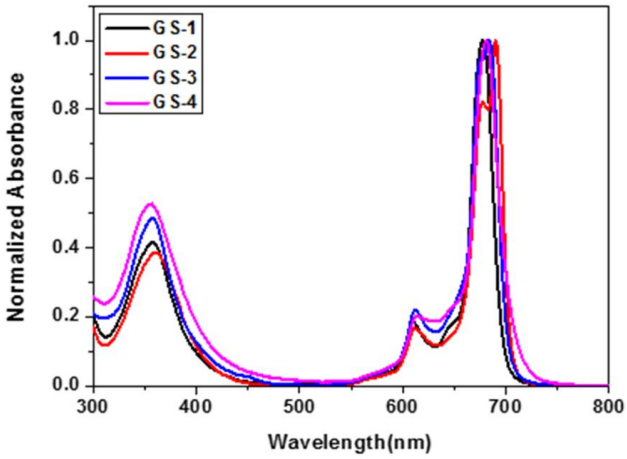

Figure 3.1. Normalized absorption spectra of the synthesized synergists in DMF (1×10^{-6}M).

The phthalocyanine structurally forms the heteroaromatic 18–π electron system of 16–membered ring, and that π-electron rich system leads to π–π* transition. This electronic transition is the origin of absorption spectra of phthalocyanine analogues. They typically present the Q-band (600–700 nm) and B-band (300–400 nm) absorption spectra. The absorption of Q-band is attributed to the electronic transition from HOMO of π-bond to LUMO of that bond, and B-band is attributed to the electronic transition from deeper HOMO to LUMO [13].

GS-1, GS-2, GS-3, and GS-4 exhibited maximum absorption at 678 nm, 690 nm, 684 nm, and 681 nm, respectively, and transmitted light in 500–550 nm

region, which is required for the green color filter. Q-band of unsubstituted zinc phthalocyanine is generally shown (or displayced) near 650 nm. On the other hand, all synthesized dye indicated bathochromically shifted Q-band, compared to unsubstituted zinc phthalocyanine. This red shift of Q-band is due to a substitution of electron donating groups on the phthalocyanine. As the electron donating substituents, such as hydroxy-, alkoxy-, and aryloxy groups, were substituted on peripheral or non-peripheral positions of phthalocyanine, the electron density of isoindole rings of phthalocyanine is increased. This enhancing of electron density on phthalocyanine core leads to a shift of the first oxidation and first reduction potential, thus decreasing the HOMO-LUMO gap. As a result, the Q-band also moves to a longer wavelength [14].

The maximum absorption wavelength of GS-2 was slightly longer than that of GS-1, and the Q-band was weakly split, unlike other synergists. This difference is due to the D_2h symmetry characteristic [15], which is enhanced by the solvation of the carboxylic acid in the DMF of a polar solvent [16]. All other synergists indicated a similar maximum absorption characteristic of approximately 680 nm.

Although GS-2 showed a weakly split Q-band, this phenomenon had little effect on its transmission wavelength range. Thereby, all synthesized synergists transmitted green light range (500–550 nm) for use in the color filter.

3.3.3. Dispersion capability of the synergists

The pigment was mixed with the prepared synergists, the dispersant, and Zr-bead in PGMEA. The mixture was then dispersed by using a paint shaker [20]. To confirm the dispersion performance, the particle size was measured by DLS.

As shown in Table 3.1, the average particle sizes of the pigment with GS-1 and GS-3 were 119.9 nm and 123.9 nm, respectively, those of GS-2 and GS-4 were 94.3 nm and 98.9 nm, respectively, and that without a synergist was 118.6 nm. These results indicate that GS-1 and GS-3 containing ester and tertiary amine were ineffective for reducing the particle size compared with the non-synergist pigment dispersant. In contrast, GS-2 and GS-4 with carboxylic acid and primary amine displayed considerably decreased particle size, indicating that those molecules are suitable as the synergist.

In GS-1 and GS-3, ethyl and methyl groups are introduced at carboxylate and amine groups, respectively, whereas hydrogen, not an alkyl group, is substituted in the cases of GS-2 and GS-4. Thus, it is assumed that because the terminal alkyl groups of ester and tertiary amine induce steric hindrance and interfere with the interaction between the pigment-affinic group of the dispersant and carboxylate and amine of GS-1 and GS-3, the dispersion was not performed properly. On the contrary, GS-2 and GS-4 contain carboxylic acid and primary amine, which have

hydrogen readily capable of hydrogen bond formation. Thus, it is inferred that an interaction such that hydrogen bonds between the dispersant and synergist could be provoked by an elimination of the steric hindrance, thereby reducing the particle size.

The polydispersity index (PDI) of all the dispersed particles was measured to be 0.1–0.2, which indicates that the size distribution of the particles in the dispersion is narrow. Moreover, the result is consistent with that of the average particle size. GS-2 and GS-4 displayed smaller values of PDI among the different dispersions. This fact confirms that these synergists are efficient in improving the dispersity of the pigment particles. The state of the pigment dispersion was also observed using TEM micrographs, indicated in Fig. 3.2. The dispersed pigment nanoparticles without a synergist exhibited a large particle size and agglomerated together forming clusters. The similar phenomenon was shown in the dispersion with GS-1 or GS-3, which were not effective in reducing particle size. In contrast, ones with GS-2 or GS-4 as a synergist displayed uniformly dispersed state. Thus, this result suggests that those pigment dispersions of the former have not only a large particle size but also a low uniformity. However, the size of agglomerates of those is smaller than that of the dispersion which does not use a synergist. Therefore, it is also inferred through the TEM images that the synergists can inhibit the agglomeration by being present between pigment particles.

Table 3.1. Average particle size, and PDI of dispersed pigment pastes in PGMEA (0.1 wt%). The samples were stored at room temperature for ten weeks and then analyzed by the same method.

Synergist	Average Particle size	Polydispersity Index (PDI)	Average Particle size after 10 weeks	Increment of particle size
-	118.6 nm	0.174	156.5 nm	37.9 nm
GS-1	119.9 nm	0.182	132.5 nm	12.6 nm
GS-2	94.3 nm	0.112	102.4 nm	8.10 nm
GS-3	123.9 nm	0.177	137.3 nm	13.4 nm
GS-4	98.9 nm	0.113	112.8 nm	13.9 nm

In the dispersion of pigments, the dispersion stability is also important. When the dispersion is labile, the particle can grow by agglomeration [21], thereby changing the color characteristic. For this, the particle size of the dispersions was evaluated after ten weeks. The results are provided in Table 3.1. In terms of the long-term stability after storage for ten weeks, dispersions with GS-2 exhibit superior stability, showing the growth of the particle by 8.1 nm, and those with GS-1, GS-3, and GS-4 showed a similar growth with an increase in the particle size by 12.6, 13.4, and 13.9, respectively. This is presumably due to the stronger electrostatic interaction between the carboxylic acid and amine groups. It is accepted that the carboxylic acid group is one of the excellent hydrogen-bond donors and acceptors. Thus, comparing GS-2 with GS-4, it can be concluded that a combination of the carboxylic acid/amine anchoring group is better than that of

the amine/amine anchoring group, inducing stronger intermolecular interaction with the dispersant. This excellent hydrogen bonding ability leads to a better stability of the pigment dispersion with GS-2 than that with GS-4.

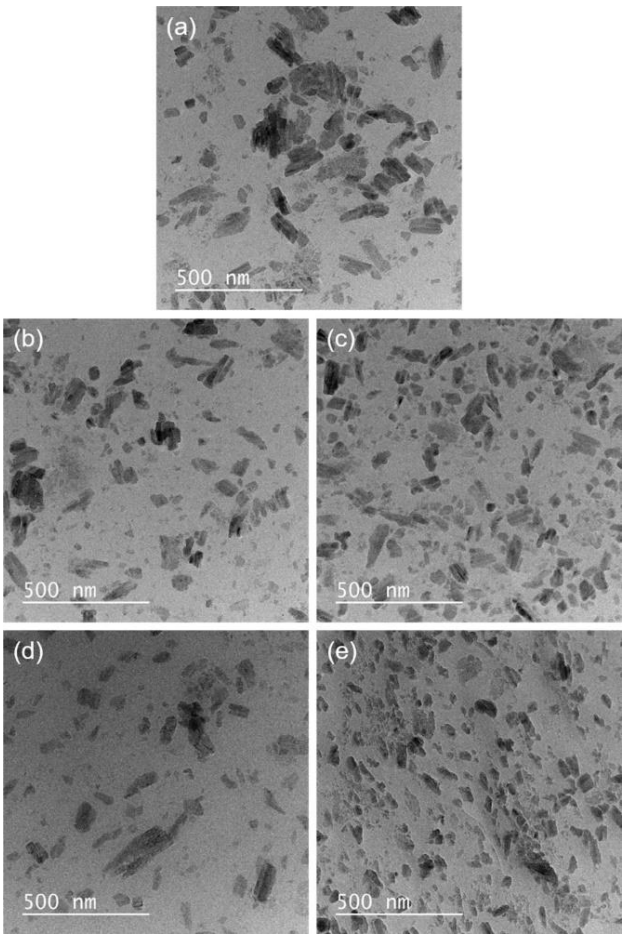

Figure 3.2. Transmission electron microscopy images of dispersed pigment nanoparticles coated on ultrathin amorphous carbon film. (a) C.I pigment green 7 without synergist; (b) with GS-1; (c) with GS-2; (d) with GS-3; (e) with GS-4.

Furthermore, it is clear that the particle size growth of the pigment dispersions with synergists was smaller than that of the dispersion without a synergist. This difference means that the synergists exist between the pigment particles and suppress an aggregation of the particles by steric hindrance of those bulky substituents, they were adsorbed on the pigment as intended. Accordingly, the introduction of the prepared synergists can be effective for enhancing the stability.

Among the synergists, GS-2 showed outstanding dispersion performance in both particle size and stability, and GS-4 also displayed similar capability in reducing the particle size. These results obtained in the pigment dispersion properties indicate that functional groups such as carboxylic acid and primary amine, which can induce electrostatic attraction such as hydrogen bonding [23, 24], can improve the dispersion of pigment green 7. Furthermore, an introduction of all prepared synergists can improve the dispersion stability, compared to the non-synergist dispersion.

However, because all pigment dispersions tend to increase in particle size over time, further studies are needed to address this issue.

3.3.4. AFM and SEM analysis of spin-coated pigment nanoparticle dispersions

The surface of spin-coated films on glass was analyzed by using AFM and

SEM, to observe coatings of pigment nanoparticle dispersions.

As displayed in Fig. 3.3, the pigment nanoparticle film without a synergist showed a rough surface with various clusters of agglomerates having a height of 50–100 nm. It appears that those clusters were caused by particles which were not properly dispersed. This result corresponds well with those found in the TEM analysis above. Because the dispersion is not uniform, particles having different sizes are present in an unstable state. Therefore, those particles can easily flocculate in the film [25, 26], and large particles can stick out of the coating. Those phenomena resulted in the surface irregularity of the film. A similar result was also exhibited in pigment dispersions using GS-1 or GS-3. Various agglomerates were observed on the surface of each film using those synergists. However, those films with GS-1 or GS-3 showed smaller agglomerates and clusters, compared with pigment dispersion film containing no synergist. As stated above, this result demonstrates that the synergists can inhibit a formation of large clusters of agglomerates on the surface of a coating.

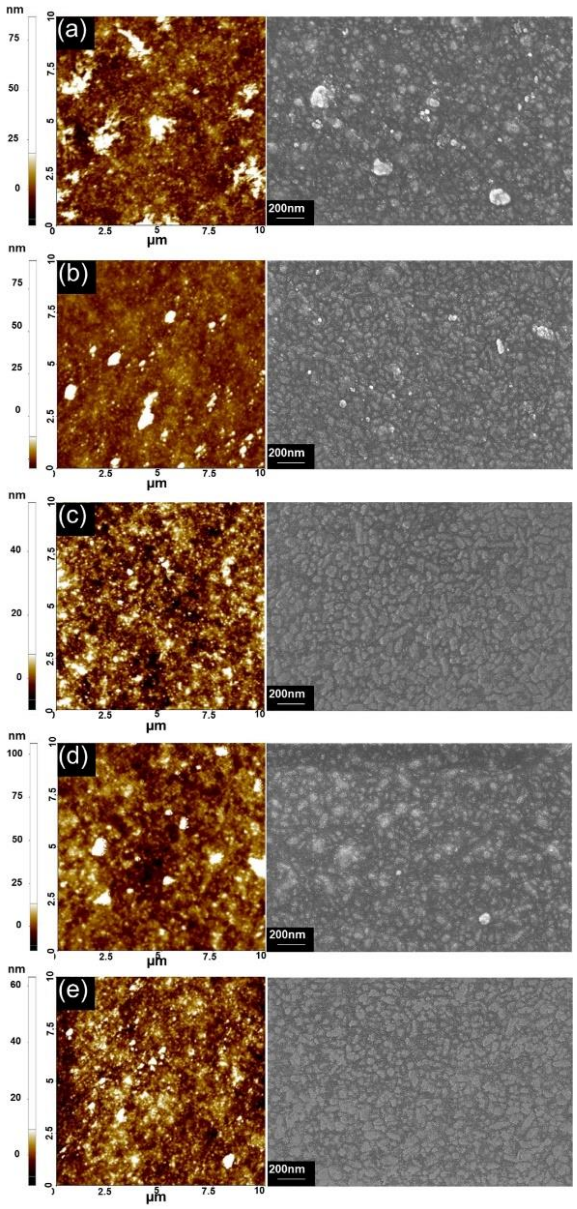

Figure 3.3. Atomic force microscopy images (10×10 µm^2) (left) and scanning electron microscopy (right) images of pigment nanoparticles dispersions spin-coated on glass. (A) C.I pigment green 7 without synergist; (B) with GS-1; (C) with GS-2; (D) with GS-3; (E) with GS-4.

Meanwhile, in the case of films with thoroughly dispersed pigments using GS-2 or GS-4, the coatings displayed few and small agglomerates and had a clearer surface than those of the dispersions with no synergist, GS-1, or GS-3. This phenomenon implies that their excellent dispersion state obtained by a suitable synergist can be efficiently retained in their coatings.

The surface analysis micrographs of the pigment dispersion coatings by AFM and SEM showed the similar tendency with those of TEM. The result revealed that all dispersions using synergists had a smaller size of agglomerates and the dispersion of GS-2 or GS-4 particularly displayed minimal agglomeration. Hence, the synergists can not only enhance the stability of dispersion particles in a liquid state but also help to sustain that in the coating.

3.3.5. FT-IR spectra of the synergists and dispersant blend

A polymeric dispersant is commonly used to disperse phthalocyanine derivatives such as pigment green 7, and an acrylic block copolymer dispersant with an amine value of 40 mg (KOH/g) was adopted in this study. The structure of a typical acrylic block copolymer dispersant is mainly composed of two parts [27, 28] as shown in Fig. 3.4. The anchoring block of a polymeric dispersant for organic pigments mainly incorporates an aminic group, because that functional group is effective in diverse pigments [29]; various aminic groups are introduced

in dispersants.

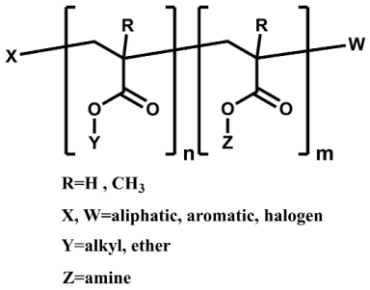

Figure 3.4. The common structure of acrylic block copolymer dispersants.

As stated above, GS-2 and GS-4, which contain carboxylic acid and primary amine, respectively, reduce the particle size of the pigment. Those functional groups have hydrogen combined with a highly electronegative atom such as oxygen and nitrogen; this circumstance can provide a proper condition for hydrogen bonds with the dispersant. Thus, it is inferred that GS-2 and GS-4 present superior dispersion properties unlike GS-1 and GS-3. Eventually, it is considered that the hydrogen bonds are provoked between those carboxylic acid and primary amine group of the synergists and the aminic group of the anchoring block in the dispersant. This interaction is briefly illustrated in Fig. 3.5.

FT-IR spectroscopy was used to identify the hydrogen bonds between the dispersant and the synthesized synergists. Films without dispersant were also prepared for comparison; the IR spectra obtained from the samples are presented in Fig. 3.6.

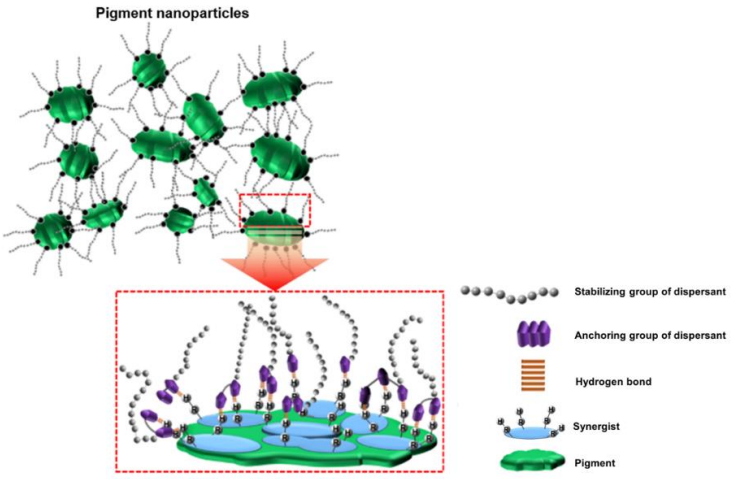

Figure 3.5. Interaction of synergists with polymeric dispersants.

In GS-1 and GS-3, the spectra showed no significant difference between the film with dispersant and that without dispersant. In the case of GS-1 without the dispersant, a strong C=O stretching band for ester near 1713 cm^{-1} appeared, and no specific absorption band of hydrogen bonding O-H was found [30]. A similar tendency was observed when dispersants were mixed with GS-1. GS-3, which is substituted the tertiary amine, also showed no absorption band for hydrogen bonding in the range of 3100–3500 cm^{-1}. For the mixture of GS-3 and the dispersant, that indicated no significant change of absorption band, identically to GS-1.

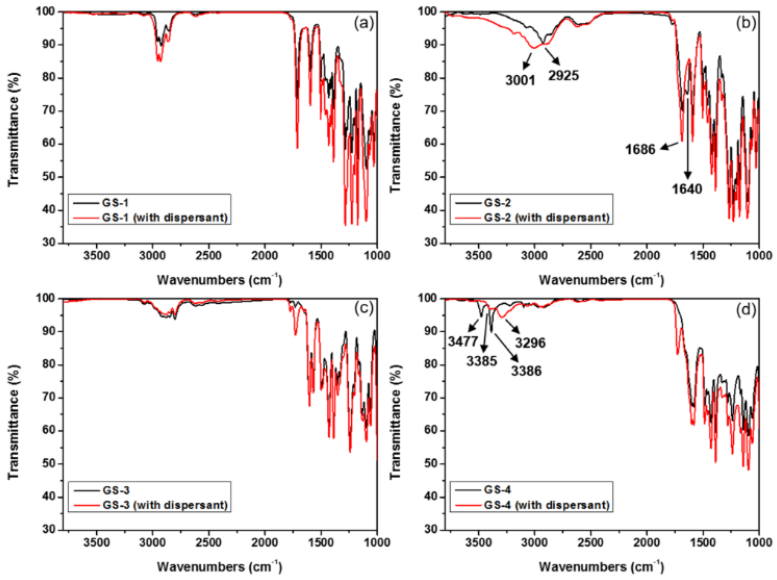

Figure 3.6. FT-IR spectra of the synergist and the dispersant blended films. The synergist and the dispersant mixtures in PGMEA were spin-coated on glass and then measured the spectra. (a) GS-1; (b) GS-2; (c) GS-3; (d) GS-4.

However, the results of GS-2 and GS-4 displayed a different propensity. The spectrum of GS-2 exhibited a broad hydrogen bonding O-H band in the range of 2700–3400 cm^{-1}; this was the result of the formation of strong self-associated hydrogen bonding between the carboxylic acids of GS-2 molecules [30]. Moreover, it should be noted that additional broad peaks were observed near 1640 cm^{-1} apart from a strong aryl conjugated C=O band at 1686 cm^{-1}. This was presumably due to the hydrogen-bonded C=O band [30, 31] Thus, the C=O stretching band can be found in company with the free C=O band at a lower wavenumber. On the contrary, in the result of GS-2 mixed with dispersant, the

hydrogen-bonded C=O band near 1640 cm^{-1} was hardly observed, and the width of the strong aryl conjugated C=O band was narrowed. This is the result of a decrease in the self-associated hydrogen bonds of the C=O group. It is inferred that the anchoring group of the dispersant and the O-H in the carboxylic acid of GS-2 were interassociated with each other, forming a hydrogen bond, and this interaction suppressed the self-associated hydrogen bond of the carboxylic acid.[32] In addition, for the non-dispersant sample of GS-2, the higher absorption peak of the self-associated O-H stretching band appeared at 2925 cm^{-1}, while that peak of the dispersant mixture moved to a 76 cm^{-1} higher frequency of 3001 cm^{-1}. It seems that the self-associated hydrogen bond of GS-2 decreased and the stretching band shifted slightly to a higher wavenumber, owing to the formation of hydrogen bond between GS-2 and the dispersant [32-34]. Therefore, these results support the formation of a hydrogen bond between GS-2 and the dispersant effectively, as suggested.

Doublet peaks were found in the range of 3386 cm^{-1} and 3477 cm^{-1}. The typical N-H stretching band for primary amine, and the N-H bending band was observed at 1535–1648 cm^{-1} in the GS-4 without the dispersant [30]. However, the GS-4 film containing the dispersant showed that those peaks at 3296 cm^{-1} and 3385 cm^{-1} broadened and moved to approximately 90 cm^{-1} lower frequency. These changes appear to be caused by the formation of the hydrogen bonding

between a dispersant and primary amine of GS-4 [35]. The hydrogen bond of amines theoretically generates shifting of the N-H stretching band to a lower wavenumber and broadening of the band. Consequently, these results suggest that GS-4 is also interassociated with the dispersant, forming a hydrogen bond.

As a result of FT-IR measurement, it was confirmed that GS-2 and GS-4 could form a hydrogen bond with the dispersant, as predicted. It is postulated that GS-2 and GS-4 showed superior dispersion performance than GS-1 and GS-3 owing to those interassociations with the dispersant.

3.3.6. Contrast ratios of spin-coated color filters

The contrast ratio of the LCD is closely related to the particle size of the pigment applied to the color filter. [1, 9] When the particle size of the pigment is large, the light from the backlight unit is scattered, and the polarization is altered; thus, uncontrolled light is transmitted, and the contrast ratio is reduced [36]. To demonstrate whether the particle size reduced by the synergist can enhance the contrast ratio, color filters using dispersed pigment pastes with the synergists were fabricated and their features were analyzed. This is shown in Table 3.2.

The contrast ratio is determined as the ratio of the maximum brightness to the minimum brightness (Y_{max}/ Y_{min}). Thus, it is necessary to increase the maximum brightness or decrease the minimum brightness to improve the contrast ratio. The

maximum brightness is influenced by the light source and can be easily enhanced by changing the type or voltage of the light source. In contrast, the minimum brightness is concerned with the material used in the color filter because the scattering occurs as the light passes through the color filter, and the light leaks out of a polarizer film, as described above. Accordingly, reducing the minimum brightness is a key point to improve the contrast ratio of the LCD.

Table 3.2. Maximum and minimum brightness (Y) and a contrast ratio (CR) of the color filter with pigment pastes. The pigment inks were spin-coated on glass, followed by baking at 230 °C.

Pigment	Synergist	Y_{max}	Y_{min}	CR	Thickness
C.I pigment green 7	-	837.6	0.171	4885	2.56
	GS-1	826.7	0.169	4904	2.60
	GS-2	843.6	0.149	5646	2.39
	GS-3	834.8	0.170	4923	2.45
	GS-4	825.1	0.150	5518	2.36

Table 3.2 shows that the contrast ratio of ref., GS-1, GS-2, GS-3, and GS-4 are 4885, 4904, 5646, 4923, and 5518, respectively, and the pigment pastes with GS-2 and GS-4 indicated higher values than the others. This is similar to the particle size measurement result above, meaning that a reduction in particle size by the synergists helps increase the contrast ratio value. This can be clearly

confirmed from the minimum brightness value. No-synergist, GS-1, GS-2, GS-3, and GS-4 displayed the Y_{min} values of 0.171, 0.169, 0.149, 0.170, and 0.150, respectively. GS-2 and GS-4 with reduced particle size exhibited reduced values 15% and 14% lower than that of ref., respectively, whereas the variations of maximum brightness values are less than 3%. It is inferred that as the particle size of the pigment dispersion decreases, the scattering of light is reduced, and the leakage of light is suppressed. Hence, the maximum brightness value was similar, but the minimum brightness value was decreased, and the contrast ratio was improved by more than 13% compared to that of the non-synergist, GS-1, and GS-3.

In conclusion, it is confirmed that the prepared synergists of GS-2 and GS-4 reduce the minimum brightness value by decreasing the particle size of the pigment dispersion, and those synergists are effective for improving the contrast ratio.

3.3.7. Spectral and chromatic properties of spin-coated color filters

Finally, the spectral and color characteristics of the spin-coated color filter with the prepared pigment dispersion were measured by using UV-vis spectrometry and color spectrometry; Table 3.3, 3.4 and Fig. 3.7 indicate each

property. The color coordinate values were compared based on the same y value to evaluate the differences precisely.

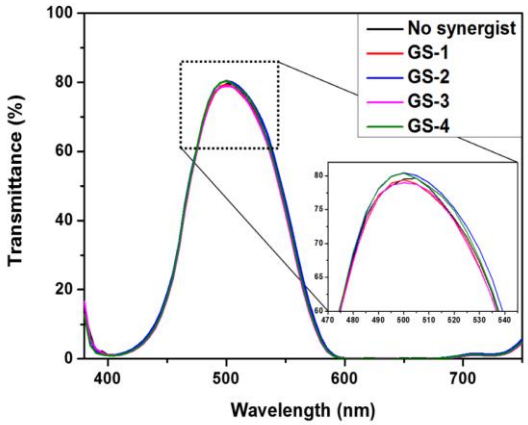

Figure 3.7. Transmittance spectra of the color filter with pigment pastes. The maximum transmittance (dashed rectangular box) was shown in an enlarged scale.

Table 3.3. The transmittance of the color filters with pigment pastes.

Pigment	Synergist	Transmittance at 500 nm	Transmittance at 505 nm
C.I pigment green 7	-	79.5%	79.6%
	GS-1	79.4%	78.8%
	GS-2	80.4%	80.0%
	GS-3	79.0%	78.7%
	GS-4	80.4%	79.6%

Table 3.4. The coordinate values corresponding to the CIE 1931 chromaticity of the color filters with pigment pastes.

Pigment	Synergist	x	y	Y
C.I pigment green 7	-	0.1552	0.4160	34.99
	GS-1	0.1556	0.4160	34.79
	GS-2	0.1581	0.4160	35.73
	GS-3	0.1567	0.4160	34.75
	GS-4	0.1592	0.4160	35.33

It is observed that all measured color properties displayed similar x values. This means that the synthesized synergists rarely influence the color of the pigment dispersion and have appropriate color characteristics for use in the green color filter. In the case of brightness (Y), GS-2 and GS-4 with superior dispersion characteristics exhibited slightly higher values than those of no synergist, GS-1, and GS-3. This difference is presumed to result from the smaller particle size of the pigment dispersion. This hypothesis can be confirmed from the transmission spectra: GS-2 and GS-4 also showed slightly higher transmittance in the range of 500–505 nm of the maximum transmission region. Thus, the difference in the transmission of the GS-2 and GS-4 appears to be reflected by the higher brightness.

It is observed that all measured color properties displayed similar x values. This means that the synthesized synergists rarely influence the color of the

pigment dispersion and have appropriate color characteristics for use in the green color filter. In the case of brightness (Y), GS-2 and GS-4 with superior dispersion characteristics exhibited slightly higher values than those of no synergist, GS-1, and GS-3. This difference is presumed to result from the smaller particle size of the pigment dispersion. This hypothesis can be confirmed from the transmission spectra; GS-2 and GS-4 also showed slightly higher transmittance in the range of 500–505 nm of the maximum transmission region. Thus, the difference in the transmission of the GS-2 and GS-4 appears to be reflected by the higher brightness.

The results of spectral and color characteristics demonstrate that the chromatic features of all prepared color filters were similar to that of the non-synergist color filter, and the synergists have a suitable spectral property as a colorant for the green color filter.

3.4 Conclusions

Four phthalocyanine-based synergists were synthesized and introduced to improve the dispersion properties of pigment green 7 and increase the contrast ratio of the color filter. All the synergists showed suitable absorption bands, transmitting in the green wavelength region (500–550 nm). GS-2 and GS-4 decreased the particle size of the pigment, thereby indicating that the carboxylic

acid and primary amine groups are effective in improving the dispersion characteristics. These functional groups can form strong hydrogen bonds with the anchoring group of the dispersant. In addition, the result of PDI confirms the stabilization of the pigment by these synergists. It is concluded that the synergists adsorb appropriately on the pigment surface and act as a bridge between the pigment and dispersing agent. The SEM and TEM images suggested a thoroughly dispersed state of the particles. The FT-IR spectra demonstrated hydrogen bonding between GS-2 or GS-4 and the dispersant, confirming the interaction between the synergist and the dispersant. Finally, it is ascertained that the pigment pastes with reduced particle sizes obtained by the use of GS-2 and GS-4 could improve the contrast ratio of the color filter without any migration of the color property.

In conclusion, it is suggested a suitable molecule structure as the synergist for dispersing phthalocyanine-based pigment used in the green color filter. However, regardless of the synergists existence, the dispersed pigment pastes were found to agglomerate over time. This issue is one of the disadvantages of the pigment dispersion method. Thus, further studies will be needed to suppress the agglomeration or introduce another color filter method that does not require the dispersion process such as a dye-based color filter.

3.5 References

[1] C.G. Jhun, J.S. Gwag, Journal of the Optical Society of Korea, 18 (2014) 184-187.

[2] B.J. Berne, R. Pecora, Dynamic Light Scattering: With Applications to Chemistry, Biology, and Physics (2013)

[3] P. Piedra, H. Moosmüller, Solar Energy, 155 (2017) 637-646

[4] F. O. Pirrung, P. H. Quednau, C. Auschra, CHIMIA International Journal for Chemistry, 56 (2002) 170-176.

[5] M.M. Gacek, J.C. Berg, Electrophoresis, 35 (2014) 1766-1772.

[6] J.J. Florio, D.J. Miller, Handbook of Coating Additives, Taylor & Francis (2004).

[7] A.T. Kelley, P.J. Alessi, J.E. Fornalik, J.R. Minter, P.G. Bessey, J.C. Garno, T.L. Royster, ACS Applied Materials & Interfaces, 2 (2010) 61-68.

[8] C. Yoon, J.-H. Choi, J.P. Kim, Molecular Crystals and Liquid Crystals, 533 (2010) 102-112.

[9] C. Yoon, J.-h. Choi, Dyes and Pigments, 101 (2014) 344-350.

[10] V.T. Verdree, S. Pakhomov, G. Su, M.W. Allen, A.C. Countryman, R.P. Hammer, S.A. Soper, J Fluoresc, 17 (2007) 547-563.

[11] K. Kadish, R. Guilard, K. M. Smith, The Porphyrin Handbook:

Phthalocyanines: Properties and Materials, Elsevier (2012)

[12] V.N. Nemykin, E.A. Lukyanets, Arkivoc, (2010) 136-208.

[13] K. J. Hamam, M. I. Alomari, Applied Nanoscience, 7 (2017) 261-268.

[14] V. N. Nemykin, E. A. Lukyanets, ARKIVOC: Online Journal of Organic Chemistry (2010) 136-208.

[15] J. Mack, N. Kobayashi, Chem. Rev., 111 (2011) 281-321.

[16] S. Gaspard, T.-H. Tran-Thi, Journal of the Chemical Society, Perkin Transactions 2, (1989) 383-389.

[20] W. Herbst, K. Hunger, Industrial Organic Pigments: Production, Properties, Applications, Wiley (2006).

[21] H.J. Spinelli, Advanced Materials, 10 (1998) 1215-1218.

[22] S. Creutz, R. Jerome, Langmuir, 15 (1999) 7145-7156.

[23] J.R.C. Costa, C. Correia, J.R. Góis, S.M.C. Silva, F.E. Antunes, J. Moniz, A.C. Serra, J.F.J. Coelho, Progress in Organic Coatings, 104 (2017) 34-42.

[24] L.S. Kotlyar, B.D. Sparks, Y. Lepage, J.R. Woods, Clay Minerals, 33 (1998) 103-107.

[25] F. Müller, W. Peukert, R. Polke, F. Stenger, International Journal of Mineral Processing, 74 (2004) S31-S41.

[26] P.T. Lee, C.W. Chiu, L.Y. Chang, P.Y. Chou, T.M. Lee, T.Y. Chang, M.T. Wu, W.Y. Cheng, S.W. Kuo, J.J. Lin, ACS Appl Mater Interfaces, 6 (2014)

14345-14352.

[27] S. Creutz, R. Jérôme, G.M.P. Kaptijn, A.W. Werf, J.M. Akkerman, Journal of Coatings Technology, 70 (1998) 41-46.

[28] C. Auschra, E. Eckstein, A. Mühlebach, M.-O. Zink, F. Rime, Progress in Organic Coatings, 45 (2002) 83-93.

[29] D.L. Pavia, G.M. Lampman, G.S. Kriz, J.A. Vyvyan, Introduction to Spectroscopy, Cengage Learning (2014).

[30] L. Guo, H. Sato, T. Hashimoto, Y. Ozaki, Macromolecules, 43 (2010) 3897-3902.

[31] N.-X. Chen, J.-h. Zhang, Chinese Journal of Polymer Science, 28 (2010) 903-911.

[32] S. Thayumanasundaram, V.S. Rangasamy, N. De Greef, J.W. Seo, J.-P. Locquet, European Journal of Inorganic Chemistry (2015) 1290-1299.

[33] M.M. Coleman, D.J. Skrovanek, J. Hu, P.C. Painter, Macromolecules, 21 (1988) 59-65.

[34] L.-S. Teo, C.-Y. Chen, J.-F. Kuo, Macromolecules, 30 (1997) 1793-1799.

[35] M. Yoneya, Y. Utsumi, Y. Umeda, Journal of Applied Physics, 98 (2005) 016106.

Chapter 4

Synthesis and characterization of metal phthalocyanine bearing carboxylic acid anchoring groups for nanoparticle dispersion and their application to color filters

4.1 Introduction

Since high durability is required in the manufacturing process and operating conditions of the color filter, the pigment is used as the major colorant for the color photoresist applied to the color filter[1]. The pigment has high stability that provides its heat resistance, chemical stability, and light fastness, which are required for the color filter. This stability exists because of its strong cohesiveness and low solubility [2]. However, the pigment has disadvantages when used as the coloring materials for the color filter. The pigment is coagulated in the polymorph crystal state, so that the absorption band is broad, and the absorbance is low. This effect results in low color purity and dimness of color

properties [3]. This color property of the pigment is not suitable for the color filter that require high transmittance and color strength in each color [4].

To overcome this drawback, various studies have been conducted to apply dyes as substitutes for the pigment [5-22]. The dye is less durable than the pigment but has high tinctorial strength and excellent brightness due to its sharp absorption band and high molar absorption coefficient. Therefore, the introduction of the dye into color filters would improve their optical properties [23].

However, since the durability required for the color filter is often higher than the durability dyes can provide, only a few dye chromophores can be applied to the color filter. In addition, general organic-solvent soluble dyes have low solubility in industrial solvents such as propylene glycol methyl ether acetate (PGMEA) and propylene glycol methyl ether (PGME) used for the color filter. Thus, it is necessary to design a molecular structure that improves the solubility of dyes in these types of solvents. For this reason, to improve solubility and obtain appropriate color characteristics, dye chromophores with superior durability have been selected, with various functional groups and auxochromes being introduced into those molecules, in earlier research studies for the development of the dye for color filters.

In this way, chromophores such as azo, perylene, anthraquinone [16], quinophthalone [13] and phthalocyanine (Pc) [17, 18] have already been studied. Our group also has reported highly soluble phthalocyanine (Pc) [15, 21, 22], perylene [19], and azo [6] derivatives with bulky substituents for the soluble-dye-based color filter, and confirmed that the dyes showed high solubility in PGMEA.

In an earlier study, it has reported a large aryloxy-substituted phthalocyanine dye with high solubility in PGMEA, and the soluble-dye-based color filter containing the dye [22]. The dye showed high solubility owing to its high bulkiness that resulted from its saddle structure. The color filter with the dye showed better color properties than the pigment-based color filters. However, not only are dyes typically less durable than the pigment, but they also may migrate in the film during the baking process of the color filter. It has been reported in other studies that color characteristics may be degraded in films due to migration and re-aggregation of dyes during high-temperature baking [13, 24]. Hence, the prepared dye-based color filter had inferior durability.

To remedy this drawback, a dye synergist-pigment-based color filter was also investigated in our earlier study [21]. Phthalocyanine-based synergist dyes containing a carboxylic acid group were synthesized and dispersed with the C.I. pigment green 7 to develop a dye synergist-pigment-based color filter. It showed that the dyes with carboxylic acid groups improve dispersibility and dispersion

stability of the C.I. pigment green 7, and increased the contrast ratio and stability of color filters.

However, in the dye synergist-pigment-based color filter, there is a limit to dispersing dye-pigment mixtures into small particles because the primary colorant is the pigment. The phthalocyanine pigment has a closed packed system due to its strong π-π stacking [25]. Hence, the pigment indicates low dispersibility and inferior re-agglomeration resistance [26]. The higher the cohesiveness the colorant causes, the lower the color characteristics in the color filter [27]. Thus, the developed color filter had superior thermal stability compared with the dye-based color filter but had inferior color properties.

To resolve these issues of color filters, a dispersed-dye-based color filter was investigated in this study. The pigment particles can change their crystalline form according to conditions including solvent and temperature, and their durability and color characteristics vary depending on the crystal state of the dispersed particles [28]. Thus, it is difficult to obtain pigment dispersed particles satisfying both color and dispersion characteristics for the color filter. On the other hand, the nature of the dye is mainly determined by substituents such as auxochromes and it is possible to control its intermolecular interaction by introducing various functional groups into dyes [2]. Therefore, the dye can be dispersed more simply than the pigment without requiring complex treatment. Furthermore, the dye can

be made into well-dispersed fine particles with superior color properties by incorporating a dispersant anchoring group [29]. It was expected that these well-dispersed dye particles can improve the durability of the color filter through the pigment-like behavior of the particles [30], while showing high color properties. In addition, it was believed that the migration of dyes, which can occur during baking, can be suppressed by the stabilization of the dispersed particles.

After review of available literature sources, the dye-based green color filters using dye dispersion have not been reported. The current study was designed to develop the dye structure that can induce high dispersion properties and the dye dispersion applicable to the green color filter. Phthalocyanine dyes bearing carboxylic acid groups were synthesized and dispersed and then applied to color filters and evaluated for their properties in this study.

For this purpose, benzoic acid derivatives and chlorine were introduced in copper phthalocyanine (CuPc) and zinc phthalocyanine (ZnPc). Thus, six phthalocyanine-based dyes were synthesized by varying the amount of substituted chlorine. Through this approach, it was intended to improve the bulkiness and dispersant anchoring ability of their molecules, and to control their spectral properties and molecular core structure. The dyes were then dispersed to application to the color filter. The characteristics of the dyes, their dispersions,

and color filters compared with those of C.I. pigment green 7, which are currently used in the green color filter.

Geometrical optimization and vertical absorption energy of the dyes were calculated using computational modeling, and the optical properties and thermal stability of the dyes were examined by UV-Vis spectrometry and thermogravimetric analysis. Average particle size and their dispersion stability of dye dispersions were measured to ascertain their dispersion properties. Color filters were then fabricated using dyes with superior dispersion properties, and their color properties, thermal fastness and thickness were compared.

4.2 Experimental

4.2.1. Materials

1,8-diazabicyclo-7-undecene (DBU), 4-nitrophthalonitrile, 4,5-dichlorophthalonitrile, 3,4,5,6-tetrachlorophthalonithrile, and ethyl 4-hydroxy-3-methoxybenzoate, C.I pigment green 7 were purchased from Tokyo Chemical Industry (TCI). Potassium carbonate anhydrous, urea, ammonium molybdate, zinc chloride, lithium hydroxide monohydrate, and 1,2,4-trichlorobenzene, 1-pentanol, tetrahydrofuran (THF), methyl methacrylic acid, benzyl methacrylate were purchased from Sigma-Aldrich. 2 2'-azobis(isobutyronitrile) was obtained

from Junsei Chemical. All the other reagents and solvents were of reagent-grade and obtained from commercial suppliers. All chemicals were reagent-grade. Transparent glass substrates were manufactured by Asahi Glass Co Ltd. Polymeric dispersants (Disperbyk LPN 6919, 21116) were acquired from BYK-Chemie GmbH.

4.2.2. Characterization and instruments

^{1}H NMR spectra were measured on a Bruker Avance 500 spectrometer (National Center for Inter-University Research Facilities at Seoul National University) at 500MHz using dimethyl sulfoxide-d6 and chloroform-d as the solvent. Tetramethylsilane (TMS) was used as an internal standard. Elemental analysis was conducted with a Thermo Scientific Flash EA 1112 elemental analyzer. Matrix-Assisted Laser Desorption/Ionization-Time of Flight (MALDI-TOF) mass spectra were collected on a Voyager-DE STR Biospectrometry Workstation (National Center for Inter-University Research Facilities at Seoul National University) with α-cyano-4-hydroxy-cynamic acid (CHCA) as the matrix. UV-Vis absorption spectra were recorded using a Lambda 25 spectrophotometer (PerkinElmer). Thermogravimetric analysis (TGA) was performed in nitrogen atmosphere at a heating rate of 10°C/min using a Thermogravimetric Analyzer 2050 (TA Instruments). The thickness of the spin-

coated color filter was measured using a Alpha step (KLA-TENCOR Nanospec AFT/200). The optical properties of the color filters were measured on a color spectrophotometer (Scinco). The particle size analysis was performed using a Litesizer 500 (Anton Paar), samples were prepared by diluting the dispersion with PGMEA (0.1 wt%). Field-emission scanning electronic microscopy (FE-SEM) images were acquired on a MERLIN Compact (Zeiss); Pt was coated on the samples using MSC-101 (JEOL) for 40 secs at a current strength of 40 mA to avoid charging of the surface. The power XRD of the dye particles was examined using a SmartLab (Rigaku) with Cu-Kα X-rays (1.5406 Å); data was recorded for the 2θ range of 3° to 40°.

4.2.3. Synthesis

4.2.3.1. Synthesis of compound 1a (ethyl 4-(3,4-dicyanophenoxy)-3-methoxybenzoate)

A synthesis of ethyl 4-(3,4-dicyanophenoxy)-3-methoxybenzoate was refers to our previous study [22]. 4-Nitrophthalonitrile (1 g, 5.77 mmol) and ethyl 4-hydroxy-3-methoxybenzoate (1.18 g, 6.00 mmol) were dissolved in dry DMF (30 ml). The temperature of the mixture was heated to 80 °C with stirring. anhydrous K_2CO_3 (1.24 g, 9.00 mmol) was then added portionwise to the solution. The mixture was heated for 5 h. All procedures were performed under nitrogen atmosphere. The solution was then poured into ice water (100 mL) with vigorous

stirring. The resulting suspension filtered to give a white-yellowish powder. The crude product was purified by column chromatography on silica gel using methylene as an eluent. The pure product was finally collected by recrystallization using a mixture of methylene chloride/methanol. Yield 89%; ^{1}H NMR (d6-DMSO, 500 MHz, 25 °C): δ 8.06 (d, J=8 Hz, 1H, Ar-H), 7.75 (d, J=2.5 Hz, 1H, Ar-H), 7.71(d, J=2 Hz, 1H, Ar-H), 7.64 (dd, J=8, 2 Hz, 1H, Ar-H), 7.33 (m, 2H, Ar-H), 4.36 (q, J=7 Hz, 2H, CH2CH3), 3.81 (s, 3H, OCH3), 1.33 (t, J=7, 3H, CH_2CH_3). Elemental analysis: Calcd for $C_{18}H_{14}N_2O_4$: C, 67.08; H, 4.38; N, 8.69; O, 19.85 %. Found: C, 66.29; H, 4.42; N, 8.71; O, 20.45.

4.2.3.2. Synthesis of compound 2a (ethyl 4-(2-chloro-4,5-dicyanophenoxy)-3-methoxybenzoate)

2a was synthesized following the same procedure for 1a using ethyl 4-hydroxy-3-methoxybenzoate (0.99 g, 5.07 mmol), 4,5-dichlorophthalonitrile (1 g, 5.07 mmol), DMF (30 ml), and anhydrous K_2CO_3 (1.06 g, 7.66 mmol). Yield 75%; ^{1}H NMR ($CDCl_3$, 500 MHz, 25 °C, TMS): δ 7.85 (s, 1H, Ar-H), 7.75 (d, J=10 Hz, 2H, Ar-H), 7.19 (d, J = 8.5 Hz, 1H, Ar-H), 6.86 (s, 1H, Ar-H), 4.43 (q, J = 7 Hz, 2H, CH_2CH_3), 3.83 (s, 3H, OCH_3), 1.41 (t, J=7.5 Hz, 3H, CH_2CH_3). Elemental analysis: Calcd for $C_{18}H_{13}ClN_2O_4$: C, 60.60; H, 3.67; N, 7.85; O, 17.94 %. Found: C, 59.49; H, 3.84; N, 7.79; O, 19.65.

4.2.3.3. Synthesis of compound 3a (ethyl 3-methoxy-4-(2,3,6-trichloro-4,5-dicyanophenoxy)benzoate)

3a was synthesized following the same procedure for 1a using ethyl 4-hydroxy-3-methoxybenzoate (0.74 g, 3.76 mmol), 3,4,5,6-tetrachlorophthalonitrile (1 g, 3.76 mmol), DMF (30 ml), and anhydrous K_2CO_3 (0.78 g, 5.64 mmol). Column chromatography with toluene as an eluent was performed to obtain the product. The pure product was finally collected by recrystallization using a mixture of methylene chloride/methanol. Yield 76%; ^{1}H NMR (d6-DMSO, 500 MHz, 25 °C): δ 7.69 (d, J=2 Hz, 1H, Ar-H), 7.49 (dd, J=8.5, 2 Hz, 1H, Ar-H), 6.84 (d, J = 8.5 Hz, 1H, Ar-H), 4.29 (q, J = 6.5 Hz, 2H, CH_2CH_3), 3.91 (s, 3H, OCH_3), 1.31 (t, J=7 Hz, 3H, CH_2CH_3). Elemental analysis: Calcd for $C_{18}H_{11}Cl_3N_2O_4$: C, 50.79; H, 2.60; N, 6.58; O, 15.04 %. Found: C, 49.18; H, 2.74; N, 7.43; O, 16.41.

4.2.3.4. Synthesis of compound 1b-CuPC (2,9(10),16(17),23(24)-tetra(4-(ethoxycarbonyl)-2-methoxyphenoxy)phthalocyaninato copper (II))

A synthesis of compound 1b-CuPc was according to our previous study [22]. 1a (1.61 g, 5.00 mmol) and $CuCl_2$ (0.22 g, 1.65 mmol) were mixed in 1-pentanol (50mL), followed by heating to 150 °C. DBU (0.50 g, 3.30 mmol) was then added dropwise to the solution. The mixture was stirred for 5h under nitrogen atmosphere. After cooling the mixture, the crude product was precipitated by

pouring the reaction solution into methanol (100mL). The collected solid was dried at 50°C in a vacuum oven. The crude product was purified by column chromatography with a 20:1 mixture of chloroform/methanol eluent. The pure product was finally collected by recrystallization using a mixture of methylene chloride/methanol. Yield 65%; MALDI-TOF MS: m/z 1352.6 (100%, $[M + H]^+$). Elemental analysis: Calcd for $C_{72}H_{56}N_8O_{16}Cu$: C, 63.92; H, 4.17; N, 8.28; O, 18.92 %. Found: C, 63.88; H, 4.25; N, 9.15; O, 19.37.

4.2.3.5. Synthesis of compound 1b-ZnPc (2,9(10),16(17),23(24)-tetra(4-(ethoxycarbonyl)-2-methoxyphenoxy)phthalocyaninato zinc (II))

1b-ZnPc was synthesized following the same procedure for 1b-CuPc using 1a (1.61 g, 5.00 mmol), ZnCl2 (0.22 g, 1.65 mmol) and DBU (0.50 g, 3.30 mmol), in 1-pentanol (50mL). The crude product was purified by column chromatography with a 10:1 mixture of methylene chloride/methanol eluent. The green solid product was finally collected by recrystallization using a mixture of methylene chloride/methanol. Yield 69%; MALDI-TOF MS: m/z 1353.8 (100%, $[M + H]^+$). Elemental analysis: Calcd for $C_{72}H_{56}N_8O_{16}Zn$: C, 63.84; H, 4.17; N, 8.27; O, 18.90 %. Found: C, 62.97; H, 4.39; N, 9.03; O, 19.98.

4.2.3.6. Synthesis of compound 2b-CuPc (2,9(10),16(17),23(24)-tetrachloro-3,9(10),16(17),23(24)-tetra(4-(ethoxycarbonyl)-2-

methoxyphenoxy)phthalocyaninato copper (II))

2b-CuPc was synthesized following the same procedure for 1b-CuPc using 2a (1.78 g, 5.00 mmol), $CuCl_2$ (0.22 g, 1.65 mmol) and DBU (0.50 g, 3.30 mmol), in 1-pentanol (50mL). Column chromatography with a 50:1 mixture of chloroform/methanol eluent was performed to obtain the product. The green solid product was finally collected by recrystallization using a mixture of methylene chloride/methanol. Yield 54%; MALDI-TOF MS: m/z 1490.8 (100%, $[M + H]^+$). Elemental analysis: Calcd for $C_{72}H_{52}Cl_4N_8O_{16}Cu$: C, 58.02; H, 3.52; N, 7.52; O, 17.17 %. Found: C, 57.55; H, 3.65; N, 8.42; O, 19.07.

4.2.3.7. Synthesis of compound 2b-ZnPc (2,9(10),16(17),23(24)-tetrachloro-3,9(10),16(17),23(24)-tetra(4-(ethoxycarbonyl)-2-methoxyphenoxy)phthalocyaninato zinc (II))

2b-ZnPc was synthesized following the same procedure for 1b-CuPc using 2a (1.78 g, 5.00 mmol), $ZnCl_2$ (0.22 g, 1.65 mmol) and DBU (0.50 g, 3.30 mmol), in 1-pentanol (50mL). Column chromatography with an 80:1 mixture of chloroform/methanol eluent was performed to obtain the product. The green solid product was finally collected by recrystallization using a mixture of methylene chloride/methanol. Yield 78%; MALDI-TOF MS: m/z 1491.6 (100%, $[M + H]^+$). Elemental analysis: Calcd for $C_{72}H_{52}Cl_4N_8O_{16}Zn$: C, 57.95; H, 3.51; N, 7.51; O, 17.15 %. Found: C, 57.12; H, 3.55; N, 7.84; O, 18.25.

4.2.3.8. Synthesis of compound 3b-CuPc (1, 2, 4, 8, 9(10), 11, 15, 16(17), 18, 22, 23(24), 25-dodecachloro-3,9(10),16(17),23(24)-tetra(4-(ethoxycarbonyl)-2-methoxyphenoxy)phthalocyaninato copper (II))

3a (2.13 g, 5.00 mmol), $CuCl_2$ (0.22 g, 1.65 mmol), and urea (1.00 g) were mixed in 1,2,4-trichlorobenzene (50mL), followed by heating to 150 °C. Ammonium molybdate (0.19 g, 1.00 mmol) was then added to the solution. The mixture was stirred for 5h under nitrogen atmosphere. After cooling the mixture, the crude product was precipitated by pouring the reaction solution into methanol (100mL). The precipitates were separated with vacuum filtration. The collected solid dried at 50°C in a vacuum oven. The solid was loaded onto a silica gel column with methylene chloride. As the crude product elutes from the column, the methanol was gradually raised to 5% volume concentration in the eluent solution. The green band was collected and dried, followed by recrystallization with a mixture of methylene chloride/methanol to obtain compound 3b-CuPc. Yield 44%; MALDI-TOF MS: m/z 1764.1 (100%, $[M + H]^+$). Elemental analysis: Calcd for $C_{72}H_{44}Cl_{12}N_8O_{16}Cu$: C, 48.97; H, 2.51; N, 6.34; O, 14.49 %. Found: C, 47.92; H, 2.67; N, 6.68; O, 14.84 %.

4.2.3.9. Synthesis of compound 3b-ZnPc (1, 2, 4, 8, 9(10), 11, 15, 16(17), 18, 22, 23(24), 25-dodecachloro-3,9(10),16(17),23(24)-tetra(4-(ethoxycarbonyl)-2-methoxyphenoxy)phthalocyaninato

zinc (II))

3b-ZnPc was synthesized following the same procedure for 3b-CuPc using 3a (2.13 g, 5.00 mmol), $ZnCl_2$ (0.22 g, 1.65 mmol), urea (1.00 g), and ammonium molybdate (0.19 g, 1.00 mmol), in 1,2,4-trichlorobenzene (50mL). Column chromatography with stepwise gradient elution (chloroform to 20% methanol/chloroform) was performed to obtain the product. The green solid product was finally collected by recrystallization using a mixture of methylene chloride/methanol. Yield 54%; MALDI-TOF MS: m/z 1767.2 (100%, $[M + H]^+$). Elemental analysis: Calcd for $C_{72}H_{44}Cl_{12}N_8O_{16}Zn$: C, 48.91; H, 2.51; N, 6.34; O, 14.48 %. Found: C, 48.84; H, 2.68; N, 6.48; O, 16.12 %.

4.2.3.10. Synthesis of compound 1c-CuPc (2,9(10),16(17),23(24)-tetra (4-carboxy-2-methoxyphenoxy)phthalocyaninato copper (II))

A synthesis of compound 1c-CuPc was refers to the literature procedures [21]. 1b-CuPc was dissolved in THF (100mL). A saturated solution (100mL) of lithium hydroxide monohydrate in a mixture of water/methanol (3:7) was then dropwise added to the 1b-CuPc solution. The mixture was stirred at 80°C for 12h under nitrogen atmosphere. After cooling the mixture, the organic solvents were evaporated under reduced pressure. The aqueous solution of the crude product was washed using methylene chloride and ethyl acetate, followed by acidification

with 1M HCl to precipitate the product. The resulting suspension filtered to give a green solid. The solid cake was dried in vacuo and recrystallized with a mixture of dimethylformamide and methanol to obtain the pure product. Yield 43%; MALDI-TOF MS: m/z 2140.9 (100%, $[M + H]^+$). Elemental analysis: Calcd for $C_{64}H_{40}N_8O_{16}Cu$: C, 61.96; H, 3.25; N, 9.03; O, 20.63%. Found: C, 61.08; H, 3.56; N, 9.10; O, 21.48%.

4.2.3.11. Synthesis of compound 1c-ZnPc (2,9(10),16(17),23(24)-tetrachloro (4-carboxy-2-methoxyphenoxy)phthalocyaninato zinc (II))

1c-ZnPc was synthesized following the same procedure for 1c-CuPc using 1b-ZnPc. Yield 40%; MALDI-TOF MS: m/z 2145.8 (100%, $[M + Li]^+$). Elemental analysis: Calcd for $C_{64}H_{40}N_8O_{16}Zn$: C, 61.87; H, 3.25; N, 9.02; O, 20.60%. Found: C, 60.96; H, 3.33; N, 9.14; O, 21.31%.

4.2.3.12. Synthesis of compound 2c-CuPc (2,9(10),16(17),23(24)-tetrachloro-3,9(10),16(17),23(24)-tetra(4-carboxy-2-methoxyphenoxy)phthalocyaninato copper (II))

2c-CuPc was synthesized following the same procedure for 1c-CuPc using 2b-CuPc. Yield 35%; MALDI-TOF MS: m/z 1416.25 (100%, $[M + K]^+$). Elemental analysis: Calcd for $C_{64}H_{36}Cl_4N_8O_{16}Cu$: C, 55.77; H, 2.63; N, 8.13; O, 18.57 %. Found: C, 55.67; H, 2.78; N, 8.34; O, 18.85 %.

4.2.3.13. Synthesis of compound 2c-ZnPc (2,9(10),16(17),23(24)-

tetrachloro-3,9(10),16(17),23(24)-tetra(4-carboxy-2-methoxyphenoxy)phthalocyaninato zinc (II))

2c-ZnPc was synthesized following the same procedure for 1c-CuPc using 2b-ZnPc. Yield 37%; MALDI-TOF MS: m/z 1379.61 (100%, $[M + H]^+$). Elemental analysis: Calcd for $C_{64}H_{36}Cl_4N_8O_{16}Zn$: C, 55.69; H, 2.63; N, 8.12; O, 18.55 %. Found: C, 55.21; H, 2.78; N, 8.15; O, 19.01 %.

4.2.3.14. Synthesis of compound 3c-CuPc (1, 2, 4, 8, 9(10), 11, 15, 16(17), 18, 22, 23(24), 25-dodecachloro-3,9(10),16(17),23(24)-tetra(4-carboxy-2-methoxyphenoxy)phthalocyaninato copper (II))

3c-CuPc was synthesized following the same procedure for 1c-CuPc using 3b-CuPc. Yield 29%; MALDI-TOF MS: m/z 1675.94 (100%, $[M + Na]^+$). Elemental analysis: Calcd for $C_{64}H_{28}Cl_{12}N_8O_{16}Cu$: C, 46.48; H, 1.71; N, 6.78; O, 15.48 %. Found: C, 45.91; H, 1.89; N, 6.89; O, 16.85 %.

4.2.3.15. Synthesis of compound 3c-ZnPc (1, 2, 4, 8, 9(10), 11, 15, 16(17), 18, 22, 23(24), 25-dodecachloro-3,9(10),16(17),23(24)-tetra(4-carboxy-2-methoxyphenoxy)phthalocyaninato zinc (II))

3c-ZnPc was synthesized following the same procedure for 1c-CuPc using 3b-ZnPc. Yield 33%; MALDI-TOF MS: m/z 1652.63 (100%, $[M + H]^+$). Elemental analysis: Calcd for $C_{64}H_{28}Cl_{12}N_8O_{16}Zn$: C, 46.43; H, 1.70; N, 6.77; O, 15.46 %. Found: C, 46.03; H, 1.81; N, 6.79; O, 16.11 %.

4.2.4. Preparation of a polymeric binder

A polymerization of methyl methacrylic acid (MAA) and benzyl methacrylate (BzMA) was performed according to the literature procedures [31]. Propylene glycol methyl ether acetate (PGMEA) was pre-heated at 100°C for 60min under nitrogen purging. After cooling the solution to room temperature, 1g of 2 2'-azobis(isobutyronitrile) (AIBN) was dissolved in a small amount of the solvent. Methyl methacrylic acid (3.44 g, 40 mmol) and benzyl methacrylate (16.56 g, 94 mmol) were added to 40.0g of the same solvent, and the solution was stirred for 30min under nitrogen purging to eject oxygen. Then, the monomers were polymerized at 90°C; the AIBN solution was added dropwise to the monomer solution during the polymerization. The product was cooled down to room temperature after 5hr, and poly(BzMA-MAA) (Fig. 1) was obtained with a polymer content of 39%. The GPC analysis for the polymer indicated that Mn was 8,582 and Mw was 15,449. The polymer solution was adopted as a binder solution without further isolation of the polymer.

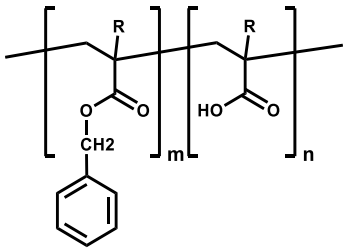

Figure 4.1. Structure of a polymeric binder. (m=7, n=3)

4.2.5. Preparation of dispersions

Dyes (0.80 g) and pigment green 7 (0.80 g) were mixed with a dispersant polymer (0.48 g) in propylene glycol methyl ether acetate (8.72 g), respectively. A pre-mixing was performed using a shaker. After pre-mixing, mixtures were dispersed using a probe sonicator at 20kHz (VCX 500, Sonics) in an ice bath; a dispersion was performed for 60min on pulse mode (10s on, 5s off).

4.2.6. Preparation of color inks and spin-coated films

Color inks for a color filter was composed of the propylene glycol methyl ether acetate (PGMEA) (0.30 g), acrylic binder (2.20 g), a dispersion (1.50 g). The prepared inks were coated on a transparent glass substrate using a MIDAS System SPIN-1200D spin coater. The spin-coated color filters were pre-baked at 100°C for 100 s and post-baked at 230°C for 30 min. After post-baking, the coordinate values of the color filters were examined.

4.2.7. Measurement of spectral and chromatic properties

Absorption spectra of the synthesized dyes and transmittance spectra of prepared color filters and pigment-based color filters were analyzed using a PerkinElmer Lambda 25 UV-vis spectrophotometer. Chromatic values were obtained by a Scinco colormate color spectrophotometer.

4.2.8. Measurement of thermal stability

Thermal stability of the synthesized dyes and C.I pigment green 7 was characterized by thermalgravimetric analysis. The colorants were heated to 230°C and held at the temperature for 30 min to simulate the color filter manufacturing thermal condition. The colorants were finally heated to 350°C to test their degradation temperature. The temperature was raised at the rate of 10 °C/ min under nitrogen atmosphere. To determin the thermal stability of the color filters, they were heated to 230°C and held at the temperature for 30 min in forced convection oven. The color difference values (ΔEab) before and after heating were measured using Scinco colormate color spectrophotometer in CIE L'a'b' mode.

4.3 Results and discussion

4.3.1. Design of the dyes

To disperse the fine particles of phthalocyanine (Pc), it is necessary to suppress the aggregation of molecules and enhance the interaction between the phthalocyanine unit and the dispersant [32]. The introduction of bulky substituents can be useful for facilitating this dispersal. Substituting those functional groups in the isoindole ring of phthalocyanine would cause steric

strain, thereby inhibiting the strong π-π interaction of the phthalocyanine core [33].

A functional group capable of maintaining strong interaction forces with the dispersant also should be introduced to the molecule to improve the dispersion stability of the dispersed particles [34]. The molecules that play this role are defined as dispersant anchoring groups. Dispersants contain the pigment-affinic groups which can adsorb to the particles. The dispersant anchoring groups interacts with the pigment-affinic groups, and this interaction makes the dispersant more adsorbable to the dispersed particles [35]. It can be said that the action of the anchoring group is important for the dispersion of the particles. Therefore, to disperse phthalocyanine particles finely, it is essential to introduce an appropriate dispersant anchoring group in the molecules.

In previous studies conducted in our laboratory, it has been shown that the 4-hydroxy-3-methoxybenzoate group enhances the bulkiness of Pc molecules, reducing the intermolecular interactions between them [22]. It has also been demonstrated that the phthalocyanine particles combined with the carboxylic acid group have superior dispersion properties since the functional group exhibits excellent properties as a dispersion anchoring group [21].

Based on these findings, for this study, the benzoate derivative was chosen as the bulky functional group, and it was introduced at the peripheral position of the

phthalocyanine to incite the same enhanced dispersion effect. Then, to increase the interaction between the dispersants and the dispersed particles, the benzoic acid group was incorporated by hydrolysis of the benzoate derivative. Furthermore, by substituting chlorine groups in both peripheral and non-peripheral positions, it was attempted to obtain Pc dyes with molecular structures favorable to dispersion and color properties suitable for the green color filter. Therefore, this study's ultimate goal was to improve the dispersion properties of the Pc particles and color properties of the color filter by enhancing the bulkiness of Pc molecule and its interaction forces with the dispersant.

Overall, 4-hydroxy-3-methoxy benzoic acid and chlorine were introduced as a bulky-dispersant anchoring group and an auxochrome, while copper and zinc were adopted as central metals of phthalocyanine

The synthesis of the six Pc dyes is shown in Scheme 4.1. The phthalocyanines were synthesized via the cyclotetramerization of its precursors, and then those dyes were purified by filtration, column chromatography, and recrystallization. The benzoate groups of the products were hydrolyzed using LiOH as a base to finally synthesize Pc dyes with benzoic acid groups [36]. Although constitutional isomers of synthesized Pc derivatives can be produced [37], these isomers were not isolated in this study.

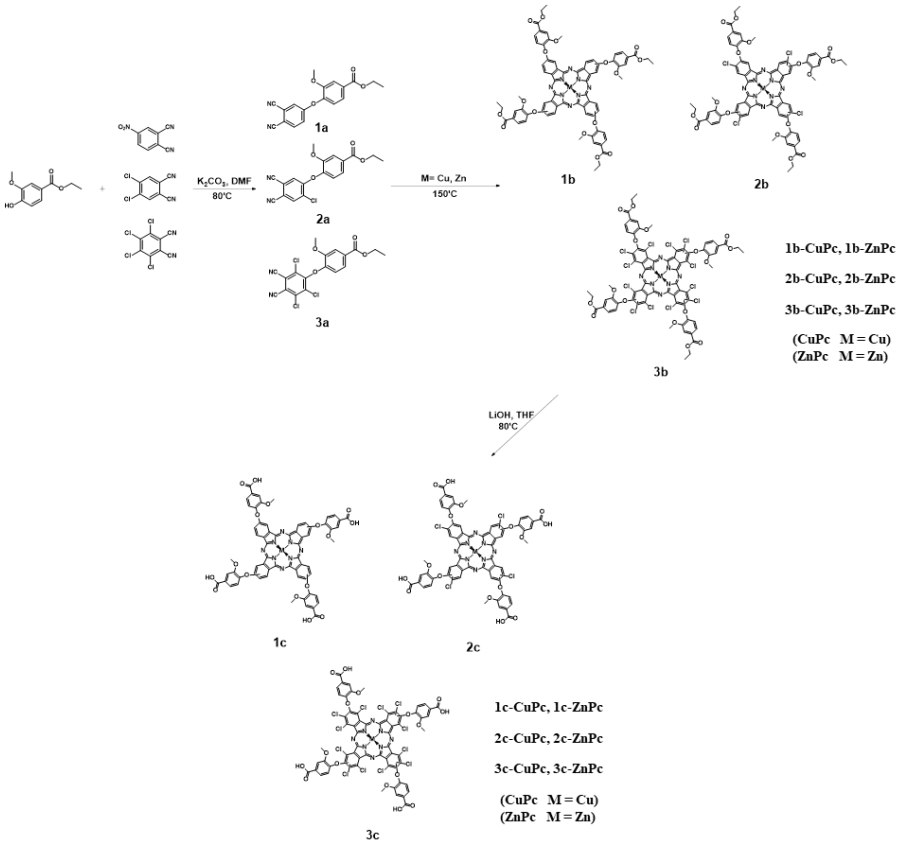

Scheme 4.1. Synthesis procedure of the designed dyes.

4.3.2. Geometry optimization, electrostatic potential (ESP) surface and TD-DFT calculations

Density functional theory (DFT) and time- dependent (TD)-DFT calculations were performed using the B3LYP function of the Gaussian09 software packages [38] with 6-311G (d) basis sets to predict the geometrically optimized structure, the optical absorption spectra, and electrostatic potential (ESP) surface.

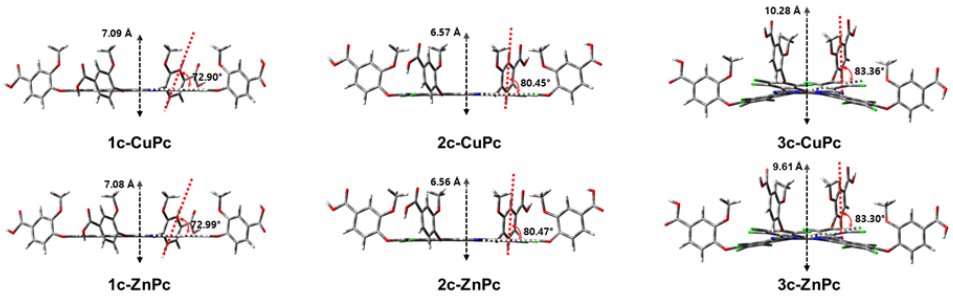

Figure 4.2. Geometry optimized structures of the dyes. (DFT calculation on B3LYP with 6-311G (d))

Fig. 4.2 and Table 4.1 display optimized structures of the dyes. The Pc cores of the dyes have planar structures, except for the 3c-CuPc and 3c-ZnPc dyes. These differences can be interpreted as follows. For 3c dyes with chlorine substituted on the non-peripheral position, the steric strain would increase due to the repulsion between adjacent Cl atoms, and this repulsive force would distort the core structure of 3c-CuPc and 3c-ZnPc, forming a saddle structure. This result is consistent with that of phthalocyanines with benzoate derivatives in our previous study [22]. These findings suggest that the transformation of the incorporated benzoate group into the benzoic acid group does not significantly affect the Pc core structure. As a result, the 1c dyes and the 2c dyes show similar bulkiness, but 3c dyes have higher bulkiness than that of those. It was expected that the formation of saddle structures of 3c-CuPc and 3c-ZnPc can increase the bulkiness of Pc molecules, thereby lowering the intermolecular forces. It is also

inferred that hindering the stacking of Pc molecules can improve the dispersion properties of their particles.

Table 4.1. Geometry optimized structures (twisted angles of the plane of benzoic acid substituents to the Pcs' isoindole ring plane, tortion angles of Pc core, and vertical bulkiness(Å) of the dyes) and ESP surface charges of the dyes.

Dye	Twisted angle[a]	Tortion angle[b]	Vertical bulkiness	ESP surface charges (a.u)	
				Center[c]	π-hole[d]
1c-CuPc	72.90°	0.453°	7.092 Å	0.057	-0.015
1c-ZnPc	72.99°	0.451°	7.088 Å	0.105	-0.019
2c-CuPc	80.45°	1.024°	6.566 Å	0.070	-0.002
2c-ZnPc	80.47°	1.014°	6.562 Å	0.120	-0.002
3c-CuPc	83.36°	18.65°	10.280 Å	0.090	0.018
3c- ZnPc	83.30°	16.33°	9.614 Å	0.129	0.020

[a]Twisted angles of the plane of benzoic acid substituents to the Pcs' isoindole ring plane
[b]Tortion angles of Pc core
[c]Central site of Pcs
[d]Center of bezene ring of isoindole ring

Fig. 4.2 also indicates that the methoxy group of the bulky benzoic acid moiety causes a steric strain on the isoindole ring of the Pc core, so that the plane of the Pc core and the plane of the phenyl are perpendicular to each other. The twisted angles of the plane of phenyl in 1c and 2c dyes, where substituents are introduced only at the peripheral position, increase as the size of atoms adjacent to the

benzoic acid group grow. This result indicates that the occupation of large atoms on adjacent positions to bulky substituents at peripheral places can promote an increase in the twisted angle of the substituent to the Pc core.

The vertical absorption energy predicted by the TD-DFT calculation and optical properties measured by UV-Vis spectrometer are described in Table 4.2. The calculated vertical absorption energy of the Q-bands of 1c-CuPc are similar to those of 1c-ZnPc. The 2c and the 3c dyes also show the same result. In addition, for the 1c and the 2c dyes that have plane structures, even though the peripheral positions of 2c dyes are fully substituted, the vertical absorption energy of the Q-band is analogous to that of 1c dyes. However, for 3c dyes with chlorines substituted at the non-peripheral position, vertical absorption energy is bathochromically shifted as the plane structure of their core deforms into a saddle structure. These results are like those of the experimentally measured properties, and in close agreement with those of our previous studies [15, 21, 22]. Hence, these findings indicate that not only the properties of the substituents introduced into the Pc but also the geometry of the Pc molecules would have a significant impact on the optical properties.

The effect of the structure of the Pc molecule was also confirmed by the oscillator strength as shown in Table 4.2. In the calculated results, the oscillator strength increases in the order 3c <1c <2c, and this order resembles the tendency

of the molar extinction coefficient values measured using UV-Vis spectrometer. In particular, the 3c dyes show the lowest oscillator strength and molar extinction coefficient. It is postulated that the inferior oscillator strength can be due to their molecular structures. Oscillator strength is determined by the transition dipole moment and depends on the degree of overlap between the molecular orbitals of the highest occupied molecular orbital (HOMO) and the lowest occupied molecular orbital (LUMO), where electron transition takes place [39, 40]. The more significant the orbital overlap of the HOMO-LUMO orbitals, the higher the probability of electron transition, thus increasing the oscillator strength [41]. In this process, the molecular structure can considerably affect the overlap of these orbitals. In this fashion, the declining of the oscillator strength of 3c dyes can be explained. Unlike 1c dyes and 2c dyes, 3c dyes have distorted structures, so the orbital overlap between HOMO and LUMO can be lowered.

Hence, the oscillator strength of 3c dyes can decrease. In other words, deforming the planar structure of the Pc molecule would be an effective method for red shifting the Q-band, but can have a detrimental effect on color strength.

Table 4.2. Experimentally measured (1×10^{-5} M in DMF) and calculated spectral properties of the prepared dyes.

Dye	Experimental		TD-DFT		
	λ_{max}[a]	ε_{max}[b]	λ_{max}	Transition	Oscillator strength
1c-CuPc	677 nm	116,250	614 nm 614 nm	H→L[c] H→L+1[c]	0.5885 0.5873
1c-ZnPc	678 nm	156,310	615 nm 615 nm	H→L H→L+1	0.6108 0.6097
2c-CuPc	678 nm	117,700	615 nm 615 nm	H→L H→L+1	0.6082 0.6064
2c-ZnPc	679 nm	159,250	616 nm 616 nm	H→L H→L+1	0.6316 0.6297
3c-CuPc	694 nm	88,280	654 nm 653 nm	H→L H→L+1	0.5745 0.5662
3c-ZnPc	695 nm	113,340	655 nm 654 nm	H→L H→L+1	0.5886 0.5988

[a]Absorption maximum wavelength of Q-band of dyes
[b]Molar extinction coefficient (L mol^{-1} cm^{-1})
[c]H: HOMO, L: LUMO, L+1: LUMO+1

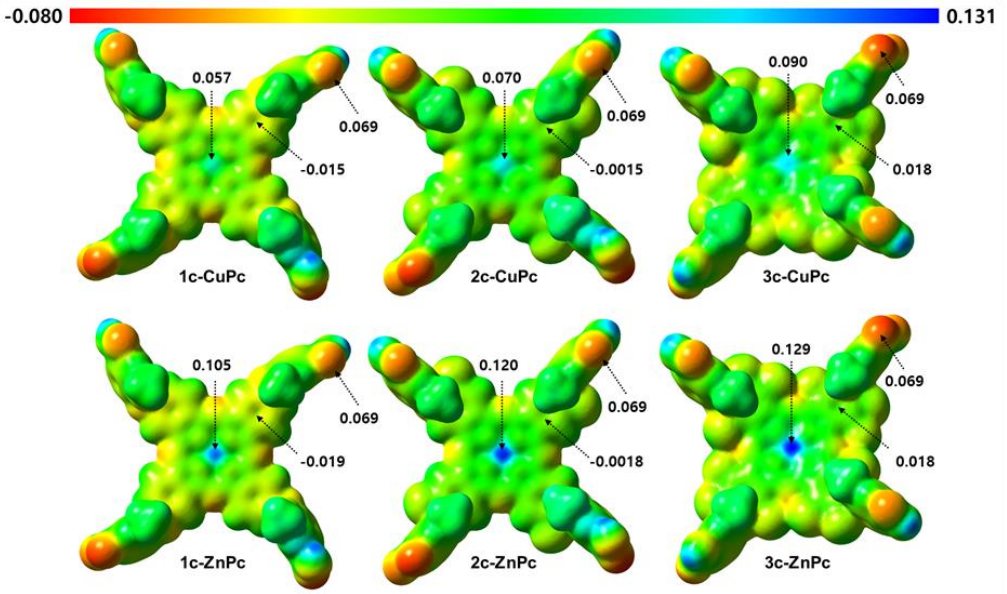

Figure 4.3. Electrostatic potential (ESP) surface maps of the prepared dyes.

All ZnPc dyes show a more positive charge on the center of the Pc than that of CuPc dyes. It seems likely that this difference is due to the higher electronegativity of Cu than Zn. Since the Cu of the central metal exhibits more negative electronegativity, it would withdraw the delocalized π electrons of the Pc core more strongly than Zn. Consequently, the electron cloud of π electrons would be further gathered in the center of the Pc molecule. These results indicate that chlorine-rich dyes and zinc Pc dyes can have higher electric polarizability [44].

4.3.3. Spectral properties of the dyes

Absorption spectra of Pc dyes were observed using a UV-Vis spectrometer, after the dyes were dissolved in DMF. The optical properties can be seen in Figs. 4.4, 4.5 and Table 4.1.

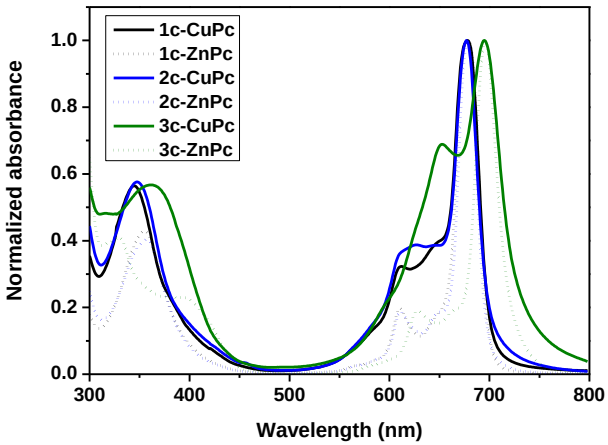

Figure 4.4. Normalized absorption spectra of the dye solutions dissolved in DMF (1×10^{-5} M).

As noted above, 1c dyes and 2c dyes show similar maximum absorption wavelengths of the Q-band. Our previous study has shown that the Q-bands of octa-benzoate substituted Pc, tetra-benzoate substituted Pc, and tetra-chloro tetra-benzoate substituted Pc were comparable [22]. These findings indicate that the addition of a substituent at the peripheral position of tetra-substituted Pc would provide a negligible shift of the Q-band, and that both chlorine and alkoxy groups would have an analogous force on the spectral properties of Pc. On the other hand,

3c dyes show a bathochromic-shifted maximum absorption wavelength of the Q-band of 16–18 nm. It is considered that this difference is owing to the molecular geometry of 3c dyes, as described above.

It should be noted that all CuPc dyes have a broader Q-band than all ZnPc dyes. Looking more closely at this, the CuPc dyes show higher absorbance with an aggregation peak around 620 nm, resulting in a broader Q-band. There are several possible explanations for such a result, one of which can be a strong intermolecular interaction. The change of the Q-band of the Pcs is explained by the following mechanism. In general, the stronger the intermolecular interaction such as π-π interaction, the higher the cohesiveness of Pc molecules [45]. Furthermore, the aggregation of these Pc molecules induces broadness and shifts of the Q-band. As the aggregate of Pc molecules grows more extensive, as in dimers, trimers, and tetramers, the excited energy states of the molecular orbital can be non-degenerate in Pcs, this effect results in a variety of electron transition [37]. In this process, the H-aggregate of Pc molecules induces hypsochromic-shift of the Q-band, and j-aggregation has the opposite effect [46]. The Q-bands of CuPc dyes seem to be affect in this way. Thus, it appears that the synthesized CuPc dyes have a higher aggregation order than ZnPc dyes. As far as is known, the aggregation order of metal Pc depends on various factors such as the solvent and substituents [47], so CuPc is not always higher in aggregate order than ZnPc.

However, in this study, it is observed that the prepared CuPc dyes exhibit higher intermolecular interaction than that of the ZnPc dyes.

The higher aggregation ability of CuPc dyes is also confirmed by the absorption spectra of the aggregates of the dyes in the mixture of DMF and aqueous 0.1 M HCl, as shown in Fig. 4.5. To measure the spectral properties of the aggregates of the synthesized dyes, aqueous 0.1 M HCl was gradually added after the dyes were dissolved in DMF. Fig. 4.5 shows that as the amount of aqueous 0.1 M HCl increases, the absorbance decreases, the Q-band broadens, and the maximum absorption wavelength of the Q-band is blue-shifted, for all dyes. In addition, this tendency is more pronounced in all CuPc dyes. The Q-bands of all CuPc dyes are more blue-shifted than those of all ZnPc dyes. These results further support our conjecture that the synthesized CuPc dyes show a higher aggregate order than ZnPc dyes [26, 33, 45].

The strong intermolecular interaction can be disadvantageous to the dispersion of dyes and the color properties of their solid states. Thus, among the synthesized dyes, ZnPc dyes are considered more appropriate for color filters.

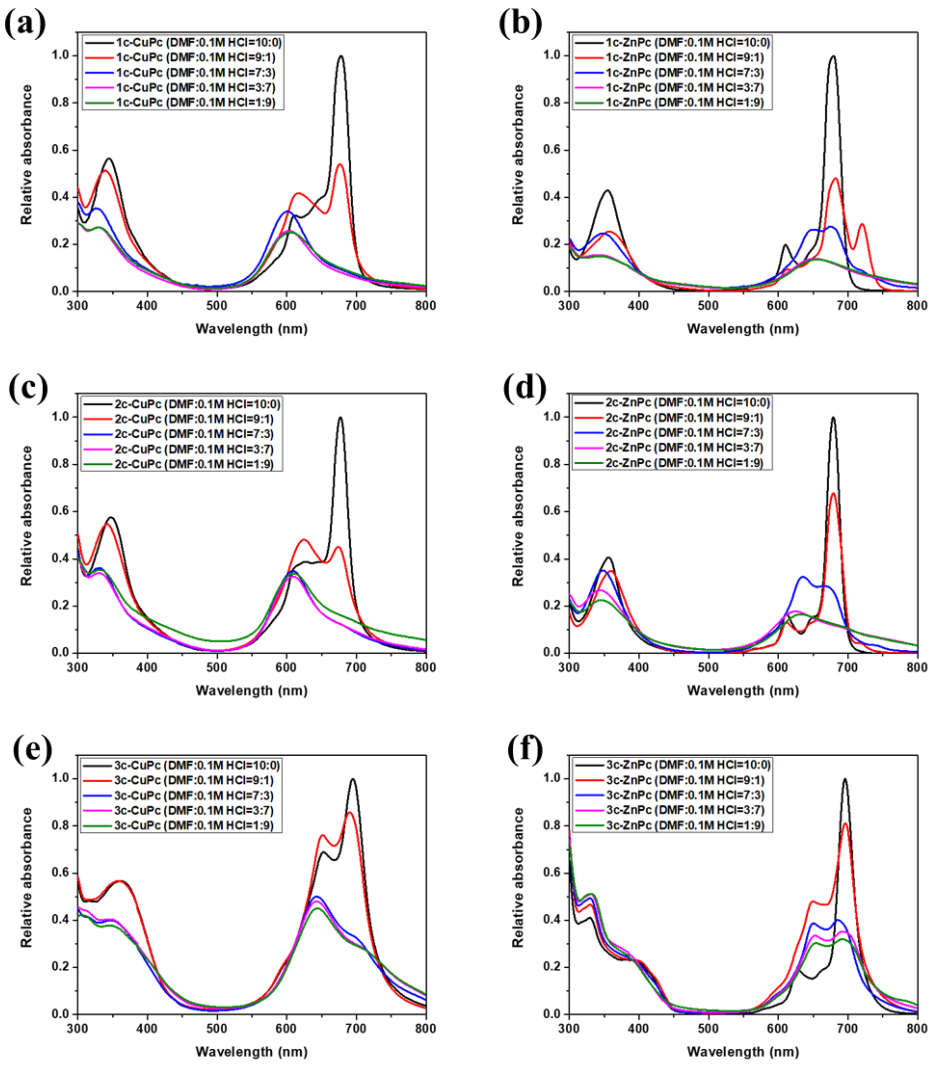

Figure 4.5. Absorption spectra of the dye solutions dissolved in DMF and aqueous 0.1M HCl (1×10^{-5} M). (a) 1c-CuPc; (b) 1c-ZnPc; (c) 2c-CuPc; (d) 2c-ZnPc; (e) 3c-CuPc; (f) 3c-ZnPc.

4.3.4. Thermal properties of the dyes

The thermal stability of the dyes and C.I pigment green 7 was measured using TGA before applying them to the color filter to confirm the heat resistance to the process temperature. Generally, the color filter is baked at 230 °C after development to remove residual solvent and cure the film. Thus, the weight loss of dyes was measured using TGA and examined under isothermal conditions at 230 °C for 30 min. Colorants can be applied to the color filter if weight loss is less than 5%. The results of TGA analysis can be seen in Fig. 4.6 and Table 4.3. A comparison of the dye and C.I. pigment green 7 was carried out along with the comparison of the properties of the dye.

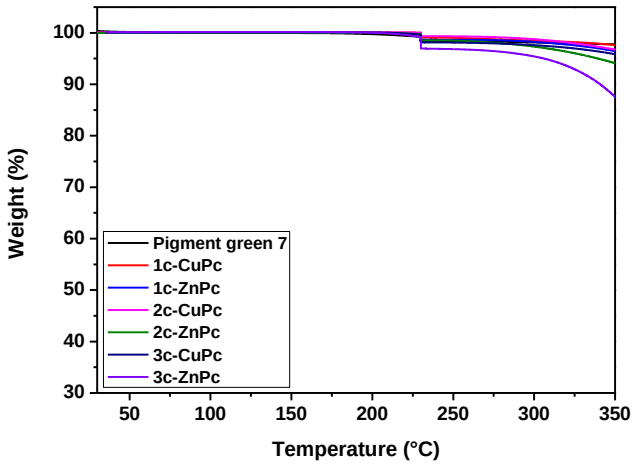

Figure 4.6. TGA analysis of the synthesized dyes. Dyes were heated to 230 °C and held at the temperature for 30 min, and then further heated to 350 °C.

Table 4.3. Weight loss (%) of the dyes in TGA.

Dye	Weight loss
C.I pigment green 7	0.78%
1c-CuPc	0.93%
1c-ZnPc	1.13%
2c-CuPc	0.95%
2c-ZnPc	1.20%
3c-CuPc	1.48%
3c-ZnPc	2.21%
3b-ZnPc	3.00%

All synthesized dyes have high thermal stability and weight loss of 2.5%. In general, except for 3b-ZnPc, CuPc dyes have less weight loss than ZnPc dyes. Moreover, 1c-CuPc and 2c-CuPc show superior thermal stability comparable to that of C.I. pigment green 7. However, the weight losses of the 3c dyes are relatively higher, and 3c-ZnPc indicates the highest weight loss of 2.21%. A point to nptice is that the decrease of thermal stability is proportional to the increase of the bulkiness of Pc molecules. The geometrical optimization results from Fig. 4.2 show that the 3c dyes have higher molecular bulkiness than the 1c and 2c dyes. As described in Section 4.3.3, the high bulkiness of a molecule would reduce intermolecular interactions thus inhibiting the aggregation of molecules. Hence, it can be inferred that the stronger the aggregation of molecules, the higher their

durability. The superior stability of CuPc dyes can be said to be due to their high aggregation ability[30].

This fact also can be illustrated by the weight loss of C.I. pigment green 7. C.I. pigment green 7, which has outstanding intermolecular forces, shows the lowest weight loss of 0.78% and indicates excellent thermal stability, whereas all dyes have higher weight losses of 0.93–2.21 wt%. Earlier studies also have demonstrated that a complex of Pc molecules exhibits superior heat and light stability than a monomer of a Pc molecule. In other words, as the aggregate order increases, the thermal stability would be enhanced.

Consequently, it is inferred that the bulkiness and thermal stability of the Pc molecules are in a trade off relationship. As a result, 3c dyes display a relatively low thermal stability. However, 3c dyes are also suitable as a colorant for the color filter because they experience a weight loss of less than 5%.

3c-ZnPc, which contains a benzoic acid moiety, shows lower weight loss than 3b-ZnPc with a benzoate moiety. This phenomenon could be the result of the formation of dimers through a strong hydrogen-bond interaction of carboxylic acid groups. Thus, it is assumed that in addition to the π-π stacking, the benzoic acid moiety also exhibits intermolecular interactions and enhances the dye stability.

4.3.5. Dispersion properties of the prepared dyes

The synthesized dyes and C.I. pigment green 7 were mixed with polymeric dispersants in PGMEA, and then the mixtures were dispersed by using a probe sonicator. Disperbyk LPN 6919 containing tertiary amine as the pigment-affinic group and disperbyk LPN 21116 containing both tertiary amine and quaternary ammonium as the pigment-affinic group were respectively applied as a polymeric dispersant, and the dispersion characteristics of the mixtures using each dispersant were compared.

It has previously reported that carboxylic acids can improve dispersion properties by forming hydrogen bonding with the amine groups of a dispersant [21]. In this study, it was further explored whether the quaternary ammonium moiety as a pigment affinic group could improve the dispersion of Pc derivatives bearing carboxylic acid as a dispersant anchoring group.

According to the dispersion properties described in Table 4.4, among the dispersions using the same dispersant, 1c-CuPc shows the largest average particle size, while 3c-ZnPc has the smallest. In comparing Pc dyes with the same central metal, 1c and 2c dyes have similar average particle sizes, and 3c dyes display the smallest average particle size. This tendency is analogous to the trend of the thermal stability discussed in Section 4.3.4. As the bulkiness of the molecules

increases, the size of dispersed particles decreases. This finding suggests that the dispersion properties would be improved by reducing the aggregate order, which is proportional to the intermolecular forces of the Pc derivatives [34]. Therefore, it is postulated that an inhibiting π-π stacking of Pc molecules is beneficial for the dispersion of particles. The results detailed in this section correspond with those found in the earlier studies in the enhancement of the solubility of Pc dyes in PGMEA.

A comparison of the dispersion properties of C.I. pigment green 7, CuPc dyes, and ZnPc dyes also provides evidence for our hypothesis. Among the colorants, C.I. pigment green 7 with the superior intermolecular stacking shows the largest average particle size, and CuPc dyes, which were believed to have higher aggregation ability than ZnPc dyes, exhibit a larger average particle size than that of ZnPc dyes. This result also indicates that superior aggregation forces induce inferior dispersion properties [48].

The difference in the intermolecular interactions also can be ascertained by X-ray powder diffraction analysis. The results are illustrated in Fig. 4.7, the measurement of all colorants was examined in their bulk states. Fig. 4.7 clearly indicates the difference in crystal structure between the synthesized dyes and C.I. pigment green 7.

Table 4.4. Dispersion properties of the prepared dyes.

Dye	Average Particle size	PDI[b]	Average Particle size after 168hr	Increment of particle size
With disperbyk LPN 6919				
Pigment[a]	154 nm	0.210	220 nm	66 nm
1c-CuPc	135 nm	0.191	197 nm	62 nm
1c-ZnPc	109 nm	0.179	164 nm	55 nm
2c-CuPc	126 nm	0.189	185 nm	59 nm
2c- ZnPc	101 nm	0.188	151 nm	50 nm
3c-CuPc	109 nm	0.178	169 nm	60 nm
3c- ZnPc	75 nm	0.165	120 nm	45 nm
With disperbyk LPN 21116				
Pigment[a]	145 nm	0.186	195 nm	50 nm
1c-CuPc	130 nm	0.182	187 nm	57 nm
1c-ZnPc	110 nm	0.167	141 nm	31 nm
2c-CuPc	127 nm	0.176	181 nm	54 nm
2c- ZnPc	103 nm	0.165	125 nm	30 nm
3c-CuPc	104 nm	0.168	144 nm	40 nm
3c- ZnPc	69 nm	0.154	79 nm	10 nm

[a]C.I Pigment green 7
[b]Polydispersity index

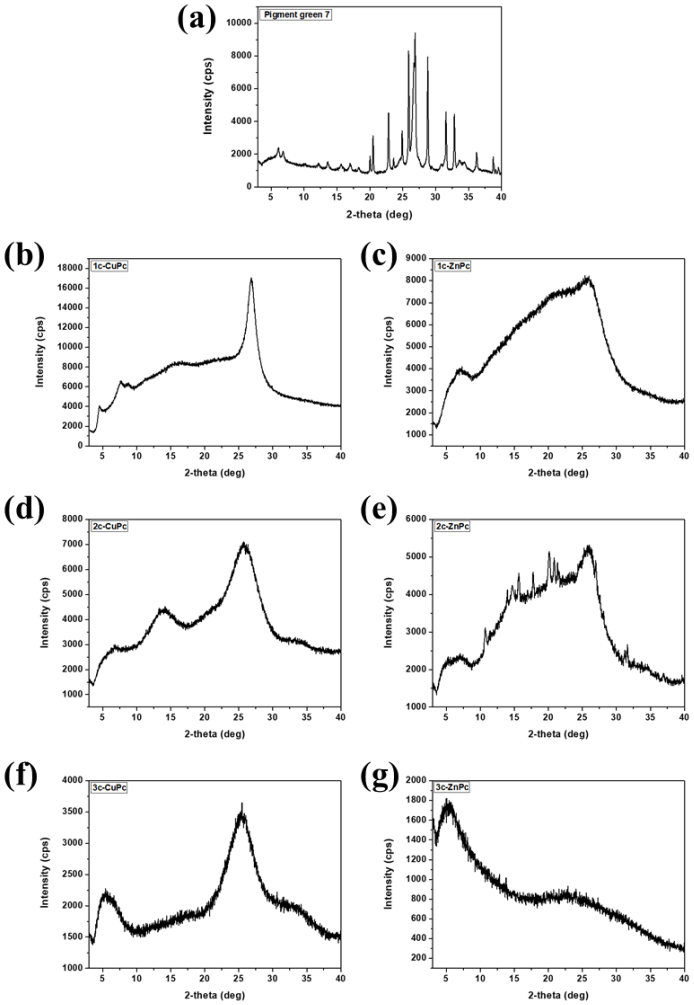

Figure 4.7. X-ray powder diffraction of the synthesized dyes. (a) C.I pigment green 7; (b) 1c-CuPc; (c) 1c-ZnPc; (d) 2c-CuPc; (e) 2c-ZnPc; (f) 3c-CuPc; (g) 3c-ZnPc.

C.I. pigment green 7 shows a polymorph crystal structure peak of sharp bandwidth and high intensity, whereas the dyes' results indicate an amorphous crystal structure pattern that is broad and weak [49]. In other words, C.I. pigment green 7 displays a strong ordered-stacking structure in spite of its bulk-state,

whereas the synthesized dyes show a disordered aggregate pattern. This fact, while preliminary, suggests that the molecules of C.I. pigment green 7 can be easily and closely packed because of its strong π-π interaction, while the stacking of the dyes is hindered by the bulky substituent and isomers they contain. Thus, it appears that the amorphous crystal structures can be created by the bulkiness of the Pc molecule and be increased by introducing the bulky substituents [50].

It was also showed that inhibiting of cohesion of the Pc molecules can also improve the dispersion stability. In Table 4.4, 3c dyes show the lowest re-agglomeration of particles among the dyes, whereas 1c-CuPc and 2c-CuPc (1c-ZnPc and 2c-ZnPc) dyes have similar tendency of re-agglomeration. This result is almost identical to that of the average particle size shown above.

However, the difference in the dispersion stability between ZnPc and CuPc dyes was observed. This consequence appears to be due not only to intermolecular interactions of Pc molecules but also to van der Waals forces with dispersants. For the dispersion of particles in organic solvents, it is difficult to stabilize particles by electrostatic stabilization methods such as electrostatic repulsion [51]. Therefore, the particles are stabilized by steric stabilization in organic-solvent dispersions. The dispersing agent is adsorbed to the particle surface by van der Waals forces such as hydrogen bonding and dipole-dipole interaction [34], so that the dispersed particles are protected by steric repulsion

of adsorbed dispersants. Therefore, the stronger the intermolecular interaction between dispersing agents and Pc molecules, the higher the dispersion stability of particles. According to the ESP surface map of the dyes in Fig. 4.3, all ZnPc dyes display a more significant positive charge in the center of molecules than that any of the CuPc dyes. Thus, the ZnPc molecules could form more powerful dipole-dipole interactions with pigment-affinic groups of dispersants such as amines with negative charges [52, 53]. Therefore, it is possible that ZnPc dyes interact with dispersant more strongly than CuPc dyes, resulting in higher dispersion stability.

Those VDW forces may also be induced on the isoindole ring of polychloro phthalocyanine [43, 54]. As described in the ESP surface map in Fig. 4.3, only 3c dyes show a positive value in the central sites of benzene in the isoindole ring. The positive center of the benzene ring of 3c dyes, thus, may interact with the lone pair of the amine pigment-affinic group, forming the lone pair···π-hole interaction. This intermolecular force may stabilize the dispersed particles. It can be assumed that this phenomenon also contributes to the superior dispersion stability of the 3c dyes. However, since the positive value is significantly smaller than that of the central site of the Pc, the interaction may have a minor impact.

Between the dispersions using disperbyk LPN 6919 and disperbyk LPN 21116, the latter displays better dispersion properties than the former. It seems likely that

the quaternary ammonium moiety would be an effective medium to adsorb on the particles of the dyes. This fact implies that the pigment-affinic groups of the disperbyk LPN 21116 interact more strongly with the carboxylic acid of the dispersion anchoring group. The ESP surface map shows that the carboxylic acid has the highest negative charge. Hence, it could be hypothesized that the negative carboxylic acid would interact actively with the positive quaternary ammonium moiety of the dispersant, so that the attractive interaction increases the stability of dispersed particles.

These findings demonstrate that 3c-ZnPc, which has a high bulkiness of molecule and a central metal of zinc, is suitable as a colorant for dispersed-dye-based color filters. It can be hypothesized that the tertiary amine part and quaternary ammonium part of disperbyk LPN 21116 interact with the isoindole ring and the carboxylic acid anchoring group, thereby improving the dispersion stability. Thus, disperbyk LPN 21116 is more effective than disperbyk LPN 6919 for the dispersion of the synthesized dyes.

4.3.6. Characterization of the spin-coated color filters

4.3.6.1. Spectral properties of the spin-coated color filters

Since 1c-ZnPc, 2c-ZnPc, and 3c-ZnPc indicated less aggregation ability and superior dispersion properties, the color filters were manufactured using those

dyes, and the pigment-based color filter was prepared using C.I pigment green 7. For the green color filter, they should have high transmittance at 500-540nm and maximum transmittance in the 510-520nm region.

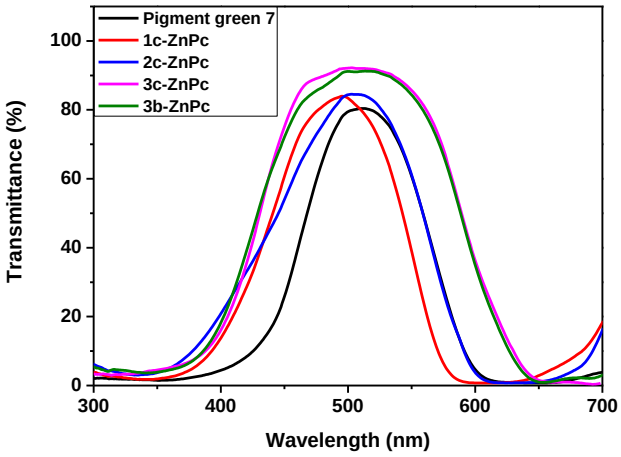

Figure 4.8. Transmittance spectra of the prepared color filters.

Fig. 4.8 and Table 4.5 present the spectral properties of the color filters. The maximum transmittance wavelengths are bathochromically-shifted in the order of 1c-ZnPc, 2c-ZnPc, and 3c-ZnPc. This spectral property can be interpreted as follows. 1c-ZnPc has a stronger re-agglomeration force in the film than 2c-ZnPc and 3c-ZnPc. The growth of particles would result in a blue-shift of the Q-band, and a diminishing of transmittance [45, 55]. In this process, 2c-ZnPc also shows inferior spectral properties compared to 3c-ZnPc. That is, as the substituents of the Pc molecule increase, the bulkiness of the molecules can rise, and the hypsochromic-shift of the Q-bands can be reduced by suppressing intermolecular

interactions in their solid-state. As a result, 3c-ZnPc shows the highest transmittance in the 480–540nm region. It is postulate that the superior transmittance of the color filter with 3c-ZnPc can be due to the superior dispersion properties resulting from the high bulkiness of the dye, a positive ESP charge of the central metal, and a strong intermolecular interaction between carboxylic acid of the Pc and pigment-affinic group of dispersant. Therefore, the aggregation between molecules is primarily limited by the bulk substituent and contorted structure of the dye, and the adsorbed dispersant then inhibits re-agglomeration in the film while inducing steric hindrance between the particles. Finally, the color properties of the color filter would be improved. Hence, it is assumed that the superior dispersion stability of 3c-ZnPc by strong intermolecular interaction between its anchoring group and the dispersant would be advantageous even in solid-state. It is also inferred this effect can prevent the migration of dyes in soluble-dye-based color filters, which has been pointed out in earlier studies. The fine particles of 3c-ZnPc in the films can be confirmed by the SEM images of the color filters. Fig. 4.9 shows the SEM images. Among the color filters, the color filter using 3c-ZnPc shows the most well-dispersed fine particles state in the film.

Table 4.5. Characterization of the prepared color filters.

Dye	Wavelength of T_{max}[b]	Transmittance	Thermal stability (ΔEab)	Thickness (μm)
Pigment[a]	512 nm	80.4%	1.02	2.51
1c-ZnPc	496 nm	83.9%	1.54	2.36
2c-ZnPc	504 nm	84.5%	1.62	2.26
3c-ZnPc	512 nm	92.0%	2.07	2.10
3b-ZnPc	513 nm	91.2%	2.89	2.11

[a]C.I pigment green 7
[b]Wavelength of maximum transmittance

In summary, the color filter using 3c-ZnPc shows the best spectral properties among the manufactured color filters. However, the transmission region of it is slightly broad for a green color filter, and it is necessary to lower its transmittance above 630 nm.

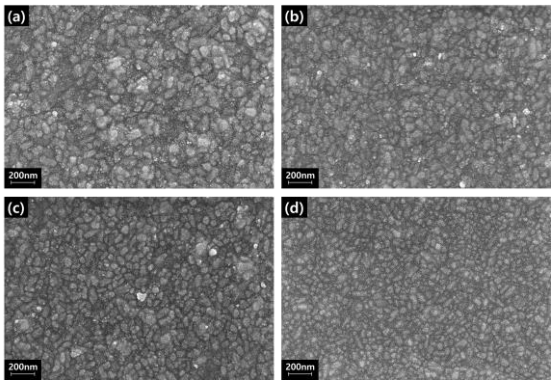

Figure 4.9. SEM images of the color filters. (a) C.I pigment green 7; (b) 1c-ZnPc; (c) 2c-ZnPc; (d) 3c-ZnPc.

4.3.6.2. Thermal properties and thickness of the spin-coated color filters

The heat fastness of the color filter was analyzed by color differential (ΔEab) before and after additional baking at the processing temperature. For this analysis, the fabricated color filter was further baked for 60 min at 230 °C after its initial baking at 230 °C. The color differential (ΔEab) must be less than 3 to be used for the color filter. The trend of heat resistance of the fabricated color filters is similar to the thermal stability (TGA) results of the dye, shown in Section 4.3.4. 3c-ZnPc which is considered to have the lowest molecule stacking, as the plane structure of the Pc core is deformed, shows the highest color difference value. However, it still indicates the proper heat resistance for use as the color filter.

Nevertheless, the color filter with 3c-ZnPc shows better heat resistance compared with a soluble-dye-based color filter using 3b-ZnPc. There are several possible explanations for such a result. First, as determined in the TGA analysis, the improvement of intermolecular interactions such as hydrogen bonding by the carboxylic acid of 3c-ZnPc would improve thermal stability of its particles. Second, the aggregate formation of 3c-ZnPc by dispersion also can enhance the durability of the dye. Lastly, the inhibition of re-agglomeration by steric stabilization of particles would suppress the migration of the dye, and thus the color filter with 3c-ZnPc exhibits higher stability than that of 3b-ZnPc. The

migration of dyes in the soluble-dye-based color filter reduces its colorfastness to the heat. As a result, 3c-ZnPc exhibits better heat resistance than 3b-ZnPc.

As shown in Table 4.5, the thickness of the manufactured color filters is reduced compared with C.I. pigment green 7. The color filter with 3c-ZnPc, particularly, shows a thickness 0.41μm lower than C.I. pigment green 7. It seems likely that this lower thickness is in fact due to the smaller particle size of 3c-ZnPc and the relatively better color properties resulting from its particle size. In general. the smaller the particle size in the film, the lower the volume of the film will be. In addition to this, the color strength is also related to the thickness of the film. In our previous study, it has reported that increasing the color strength of the colorant can reduce the thickness of its film [22]. The color properties of organic colorants are highly dependent on their particle size. In general, the smaller particle size, the stronger color strength [27]. In other words, the color strength of 3c-ZnPc would be stronger because the size of dispersed particles of the dye is smaller than that of C.I. pigment green 7, and thus this provides the dye higher tinctorial strength with fewer molecules. Hence, it is possible that 3c-ZnPc have superior color properties despite the presence of a smaller quantity of molecules, owing to the larger molecular weight of the dye, in the same wt% concentration. Therefore, the thickness of the color filter can be reduced by decreasing the number of colorant molecules present in the film. These results

match those mentioned in the earlier study of the fact that the dye-based color filter indicates lower film thicknesses than the pigment-based color filter in the same wt% concentration because the dye has better color strength.

The characteristics of the prepared color filters using 1c-ZnPc, 2c-ZnPc, and 3c-ZnPc dyes reveal that 3c-ZnPc, which has the best dispersion properties among the dyes, has superior color properties in its color filter. Moreover, all color filters show acceptable reliability of thermal stability ($\Delta Eab<3$).

4.4 Conclusion

In this study, six metal phthalocyanine dyes containing bulky benzoic acid groups and chlorine were synthesized and the dispersed-dye-based color filter was fabricated exhibiting superior optical and dispersion properties.

Among the dyes, all ZnPc dyes had lower aggregation tendency than CuPc dyes, and thus showed narrower bandwidth and higher absorbance of the Q-band. Polychloro zinc phthalocyanine derivative (3c-ZnPc) showed high bulkiness, electric polarizability of molecule, and the most red-shifted Q-band. X-ray powder diffraction also confirmed that C.I. pigment green 7 had polymorph closed packing structure while all dyes indicated amorphous crystal structures. In the TGA analysis, all synthesized dyes demonstrated thermal stability applicable to the color filter manufacturing process. For the dispersion of the dyes,

dispersants containing both tertiary amine and quaternary ammonium moiety were more effective in dispersing the synthesized dyes.

The results of these characterizations confirm that the high bulkiness of molecule, the amorphous crystal structure, and the attractive interactions with dispersant would reduce the size of dispersed particles and further stabilize them. Thus, 3c-ZnPc was able to achieve the smallest average particle size and superior dispersion stability.

Among the fabricated color filters, the color filter with 3c-ZnPc showed the highest transmittance, and exhibited stronger heat resistance compared with the color filter with soluble-dye. This result suggests that the polychloro zinc phthalocyanine derivative bearing carboxylic acid is appropriate for obtaining the well-dispersed fine particles for the color filter, and the dispersed-dye-based color filter would remedy the drawbacks of the soluble-dye and pigment-based color filters, thus improving of the bulkiness of the dye and enhancing dispersion properties.

In conclusion, it is investigated that the distortion of the core structure of the Pc molecule and introduction of a bulky acid moiety were effective in improving the dispersibility and dispersion stability of Pc dyes. It is also confirmed that the color filter using these well-dispersed fine particles provides better stability than the soluble-dye-based color filter, and superior color properties than the pigment-

based color filter. This paper presents the case that the dispersed-dye-based color filter can be a dye-based color filter capable of overcoming the disadvantages of the soluble-dye-based color filter while maintaining the advantages of the superior color properties of the dye.

However, the stability of the color filter using 3c-ZnPc was still lower than the pigment-based color filter and the transmittance spectra of the color filter was somewhat broad for the green color filter. Further studies for the development of Pc dyes to overcome these drawbacks should be undertaken.

4.5 References

[1] Sabnis RW. Color filter technology for liquid crystal displays. Displays. 1999;20(3):119-29.

[2] Freeman HS, Peters AT. Colorants for Non-Textile Applications: Elsevier Science, 2000.

[3] Herbst W, Hunger K. Industrial Organic Pigments: Production, Properties, Applications: Wiley, 2006.

[4] Sugiura T. A History of CFs Development for Color LCD. Journal of Printing Science and Technology. 1996;33(6):356-68.

[5] Kim YD, Kim JP, Kwon OS, Cho IH. The synthesis and application of thermally stable dyes for ink-jet printed LCD color filters. Dyes and Pigments.

2009;81(1):45-52.

[6] Kim YD, Cho JH, Park CR, Choi J-H, Yoon C, Kim JP. Synthesis, application and investigation of structure–thermal stability relationships of thermally stable water-soluble azo naphthalene dyes for LCD red color filters. Dyes and Pigments. 2011;89(1):1-8.

[7] Sakong C, Kim YD, Choi J-H, Yoon C, Kim JP. The synthesis of thermally-stable red dyes for LCD color filters and analysis of their aggregation and spectral properties. Dyes and Pigments. 2011;88(2):166-73.

[8] Choi J, Sakong C, Choi J-H, Yoon C, Kim JP. Synthesis and characterization of some perylene dyes for dye-based LCD color filters. Dyes and Pigments. 2011;90(1):82-8.

[9] Choi J, Kim SH, Lee W, Yoon C, Kim JP. Synthesis and characterization of thermally stable dyes with improved optical properties for dye-based LCD color filters. New Journal of Chemistry. 2012;36(3):812.

[10] Choi J, Lee W, Sakong C, Yuk SB, Park JS, Kim JP. Facile synthesis and characterization of novel coronene chromophores and their application to LCD color filters. Dyes and Pigments. 2012;94(1):34-9.

[11] Choi J, Lee W, Namgoong JW, Kim T-M, Kim JP. Synthesis and characterization of novel triazatetrabenzcorrole dyes for LCD color filter and black matrix. Dyes and Pigments. 2013;99(2):357-65.

[12] Lee J-Y, Kim J-H, Bae J-H, Yoon C, Kim J-P, Choi J-H. The Synthesis and Characterizations of Thermally-Stable Yellow Metal Complex Dyes for LCD Color Filters. Molecular Crystals and Liquid Crystals. 2013;583(1):60-9.

[13] Choi J, Kim SH, Lee W, Chang JB, Namgoong JW, Kim YH, et al. The influence of aggregation behavior of novel quinophthalone dyes on optical and thermal properties of LCD color filters. Dyes and Pigments. 2014;101:186-95.

[14] Kim JY, Choi J, Namgoong JW, Kim SH, Sakong C, Yuk SB, et al. Synthesis and characterization of novel perylene dyes with new substituents at terminal-position as colorants for LCD color filter. Journal of Inclusion Phenomena and Macrocyclic Chemistry. 2015;82(1-2):203-12.

[15] Kim SH, Namgoong JW, Yuk SB, Kim JY, Lee W, Yoon C, et al. Synthesis and characteristics of metal-phthalocyanines tetra-substituted at non-peripheral (α) or peripheral (β) positions, and their applications in LCD color filters. Journal of Inclusion Phenomena and Macrocyclic Chemistry. 2015;82(1-2):195-202.

[16] Park S, Park J, Lee S, Park J. New Dyes Based on Anthraquinone Derivatives for Color Filter Colorants. Journal of Nanoscience and Nanotechnology. 2014;14(8):6435-7.

[17] Muthukumar P, Kim H-S, Jeong JW, Son Y-A. Synthesis and characterization of tetra phenoxy-substituted halogen-rich metallophthalocyanine derivatives: A study on their LCD color filter

requirements. Journal of Molecular Structure. 2016;1119:325-31.

[18] Kim IJ, Palanisamy M, Jeong J, Son Y-A. Synthesis of octa-phenoxy substituted metallophthalocyanines and their green color filter application in liquid crystal display. Molecular Crystals and Liquid Crystals. 2017;644(1):88-97.

[19] Kim JY, Hwang TG, Kim SH, Namgoong JW, Kim JE, Sakong C, et al. Synthesis of high-soluble and non-fluorescent perylene derivatives and their effect on the contrast ratio of LCD color filters. Dyes and Pigments. 2017;136:836-45.

[20] Kong NS, Jung H, Kim B, Lee CK, Kong H, Jun K, et al. Development of dimeric triarylmethine derivatives with improved thermal and photo stability for color filters. Dyes and Pigments. 2017;144:242-8.

[21] Namgoong JW, Chung S-W, Jang H, Kim YH, Kwak MS, Kim JP. Improving nanoparticle dispersions of pigment and its application to a color filter: New phthalocyanine derivatives as synergist. Journal of Industrial and Engineering Chemistry. 2018;58:266-77.

[22] Namgoong JW, Kim SH, Chung S-W, Kim YH, Kwak MS, Kim JP. Aryloxy- and chloro-substituted zinc(II) phthalocyanine dyes: Synthesis, characterization, and application for reducing the thickness of color filters. Dyes and Pigments. 2018;154:128-36.

[23] Sugiura T. Dyed color filters for liquid-crystal displays. Journal of the Society for Information Display. 1993;1(2):177.

[24] Kalugasalam P, Ganesan S. Surface morphology of annealed lead phthalocyanine thin films. International journal of engineering science and technology. 2010;2(6):1773-9.

[25] Löbbert G. Phthalocyanines. Ullmann's Encyclopedia of Industrial Chemistry: Wiley-VCH Verlag GmbH & Co. KGaA; 2012. p. 181-213.

[26] Kobak RZU, Arı MU, Tekin A, Gül A. Aggregation behavior in unsymmetrically substituted metal-free phthalocyanines. Chemical Physics. 2015;448:91-7.

[27] Gueli AM, Bonfiglio G, Pasquale S, Troja SO. Effect of particle size on pigments colour. Color Research & Application. 2017;42(2):236-43.

[28] Müller M, Dinnebier RE, Jansen M, Wiedemann S, Plüg C. The influence of temperature, additives and polymorphic form on the kinetics of the phase transformations of copper phthalocyanine. Dyes and Pigments. 2010;85(3):152-61.

[29] Müller F, Peukert W, Polke R, Stenger F. Dispersing nanoparticles in liquids. International Journal of Mineral Processing. 2004;74:S31-S41.

[30] Kim JP, Kim JS, Park JS, Jang SS, Lee JJ. Synthesis of temporarily solubilised azo disperse dyes containing a β-sulphatoethylsulphonyl group and

dispersant-free dyeing of polyethylene terephthalate fabric. Coloration Technology. 2016;132(5):368-75.

[31] Yoon C, Kwon H-S, Yoo J-S, Lee H-Y, Bae J-H, Choi J-H. Preparation of thermally stable dyes derived from diketopyrrolopyrrole pigment by polymerisation with polyisocyanate binder. Coloration Technology. 2015;131(1):2-8.

[32] McDowell R. Particle size reduction of phthalocyanine blue pigment. Electronic Theses and Dissertations. 2006.

[33] Özçeşmeci İ, Tekin A, Gül A. Synthesis and aggregation behavior of zinc phthalocyanines substituted with bulky naphthoxy and phenylazonaphthoxy groups: An experimental and theoretical study. Synthetic Metals. 2014;189:100-10.

[34] Naito M, Yokoyama T, Hosokawa K, Nogi K. Characteristics and Behavior of Nanoparticles and Its Dispersion Systems. Nanoparticle Technology Handbook (Third Edition): Elsevier; 2018. p. 109-68.

[35] Auschra C, Eckstein E, Mühlebach A, Zink M-O, Rime F. Design of new pigment dispersants by controlled radical polymerization. Progress in Organic Coatings. 2002;45(2–3):83-93.

[36] Verdree VT, Pakhomov S, Su G, Allen MW, Countryman AC, Hammer RP, et al. Water soluble metallo-phthalocyanines: the role of the functional groups on

the spectral and photophysical properties. J Fluoresc. 2007;17(5):547-63.

[37] Gregory P. Industrial applications of phthalocyanines. Journal of Porphyrins and Phthalocyanines. 2000;04(04):432-7.

[38] Frisch MJ, Trucks GW, Schlegel HB, Scuseria GE, Robb MA, Cheeseman JR, et al. Gaussian 09, Revision E.01. Wallingford CT2009.

[39] Zeng W, Gong S, Zhong C, Yang C. Prediction of Oscillator Strength and Transition Dipole Moments with the Nuclear Ensemble Approach for Thermally Activated Delayed Fluorescence Emitters. The Journal of Physical Chemistry C. 2019;123(15):10081-6.

[40] Irie M, Yokoyama Y, Seki T. New Frontiers in Photochromism: Springer Japan, 2013.

[41] Corsini NR, Hine ND, Haynes PD, Molteni C. Unravelling the Roles of Size, Ligands, and Pressure in the Piezochromic Properties of CdS Nanocrystals. Nano Lett. 2017;17(2):1042-8.

[42] Egli M, Sarkhel S. Lone Pair−Aromatic Interactions: To Stabilize or Not to Stabilize. Accounts of Chemical Research. 2007;40(3):197-205.

[43] Liu JJ, Guan YF, Chen Y, Lin MJ, Huang CC, Dai WX. The impact of lone pair-pi interactions on photochromic properties in 1-D naphthalene diimide coordination networks. Dalton Trans. 2015;44(39):17312-7.

[44] Klyamer D, Sukhikh A, Gromilov S, Krasnov P, Basova T. Fluorinated

Metal Phthalocyanines: Interplay between Fluorination Degree, Films Orientation, and Ammonia Sensing Properties. Sensors (Basel). 2018;18(7).

[45] Bayda M, Dumoulin F, Hug GL, Koput J, Gorniak R, Wojcik A. Fluorescent H-aggregates of an asymmetrically substituted mono-amino Zn(ii) phthalocyanine. Dalton Trans. 2017;46(6):1914-26.

[46] Bächle F, Maichle-Mössmer C, Ziegler T. Helical Self-Assembly of Optically Active Glycoconjugated Phthalocyanine J-Aggregates. ChemPlusChem. 2019;84(8):1081-93.

[47] Bıyıklıoğlu Z, Çakır V, Çakır D, Kantekin H. Crown ether-substituted water soluble phthalocyanines and their aggregation, electrochemical studies. Journal of Organometallic Chemistry. 2014;749:18-25.

[48] Hughes DFK, Robb ID, Dowding PJ. Stability of Copper Phthalocyanine Dispersions in Organic Media. Langmuir. 1999;15(16):5227-31.

[49] Squires AD, Lewis RA. Terahertz Analysis of Phthalocyanine Pigments. Journal of Infrared, Millimeter, and Terahertz Waves. 2019;40(7):738-51.

[50] Denekamp IM, Veenstra FLP, Jungbacker P, Rothenberg G. A simple synthesis of symmetric phthalocyanines and their respective perfluoro and transition-metal complexes. Applied Organometallic Chemistry. 2019;33(5).

[51] Schofield JD. Extending the boundaries of dispersant technology. Progress in Organic Coatings. 2002;45(2-3):249-57.

[52] Ridhi R, Saini GSS, Tripathi SK. Study of interaction mechanism of metal phthalocyanines dispersed sol-gel glasses with chemical vapours. Sensors and Actuators B: Chemical. 2018;255:1849-68.

[53] Mooibroek TJ, Gamez P, Reedijk J. Lone pair–π interactions: a new supramolecular bond? CrystEngComm. 2008;10(11):1501-15.

[54] Wheeler SE, Seguin TJ, Guan Y, Doney AC. Noncovalent Interactions in Organocatalysis and the Prospect of Computational Catalyst Design. Acc Chem Res. 2016;49(5):1061-9.

[55] Jones FN, Nichols ME, Pappas SP. Effect of Pigments on Coating Properties. Organic Coatings: John Wiley & Sons, Inc.; 2017. p. 323-30.

Chapter 5

Synthesis and characterization of asymmetric polychloro phthalocyanine derivatives and preparation of their nanoparticle dispersions for a color filter

5.1 Introduction

Phthalocyanine (Pc) is one of the most durable organic materials in heat, light, and chemical stability [1]. Furthermore, in terms of coloration, the material exhibits vivid color in the range of blue and green [2]. Owing to its superior characteristics, dispersions of phthalocyanine (Pc) pigments are used as blue and green colorant in color filters for display devices and CMOS image sensors [3, 4].

However, the application of phthalocyanine (Pc) pigment to color filters has various disadvantages. Firstly, it has strong intermolecular interactions, such as π-π stacking due to the symmetry and rigidity of the molecular structure [5]. This strong interaction interferes with nanosized-pigment particle formation and

stabilization [6]. Secondly, the aggregate behavior of the phthalocyanine (Pc) pigment adversely affects the color characteristics of the color filter [2]. The strong π-π stacking of phthalocyanine (Pc) pigment widens the absorption band and reduces the absorbance, resulting in reducing the brightness and contrast ratio of the color filter [7-10]. Lastly, the durability and color characteristics of phthalocyanine (Pc) pigment are significantly affected by the crystal state and size of the particles [11]. For this reason, careful attention must be given to it from synthesis to mill-base manufacturing.

To address these drawbacks, several studies have been conducted to develop dyes for a soluble-dye-based color filter [12-25]. Our group has also reported various phthalocyanine (Pc) derivatives, which contain differing bulky substituents and have a deformed-core structure, for soluble-dye-based color filters [12, 17, 26]. These works have demonstrated that the dye can show a narrower absorption band and a higher molar extinction coefficient than the pigment, and it can be applied to color filters without complicated processes that use in the preparation of pigment. It has been also suggested that the dye decreases the film thickness due to its higher color strength than the pigment in our previous study [12]. As a result, the soluble-dye-based color filters have superior color characteristics than pigment-based color filters.

However, dyes have the disadvantage of lacking the durability required for color filters [27]. The color filter is cured at high temperatures (≥230°C) and washed in an organic solvent and a strong basic solvent during the manufacturing process. The baking is performed under severe conditions, particularly for a color filter for white-OLED display, to completely remove impurities that may contaminate the electroluminescent layer. Furthermore, the color filter is continuously exposed to light during its lifetime. In these processes, the dye should maintain its color properties ($\Delta Eab < 3$) and not be eluted in solvents. It is not common for dyes to have such heat, light, and chemical resistance [4]. Therefore, dye-based color filters exhibit excellent optical properties, whereas show low durability [12]. For this reason, the soluble-dye-based color filters are not currently applied to devices.

To overcome shortcomings of the soluble-dye-based color filter, it has presented a dispersed-dye-based color filter in a previous study. The result of our efforts confirmed that the application of dye dispersions rather than the solution of dyes improves the durability while sustaining superior color properties of the dyes.

In previous works, phthalocyanine (Pc) derivatives containing a carboxylic acid group were prepared for a dispersed-dye-based green color filter and the color filters were manufactured using dispersions [26]. This investigation

demonstrated that a polychloro zinc phthalocyanine (Pc) derivate with an acid dispersant anchoring group can form superior dispersions owing to its high bulkiness and high degree of intermolecular interaction with a dispersant. It is also indicated that the dispersed-dye-based color filter has superior color properties and heat resistance compared to soluble-dye-based color filters.

However, the reported color filter still had lower durability than the pigment-based color filter and showed undue transmission regions for use in the green color filter. Therefore, the current study was conducted to improve the durability and spectral properties of the dispersed-dye-based green color filter. In the previous work, bulky substituents were adopted to improve the dispersion of phthalocyanine (Pc) molecules. However, it seems likely that durability has not increased as intended due to its excessive bulkiness. Thus, it was inferred that inducing the appropriate level of aggregate order of the phthalocyanine (Pc) dye by reducing its bulkiness could improve the durability of the dye [28]. In addition, it was postulated that increasing the aggregate order can also broaden the Q-band of the phthalocyanine (Pc) molecule, leading to a narrowing of the transmission region of the color filter [29, 30]. Thus, this approach is expected to improve both the color characteristics and the durability of the color filter [31].

There are several ways to regulate the aggregation of phthalocyanine (Pc) derivatives [32]. Here this work presents a way to control aggregate order by

fine-tuning the bulkiness of the molecules. The aggregation force of the phthalocyanine (Pc) molecule was adjusted by changing the number of functional groups contained in polychloro phthalocyanine (Pc) and was intended to improve the durability and spectral property of the color filter [33]. This method fixes the kind of functional group substituted and does not significantly change the molecular structure of the polychloro phthalocyanine (Pc). Therefore, it was expected to be able to finely adjust the bulkiness of the molecule, resulting in the acquisition of phthalocyanine (Pc) dyes with various aggregation orders [34]. It was also expected that, if the number of bulky substituents on a phthalocyanine (Pc) molecule is reduced, not only the would the aggregate ability of the phthalocyanine (Pc) molecule increase, but also that defects (which are decomposed by external energy, i.e. heat and light) would be reduced. Hence, it was inferred that the durability of phthalocyanine (Pc) dyes would be improved [35]. However, it also can be supposed that due to the reduction of the functional group, the suppression of intermolecular interaction and anchoring force with the dispersant is reduced. This action would increase the π-π stacking of phthalocyanine (Pc), which can reduce dispersibility of it [36]. Therefore, it is important to properly control the bulkiness and cohesion of the molecules. To the best of our knowledge, there are few studies applying this method of dye dispersions to color filters.

For this purpose, polychloro phthalocyanine (Pc) derivatives, which contain one(mono-substituted), two(di-substituted), and four(tetra-substituted) dispersant anchoring groups at peripheral positions and optimized their dispersions, were synthesized. The features of the dyes and dispersibility were then compared with each other. C.I pigment green 7, which is currently used as a green colorant for color filters, was also adopted for comparison.

The prepared dyes and the dye dispersions were characterized by computational quantum mechanical modelling, UV-Vis spectroscopy, thermogravimetric analysis, and dynamic light scattering. The dispersed-dye-based color filters were prepared using the dye dispersions, and their spectral properties, thermal stability, light stability, surface property, and thicknesses were measured.

5.2 Experimental

5.2.1. Materials

3,4,5,6-tetrachlorophthalonithrile, and ethyl 4-hydroxy-3-methoxybenzoate, C.I pigment green 7 were purchased from Tokyo Chemical Industry (TCI). Urea, ammonium molybdate, zinc chloride, lithium hydroxide monohydrate, and 1,2,4-trichlorobenzene, methyl methacrylic acid, benzyl methacrylate were purchased

from Sigma-Aldrich. 2 2'-azobis(isobutyronitrile) was obtained from Junsei Chemical. All the other reagents and solvents were of reagent-grade and obtained from commercial suppliers. All chemicals were reagent-grade. Transparent glass substrates were manufactured by Asahi Glass Co Ltd. Polymeric dispersants (Disperbyk LPN 6919, 21116) were acquired from BYK-Chemie.

5.2.2. Characterization and instruments

^{1}H NMR spectra were measured on a Bruker Avance 500 spectrometer (National Center for Inter-University Research Facilities at Seoul National University) at 500MHz using dimethyl sulfoxide-d6 and chloroform-d as the solvent. Tetramethylsilane (TMS) was used as an internal standard. Elemental analysis was conducted with a Thermo Scientific Flash EA 1112 elemental analyzer. Matrix-Assisted Laser Desorption/Ionization-Time of Flight (MALDI-TOF) mass spectra were collected on a Voyager-DE STR Biospectrometry Workstation (National Center for Inter-University Research Facilities at Seoul National University) with α-cyano-4-hydroxy-cynamic acid (CHCA) as the matrix. UV-Vis absorption spectra were recorded using a Lambda 25 spectrophotometer (PerkinElmer). Thermogravimetric analysis (TGA) was performed in nitrogen atmosphere at a heating rate of 10°C/min using a Thermogravimetric Analyzer 2050 (TA Instruments). The thickness of the spin-

coated color filter was measured using a Alpha step (KLA-TENCOR Nanospec AFT/200). The optical properties of the color filters were measured on a color spectrophotometer (Scinco). The particle size analysis was performed using a Litesizer 500 (Anton Paa), samples were prepared by diluting the dispersion with PGMEA (0.1 wt.%). Field-emission scanning electronic microscopy (FE-SEM) images were acquired on a MERLIN Compact (Zeiss); Pt was coated on the samples using MSC-101 (JEOL) for 40 secs at a current strength of 40 mA to avoid charging of the surface. The power XRD of the dye particles was examined using a SmartLab (Rigaku) with Cu-Kα X-rays (1.5406 Å); data was recorded for the 2θ range of 3° to 40°.

5.2.3. Synthesis

5.2.3.1. Synthesis of compound 1 (ethyl 3-methoxy-4-(2,3,6-trichloro-4,5-dicyanophenoxy)benzoate)

A synthesis of ethyl 3-methoxy-4-(2,3,6-trichloro-4,5-dicyanophenoxy)benzoate was refers to our previous study[12]. 3,4,5,6-tetrachlorophthalonitrile (1 g, 3.76 mmol), and ethyl 4-hydroxy-3-methoxybenzoate (0.74 g, 3.76 mmol) were dissolved in dry DMF (30 ml). The temperature of the mixture was heated to 80 °C with stirring. Anhydrous K_2CO_3 (0.78 g, 5.64 mmol) was then added portionwise to the solution. The mixture was heated for 5 h. All procedures were performed under nitrogen atmosphere. The

solution was then poured into ice water (100 mL) with vigorous stirring. The resulting suspension filtered to give a white-yellowish powder. The crude product was purified by column chromatography on silica gel using toluene as an eluent. The pure product was finally collected by recrystallization using a mixture of methylene chloride/methanol. Yield 76%; ^{1}H NMR (d6-DMSO, 500 MHz, 25 °C): δ 7.69 (d, J=2 Hz, 1H, Ar-H), 7.49 (dd, J=8.5, 2 Hz, 1H, Ar-H), 6.84 (d, J = 8.5 Hz, 1H, Ar-H), 4.29 (q, J = 6.5 Hz, 2H, CH_2CH_3), 3.91 (s, 3H, OCH_3), 1.31 (t, J=7 Hz, 3H, CH_2CH_3). Elemental analysis: Calcd for $C_{18}H_{11}Cl_3N_2O_4$: C, 50.79; H, 2.60; N, 6.58; O, 15.04 %. Found: C, 49.18; H, 2.74; N, 7.43; O, 16.41.

5.2.3.2. Synthesis of compound 2a (pentadecachloro(4-(ethoxycarbonyl)-2-methoxyphenoxy)phthalocyaninato zinc (II))

Compound 1 (1.61 g, 5.00 mmol), 3,4,5,6-tetrachlorophthalonitrile (13.30 g, 50 mmol), urea (6.00 g), and $ZnCl_2$ (2.49 g, 18.33 mmol) were mixed in 1,2,4-trichlorobenzene (50mL), followed by heating to 150 °C. Ammonium molybdate (0.19 g, 1.00 mmol) was then added to the solution. The mixture was stirred for 5h under nitrogen atmosphere. After cooling the mixture, filtration was performd to remove insoluble impurities. The filtrate was then evaporated under reduced pressure. The crude product was dissolved in methylene chloride (50mL), and precipitated by pouring into methanol (500mL). The resultant precipitates were

separated with vacuum filtration. The solid cake dried at 50°C in vacuo. The solid was roughly purified using flash column chromatography with methylene chloride. The resultant product was then concentrated, loaded again onto a silica gel column with a 20:1 mixture of methylene chloride/methanol. The obtained green solid was recrystallized with a mixture of methylene chloride/methanol to afford compound 2a. Yield 8%; MALDI-TOF MS: m/z 1289.15 (100%, $[M + H]^+$). Elemental analysis: Calcd for $C_{42}H_{11}Cl_{15}N_8O_4Zn$: C, 39.14; H, 0.86; N, 8.70; O, 4.97 %. Found: C, 39.01; H, 0.99; N, 8.78; O, 5.28.

5.2.3.3. Synthesis of compound 2b (tetradecachloro-di(4-(ethoxycarbonyl)-2-methoxyphenoxy)phthalocyaninato zinc (II))

2b was synthesized following the same procedure for 1b using compound 1 (1.61 g, 5.00 mmol), 3,4,5,6-tetrachlorophthalonitrile (6.65 g, 25 mmol), urea (6.00 g), and ZnCl2 (1.16 g, 8.50 mmol) ammonium molybdate (0.19 g, 1.00 mmol), in 1,2,4-trichlorobenzene (50mL). Yield 9%; MALDI-TOF MS: m/z 1443.81 (100%, $[M]^+$). Elemental analysis: Calcd for $C_{52}H_{22}Cl_{14}N_8O_8Zn$: C, 43.12; H, 1.53; N, 7.74; O, 8.84 %. Found: C, 42.99; H, 1.63; N, 7.81; O, 9.48.

5.2.3.4. Synthesis of compound 2c (1, 2, 4, 8, 9(10), 11, 15, 16(17), 18, 22, 23(24), 25-dodecachloro-3,9(10),16(17),23(24)-tetra(4-(ethoxycarbonyl)-2-methoxyphenoxy)phthalocyaninato zinc

(II))

Compound 2c was synthesized following the same procedure for 1c using compound 1 (1.61 g, 5.00 mmol), urea (1.00 g), and $ZnCl_2$ (0.22 g, 1.65 mmol) ammonium molybdate (0.19 g, 1.00 mmol), in 1,2,4-trichlorobenzene (50mL). Column chromatography with stepwise gradient elution (chloroform to 20% methanol/chloroform) was performed to obtain the product. The green solid product was finally collected by recrystallization using a mixture of methylene chloride/methanol. Yield 54%; MALDI-TOF MS: m/z 1767.2 (100%, $[M + H]^+$). Elemental analysis: Calcd for $C_{72}H_{44}Cl_{12}N_8O_{16}Zn$: C, 48.91; H, 2.51; N, 6.34; O, 14.48 %. Found: C, 48.84; H, 2.68; N, 6.48; O, 16.12 %.

5.2.3.5. Synthesis of compound 3a (pentadecachloro(4-carboxy-2-methoxyphenoxy)phthalocyaninato zinc (II))

A synthesis of compound 3a was refers to the literature procedures [26]. 2a was dissolved in THF (100mL). A saturated solution (100mL) of lithium hydroxide monohydrate in a mixture of water/methanol (3:7) was then dropwise added to the 2a solution. The mixture was stirred at 80°C for 12h under nitrogen atmosphere. After cooling the mixture, the organic solvents were evaporated under reduced pressure. The aqueous solution of the crude product was washed using methylene chloride and ethyl acetate, followed by acidification with 1M HCl to precipitate the product. The resulting suspension filtered to give a green

solid. The solid cake was dried in vacuo and recrystallized with a mixture of dimethylformamide and methanol to obtain the pure product. Yield 45%; MALDI-TOF MS: m/z 1280.14 (100%, $[M + Na]^+$). Elemental analysis: Calcd for $C_{40}H_7Cl_{15}N_8O_4Zn$: C, 38.11; H, 0.56; N, 8.89; O, 5.08 %. Found: C, 37.99; H, 0.64; N, 8.97; O, 5.56.

5.2.3.6. Synthesis of compound 3b (tetradecachloro-di(4-carboxy-2-methoxyphenoxy)phthalocyaninato zinc (II))

Compound 3b was synthesized following the same procedure for 3a using 2b. Yield 49%; MALDI-TOF MS: m/z 1413.51 (100%, $[M + Na]^+$). Elemental analysis: Calcd for $C_{48}H_{14}Cl_{14}N_8O_8Zn$: C, 41.41; H, 1.01; N, 8.05; O, 9.19 %. Found: C, 41.21; H, 1.04; N, 8.17; O, 9.58 %.

5.2.3.7. Synthesis of compound 3c (1, 2, 4, 8, 9(10), 11, 15, 16(17), 18, 22, 23(24), 25-dodecachloro-3,9(10),16(17),23(24)-tetra(4-carboxy-2-methoxyphenoxy)phthalocyaninato zinc (II))

Compound 3c was synthesized following the same procedure for 3a using 2c. Yield 43%; MALDI-TOF MS: m/z 1652.63 (100%, $[M + H]^+$). Elemental analysis: Calcd for $C_{64}H_{28}Cl_{12}N_8O_{16}Zn$: C, 46.43; H, 1.70; N, 6.77; O, 15.46 %. Found: C, 46.03; H, 1.81; N, 6.79; O, 16.11 %.

5.2.4. Preparation of a polymeric binder

A polymeric binder was obtained by a polymerization of methyl methacrylic acid (MAA) and benzyl methacrylate (BzMA). The polymerization was referred to the literature procedures [8]. Propylene glycol methyl ether acetate (PGMEA) was pre-heated at 100°C for 60min under nitrogen purging to expel oxygen. The solvent was cooled down to room temperature, 1g of 2 2'-azobis(isobutyronitrile) (AIBN) was then dissolved in a small amount of the solvent. Methyl methacrylic acid (3.44 g, 40 mmol) and benzyl methacrylate (16.56 g, 94 mmol) were mixed in 40.0g of the same solvent, and the solution was stirred for 30min under nitrogen purging to eject oxygen. The monomers were polymerized at 90°C for 5hr; the AIBN solution was added dropwise to the monomer solution during the polymerization. The product of poly (BzMA-MAA) (Fig.1) was obtained with a polymer content of 39%. The molecular weight of the polymer was examined by GPC analysis, indicated that Mn was 8,582 and Mw was 15,449. The polymer solution was adopted as a binder solution without further isolation of the polymer.

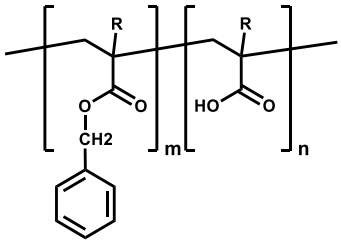

Figure 5.1. Structure of a polymeric binder. (m=7, n=3)

5.2.5. Preparation of dispersions

Dyes (0.80 g) and pigment green 7 (0.80 g) were mixed with a dispersant polymer (0.48 g) in propylene glycol methyl ether acetate (8.72 g), respectively. A pre-mixing was performed using a shaker. After pre-mixing, mixtures were dispersed using a probe sonicator at 20kHz (VCX 500, Sonics) in an ice bath; a dispersion was performed for 60min on pulse mode (10s on, 5s off).

5.2.6. Preparation of color inks and spin-coated films

Color inks for a color filter was composed of the propylene glycol methyl ether acetate (PGMEA) (0.30 g), acrylic binder (2.20 g), a dispersion (1.50 g). The prepared inks were coated on a transparent glass substrate using a MIDAS System SPIN-1200D spin coater. The spin-coated color filters were pre-baked at 100°C for 100 s and post-baked at 230°C for 30 min. After post-baking, the coordinate values of the color filters were examined.

5.2.7. Measurement of spectral and chromatic properties

Absorption spectra of the synthesized dyes and transmittance spectra of prepared color filters and pigment-based color filters were analyzed using a PerkinElmer Lambda 25 UV-vis spectrophotometer. Chromatic values were obtained by a Scinco colormate color spectrophotometer.

5.2.8. Measurement of thermal stability

Thermal stability of the synthesized dyes and C.I pigment green 7 was characterized by thermalgravimetric analysis. The colorants were heated to 230°C and held at the temperature for 30 min to simulate the color filter manufacturing thermal condition. The colorants were finally heated to 350°C to test their degradation temperature. The temperature was raised at the rate of 10 °C/ min under nitrogen atmosphere. To determin the thermal stability of the color filters, they were heated to 230°C and held at the temperature for 30 min in forced convection oven. The color difference values (ΔEab) before and after heating were measured using Scinco colormate color spectrophotometer in CIE L'a'b' mode.

5.2.9. Measurement of light stability

To determin the light stability of the color filters, they were exposed under a xenon lamp (350 W) for 30 h at room temperature. The color difference values (ΔEab) before and after exposure were measured using Scinco colormate color spectrophotometer in CIE L'a'b' mode.

5.3 Results and discussion

5.3.1. Design and synthesis of the dyes

For good dispersibility of phthalocyanine (Pc) in organic solvents, functional groups capable of anchoring the dispersant to the Pc molecule are required [37]. In our previous study, it was confirmed that a benzoic acid derivative has excellent performance as a dispersant anchoring group [26], and the chlorine-rich zinc Pc with this dispersant anchoring group has superior dispersion properties. Therefore, in this study, 4-hydroxy-3-methoxy benzoic acid was introduced as the anchoring group. This benzoic acid moiety was substituted at the peripheral position of polychloro zinc Pc. The number of the functional group contained in the Pc molecule was varied to control the dispersibility and the durability of the dyes. As the number of bulky substituents decreases, steric repulsion between Pc molecules can be reduced [33]. It was supposed that the diminution of the molecular repulsion could increase the likelihood of aggregation of the Pc molecules, and the dispersibility of particles could decline. This rise in intermolecular forces could have a good effect on the durability of a solid-state film but negatively impact the color properties of it. Therefore, it is important to design the synthesized Pc molecule to have optimal bulkiness and balanced effects.

Mono-substituted polychloro zinc Pc (mono-substituted Pc), di-substituted polychloro zinc Pc (di-substituted Pc), and tetra-substituted polychloro zinc Pc (tetra-substituted Pc) with different bulkiness were designed. Using this method, it is possible to take advantage of the deformed structure of polychloro Pc to achieve a certain level of bulkiness inherent in the molecules. Moreover, irregular changes in the bulkiness of molecules can be prevented by focusing on a particular kind of a functional group.

The general synthesis method of the dyes is as follows. To synthesize zinc Pc dyes, trichlorophthalonitrile with ethyl 4-Hydroxy-3-methoxybenzoate was synthesized and subjected to cyclotetramerization. Subsequently, polychloro zinc Pc containing benzoic acid was finally obtained by hydrolysis of the benzoate group of the products. The synthesis process is shown in scheme 5.1.

There are various ways to synthesize asymmetric Pc [38, 39]. Among them, the cyclotetramerization method via the equivalent control of precursors and sub-phthalocyanine method are widely used. However, the sub-phthalocyanine method has limited application because the reaction control is difficult, and the reactivity depends on the structure of phthalonitrile [32, 40]. Therefore, zinc Pc was synthesized using the former. The synthesized zinc Pcs were purified by filtration, recrystallization, and column chromatography. The constituent isomers of the products were not further separated.

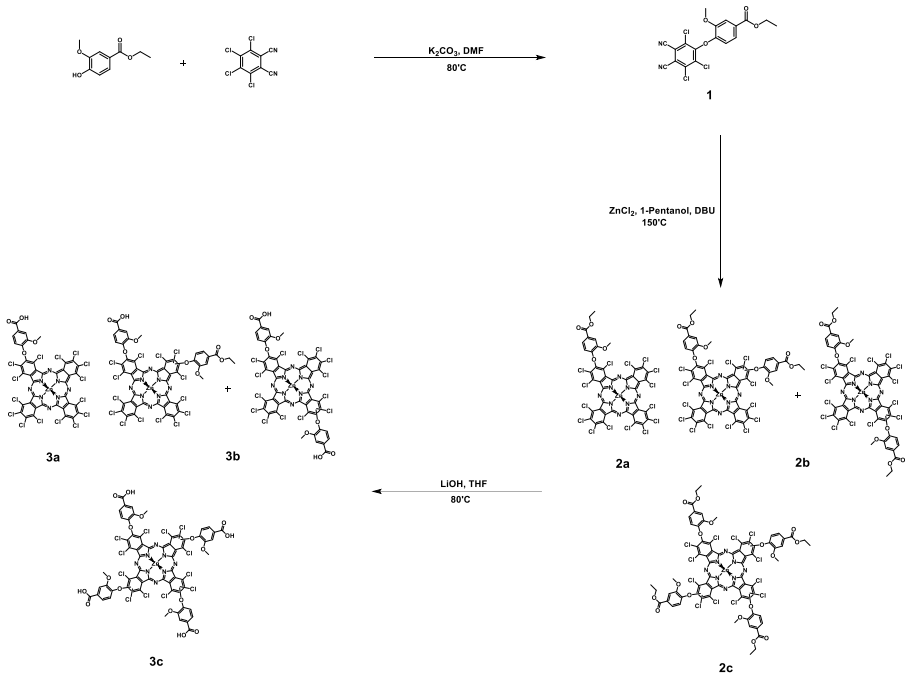

Scheme 5.1. Synthesis procedure of the designed dyes

5.3.2. Geometry optimization, electrostatic potential (ESP) surface, and TD-DFT calculations

In order to determine the optimized structure, the electrostatic potential (ESP) surface map, and the excited state transition, the dyes were subjected to density functional theory (DFT) and time-dependent (TD)-DFT calculations using Gaussian 09[41] (B3LYP with 6-311G (d)). The calculated result is shown in Fig. 2, Fig. 3, Table 5.1, and Table 5.2.

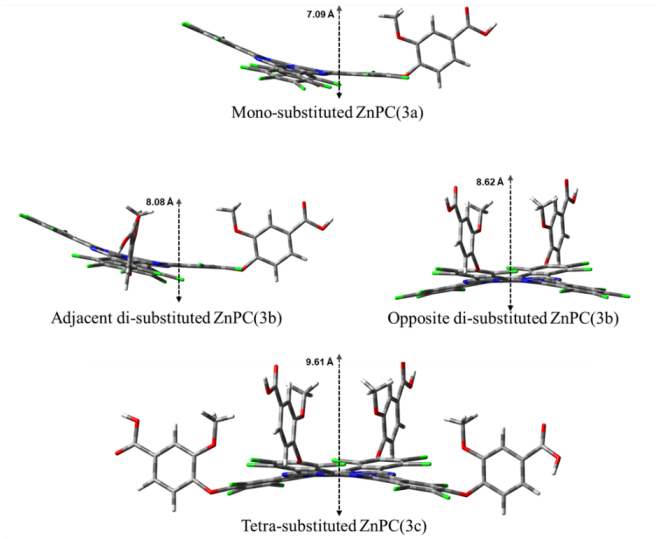

Figure 5.2. Geometry optimized structures of the dyes. (DFT calculation on B3LYP with 6-311G (d))

Table 5.1. Geometry optimized structures (twisted angles of the plane of benzoic acid substituents to the Pcs' isoindole ring plane, tortion angles of Pc core, and vertical bulkiness (Å) of the dyes) and ESP surface charges of the dyes.

Dye	Twisted angle[a]	Tortion angle[b]	Vertical bulkiness	ESP surface charges (a.u)	
				Center[c]	π-hole[d]
3a	82.25°	15.45°	7.090 Å	0.134	0.024
Adjacent-3b	82.42°	15.83°	8.085 Å	0.130	0.022
Opposite-3b	81.89°	15.79°	8.614 Å	0.130	0.022
3c	83.30°	16.33°	9.614 Å	0.129	0.020

[a]Twisted angles of the plane of benzoic acid substituents to the Pcs' isoindole ring plane
[b]Tortion angles of Pc core
[c]Central site of Pcs
[d]Center of bezene ring of isoindole ring

For the optimized structures of the dyes in Fig. 5.2, the twisted angles of all dyes between the isoindole ring plane of Pc and the phenyl plane of benzoic acid moiety are close to vertical (82-84°). It can be also seen that all dyes have a saddle structure, which is a distorted core structure of Pc. The formation of the deformed structure in polychloro zinc Pc has been confirmed in our previous works [12, 42]. These bulky molecular structures of the dyes could have the following explanation. The synthesized dyes have chlorines at the non-peripheral positions of the isoindole rings. The substituents in those positions of the Pc would cause repulsion between nearby atoms because the distance between non-peripheral positions is quite close. Therefore, these interaction forces can lead to distortion of the Pc core due to the steric effect, which forms a saddle-like structure.

In this situation, the torsion angle of the core structure has the smallest value for mono-substituted Pc, and the value increases with the number of benzoic acid substituents which are introduced to peripheral positions. This result suggests that not only the substituents at the non-peripheral positions but also the bulky substituents in the peripheral positions can affect the core structure of the Pc molecule.

In terms of the vertical bulkiness of the Pc dyes in Table 5.1, mono-substituted Pc shows the lowest value, and tetra-substituted Pc indicates the highest value. This tendency similar to that of the torsion angle of Pc core. It appears that the

decrease in the bulkiness owes to the elimination of bulky substituents of the dyes. As shown in Fig. 5.2, the mono-substituted Pc has a benzoic acid moiety in one of the four isoindole rings, so the steric hindrance is reduced on the opposite side. A similar phenomenon is observed for the adjacent di-substituted Pc. In contrast, tetra-substituted Pc contains the bulky substituent on all four isoindole rings, resulting in steric hindrance in all directions. As a result, the bulkiness declines in the order of the tetra-substituted Pc > opposite di-substituted Pc > adjacent di-substituted Pc > mono-substituted Pc. This result demonstrates that our approach can finely control the bulkiness of Pc, as intended. Thus, it can be inferred that as the number of bulky substituents introduced into the Pc decreases, intermolecular interactions, such as π-π stacking of the Pc molecule, can increase [34].

According to the ESP surface map (Fig. 5.3), all four dyes have a similar charge distribution on the molecule. However, there is a slight difference in the central metal and the benzene of the isoindole ring. While tetra-substituted Pc has the smallest positive values for both the central metal and the center of the benzene ring, mono-substituted Pc has the largest positive values. This difference could be attributed to the inductive effect caused by substituted chlorines. As the number of Cl atoms in the Pc molecule increases, the electron-withdrawing effect can increase, which can reduce the electron density of the Pc core. Among the

synthesized dyes, the mono-substituted Pc contains the highest quantity of chlorine. Therefore, by this inductive effect, the central site and the center of the benzene part of isoindole ring of mono-substituted Pc can be slightly more positively charged [43, 44]. However, since the difference is not large, it is not considered to be a significant factor on the dispersion of the dyes.

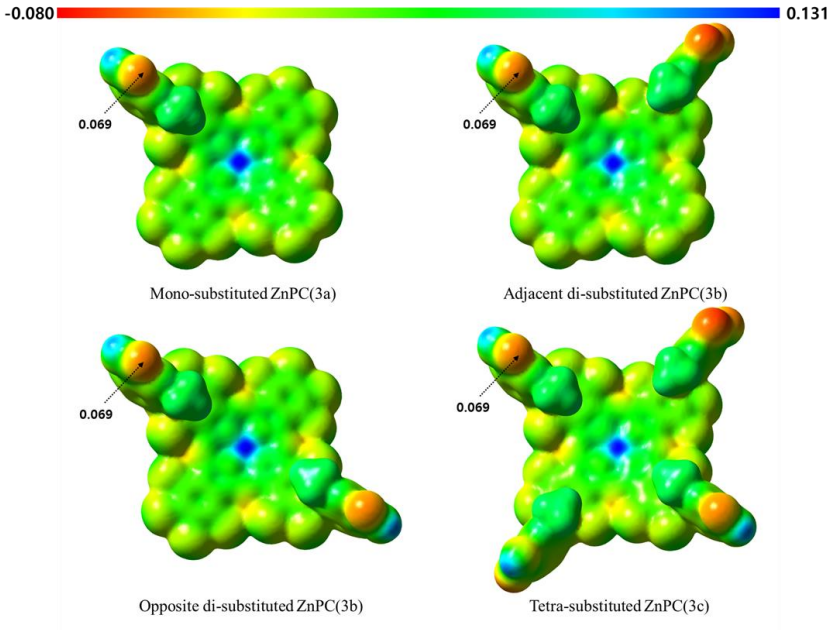

Figure 5.3. Electrostatic potential (ESP) surface maps of the dyes.

Next, in the TD-DFT calculation of Table 5.2, all dyes show analogous vertical absorption energy, which is similar to the tendency of the maximum absorption wavelengths of the Q-band measured experimentally. This finding demonstrates that both chlorine and alkoxy (-OR) groups as substituents introduced at the

peripheral position of the Pc can provide a comparable effect on the Q-band of the Pc molecule. This result is in agreement with those of previous studies [12, 26, 45].

Table 5.2. Experimentally measured (1×10^{-5} M in DMF) and calculated spectral properties of the prepared dyes.

Dye	Experimental		TD-DFT		
	λ_{max}[a]	ε_{max}[b]	λ_{max}	Transition[c]	Oscillator strength
3a	659 nm	54,174	653 nm	H→L	0.4866
			647 nm	H→L+1	0.5421
Adjacent-3b	696 nm	86,684	652 nm	H→L	0.5443
			651 nm	H→L+1	0.5369
Opposite-3b			658 nm	H→L	0.4830
			646 nm	H→L+1	0.5915
3c	695 nm	113,340	655 nm	H→L	0.5886
			654 nm	H→L+1	0.5988

[a]Absorption maximum wavelength of Q-band of dyes
[b]Molar extinction coefficient (L mol^{-1} cm^{-1})
[c]H: HOMO, L: LUMO, L+1: LUMO+1

By contrast, oscillator strength decreases with an increase in the number of chlorines, so that mono-substituted Pc has the smallest value. It is proposed that the following mechanism to explain this phenomenon. The π-electron cloud of the Pc molecule would withdraw due to the inductive effect of chlorine, which

can reduce a portion of the π electrons that π-π* transitions occur. Lowering of the probability of electron transition can reduce the oscillator strength [46-48]. Hence, the electron-withdrawing effect of chlorine can decrease the oscillator strength. This finding is also confirmed by the result of the molar extinction coefficient analysis of the dyes. The molar extinction coefficient of the dyes decreases as the quantity of chlorine substituted increases. Thus, it could be hypothesized that the incorporation of substituents with high electronegativity, such as halogens, into a Pc molecule can negatively affect color strength.

5.3.3. Spectral properties of the dyes

The spectral properties of the dyes were measured in dimethylformamide (DMF). Aqueous 0.1M HCl was subsequently gradually added to the dye solutions to characterize the optical properties of the dye aggregates. This is shown in Figs 5.4, 5.5, and Table 5.2.

Q-band becomes broader as the number of benzoic acid substituents decreases (Fig 5.4). Tetra-substituted Pc has a sharp Q-band, while mono-substituted Pc shows the broadest absorption and the lowest absorbance of Q-band. Furthermore, the unnecessary absorption in 450-550 nm range increases in the order of tetra-substituted Pc, di-substituted Pc, mono-substituted Pc. In earlier studies, it has

shown that aggregation of Pc molecules results in broadening of the absorption bands, and additional absorption can occur [1, 34, 49].

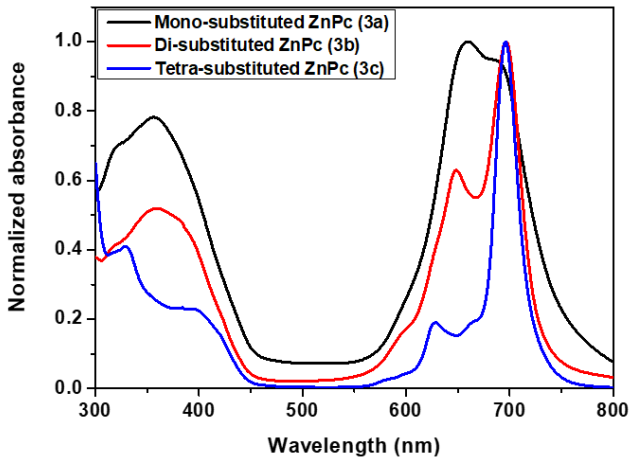

Figure 5.4. Normalized absorption spectra of the dye solutions dissolved in DMF (1×10^{-5} M).

Based on this fact, those results can be considered to be in fact due to the rise of the aggregate order of dyes [33]. It is postulate that the incipient aggregation of dyes may be observed with reduced bulkiness, due to the decreasing number of benzoic functional groups. The result of computational calculation supports our assumption. The geometry optimization results revealed that the bulkiness is lowered as the number of benzoic acid derivative substituents decreased in the synthesized Pc dye. This decrease in the bulkiness of Pc molecules can be said to increase their aggregate order. Eventually, it is regarded that this effect can

broaden the Q-band of mono-substituted Pcs and leads to the absorption of unnecessary wavelength regions. These results show that controlling the molecular bulkiness of Pcs is practical to change Pc dye aggregation. The maximum absorption wavelength of Q-band of mono-substituted Pc, and di-substituted Pc does not red-shift. Therefore, it is assumed that the synthesized dyes mainly form H-aggregates [50].

Similarly, the molar extinction coefficient of the dyes rapidly decreases in the order of tetra-substituted Pc > di-substituted Pc > mono-substituted Pc. In Section 5.3.2, it was proposed that the electron-withdrawing effect of chlorines can reduce the oscillator strength of the dye molecules. However, the oscillator strength in Table 5.2 did not show such a sharp decrease. It seems likely that there are other factors that contribute to this phenomenon. It should be noted that the trend of decrease in molar extinction coefficient is consistent with the tendency of reduction of the bulkiness of dyes. Therefore, it can be supposed that the absorbance of the Q-band can decrease as the aggregate order of the dye rises [29]. This finding coincides well with the results reported in previous studies that the color strength decreases with increasing particle size of organic colorants [51, 52]. Hence, it appears that changes in the molar extinction coefficient of the dyes are due to not only the inductive effect of chlorine but also the aggregation ability of the Pc molecules.

The excellent aggregation ability of di-substituted Pc and mono-substituted can also be confirmed by the absorption spectra in mixtures of DMF and aqueous 0.1M HCl solution. To measure the spectral properties of the aggregates of the synthesized dyes, the dyes were dissolved in DMF, and then slowly added to the solution with aqueous 0.1 M HCl. This result is illustrated in Fig. 5.5.

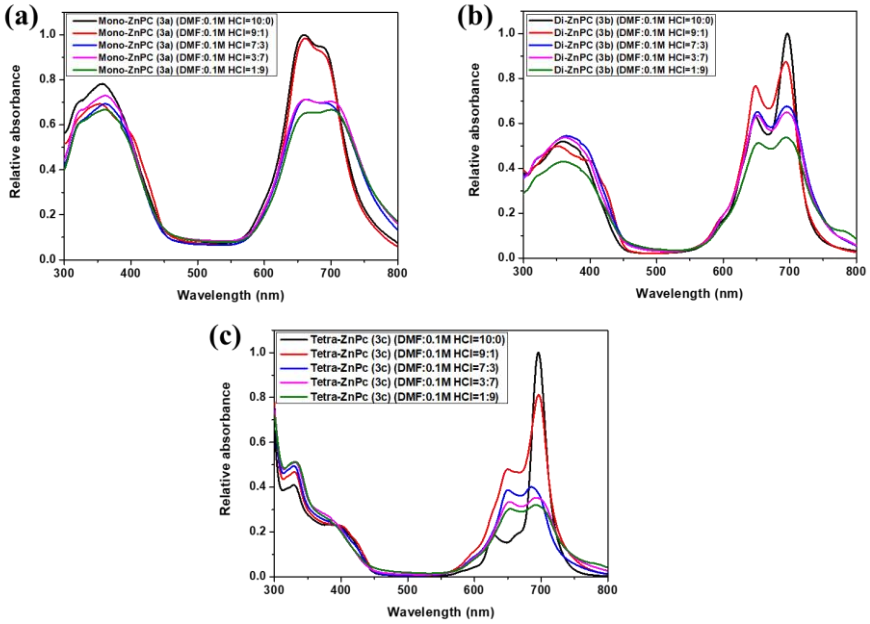

Figure 5.5. Absorption spectra of the dye solutions dissolved in DMF and aqueous 0.1M HCl (1×10^{-5} M). (a) mono-substituted ZnPc; (b) di-substituted ZnPc; (c) tetra-substituted ZnPc.

The Q-band of tetra-substituted Pc is rapidly expanded and the absorbance of the Q-band decreases, as aqueous 0.1M HCl increases. It appears that the dye is initially dissolved and gradually aggregates. However, for the di-substituted Pc,

the aggregate peak, in the range of 620-650 nm, is already considerably increased in the initial dye solution. As aqueous 0.1M HCl increases, the Q-band is slightly broadened, while the absorbance of Q-band decreases significantly. This tendency is more pronounced in mono-substituted Pc. The variation of the broadness and the absorbance of the Q-band of the mono-substituted Pc is smaller than that of the di-substituted Pc. These results suggest that the di-substituted Pc has a higher aggregate order than tetra-substituted Pc and are somewhat aggregated in the solution. Hence, the aggregate order is thought to increase in the order of tetra-substituted Pc, di-substituted Pc, and mono-substituted Pc.

The UV-Vis absorption results demonstrate that the mono-substituted Pc has the highest aggregate order among the synthesized dyes, resulting in the most inferior spectral properties [33]. The observations are in keeping with the aims of the study, i.e., to optimize the structure of the dyes. Thus, it can be concluded that the bulkiness and aggregation of the dyes were well controlled by removing the substituents. Moreover, this method is believed to be useful for the aim of this study, which is to finely adjust the aggregation to increase the absorbance of the dye at 600-700 nm, without a Q-band shift.

5.3.4. Thermal properties of the dyes

Thermalgravimetric analysis was used in this study to determine the thermal stability of the dyes and C.I pigment green 7. The color filter is typically manufactured by baking each pixel at 230 °C for 30 min; the colorant for the color filter must withstand these conditions. Thus, the experiment was conducted under isothermal conditions at 230 °C for 30 min, and the dyes were finally heated to 350°C. The weight loss must be less than 5% to apply the color filter. Fig. 5.6 and Table 5.3 show the results of the thermalgravimetric analysis (TGA) measurements. Since C.I pigment green 7 is currently one of the main colorants in the green color filter, it was introduced as a control for the characterization of the dyes.

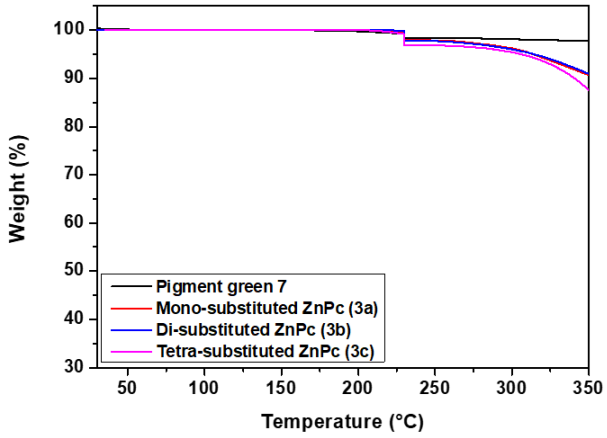

Figure 5.6. TGA analysis of the synthesized dyes. Dyes were heated to 230 °C and held at the temperature for 30 min, and then further heated to 350 °C.

Table 5.3. Weight loss (%) of the dyes in TGA

Dye	Weight loss
C.I pigment green 7	0.78%
Mono-substituted ZnPc (3a)	1.61%
di-substituted ZnPc (3b)	1.94%
Tetra-substituted ZnPc (3c)	2.21%

All synthesized dyes display superior thermal stability, with a weight loss of less than 2.5%. The weight loss declines in order of tetra-substituted Pc > di-substituted Pc > mono-substituted Pc. This trend is in line with the decrease in the bulkiness of Pc dyes and the increase in the aggregation ability of Pc dyes. This phenomenon can be explained as follows. As the bulkiness of Pc dyes diminishes, steric repulsion between Pc molecules would decline, thereby it is possible to grow π-π stacking of units. It is postulated that this strengthening of aggregation forces can increase the heat resistance of the dyes [35]. As a result, mono-substituted Pc exhibits the highest thermal stability.

This result proves that our approach is effective, increasing the stability in the solid-state of dyes by reducing the bulkiness of molecules owing to eliminate the bulky substituents in the Pc molecule.

5.3.5. Dispersion properties of the prepared dyes

To test the dispersibility, the dyes and C.I pigment green 7 were mixed with a polymeric dispersant (disperbyk LPN 21116) in PGMEA, and then dispersed using a probe sonicator. The results can be found in Table 5.4.

In Table 5.4, the dispersions of all dyes show smaller average particle size than the C.I. pigment green 7 dispersions. This result reveals that the C.I. pigment green 7 has higher aggregation forces than the dyes [53]. The adopted anchoring group seems to be helping to interact with the dispersant and to suppress the stacking of Pc. This difference in intermolecular interaction of Pc molecules can also be confirmed by X-ray powder diffraction, shown in Fig. 5.7.

Table 5.4. Dispersion properties of the prepared dyes.

Dye	Average particle size	PDI[b]	Average particle size after 168hr	Increment of particle size
Pigment[a]	145 nm	0.186	195 nm	50 nm
3a	134 nm	0.171	174 nm	40 nm
3b	112 nm	0.168	143 nm	31 nm
3c	69 nm	0.154	79 nm	10 nm

[a]C.I pigment green 7
[b]Polydispersity index

The C.I. pigment green 7 diffraction pattern is that of a polymorph crystal structure, despite its bulk-state [54]. The synthesized dyes exhibit an amorphous crystal structure, or a mixed amorphous and polymorph semicrystalline structure [55]. This relatively weak aggregation ability of dyes is postulated to result in better dispersibility.

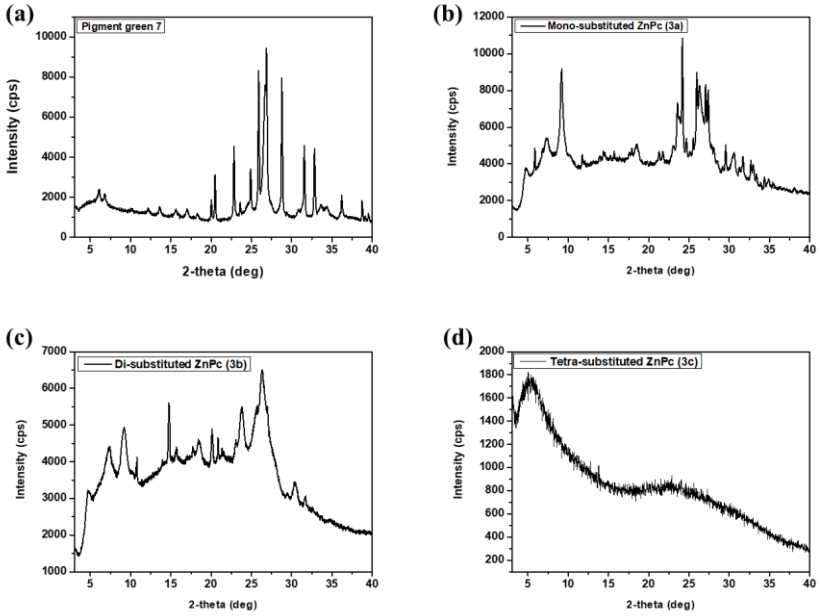

Figure 5.7. X-ray powder diffraction of the synthesized dyes. (a) C.I pigment green 7; (b) mono-substituted ZnPc; (c) di-substituted ZnPc; (d) tetra-substituted ZnPc.

As shown in Table 5.4, among the dyes, the average size of dispersed particles decreases in the order of mono-substituted Pc < di-substituted Pc < tetra-substituted Pc. The dispersibility decreases with a reduction in the number of bulky substituents in the dyes. This finding is consistent with the relationship

between thermal stability and molecular bulkiness discussed above. Thus, this phenomenon can be interpreted as a follow. Lowering the bulkiness of the Pc molecules would enhance the intermolecular stacking, which may reduce the dispersibility. This assumption can be also seen in the result of the X-ray powder diffraction. As mentioned above, tetra-substituted Pc shows an amorphous diffraction pattern, while di-substituted Pc and mono-substituted Pc display relatively mixed diffraction peaks of a polymorph and an amorphous crystal. In particular, mono-substituted Pc exhibits the diffraction pattern closest to polymorph crystal [1]. Hence, it is inferred that ordered molecular packing can increase as the number of benzoic acid moieties decrease. These results also support our argument that the dispersibility can improve as the bulky anchoring group is added.

The presence of constitutional isomers may also cause differences in dispersibility. Mono-substituted Pc and C.I. pigment green 7 do not have isomers, while tetra-substituted Pcs and di-substituted Pc contain isomers. It is believed that these isomers act as a kind of impurity, which can interfere with the aggregation of Pc molecules and increase dispersibility. As a result, tetra-substituted Pcs and di-substituted Pc indicate better dispersibility than mono-substituted Pc and C.I. pigment green 7.

To analyze dispersion stability, the initial dispersion was stored at room temperature for 168 hours and then the average particle size of the dispersion was measured again (Table 5.4). The dispersion stability is similar to the tendency of average particle size of dispersions. Among the dyes, tetra-substituted Pc shows the smallest increase in particle size, and mono-substituted Pc has the largest growth of particle size. This phenomenon can be explained as follows. As the carboxylic acid anchoring group is added, the probability of intermolecular interaction between Pc dyes and dispersants can be elevated. The improvement of these anchoring forces can lead to an enlargement of steric repulsion between the particles, thus decreasing in the re-agglomeration of dispersed particles [56-58]. In addition to this cause, the factors on the increase in dispersibility are also considered to help enhance dispersion stability. Thus, this tendency can be attributed to the fact that the increase in the number of dispersant anchoring groups and the more various isomers of Pc molecules, the more likely it is for inhibition of re-agglomeration, in conjunction with the greater the bulkiness of molecules.

All dyes show better dispersion properties than C.I. pigment green 7. Among the dyes, mono-substituted Pc displays the lowest the dispersion properties. Surprisingly, although di-substituted Pc contains isomers and has greater bulkiness than mono-substituted Pc, its dispersion properties fell short of

expectations. As a result, except for tetrasubstituted Pc, the dispersion of dyes showed insufficient properties for application to color filters.

5.3.6. Dispersion of the di-substituted phthalocyanine with a dispersion synergist

The dispersion characteristics of the di-substituted Pc were somewhat inadequate, but its durability and color characteristics were excellent for application to color filters. Therefore, in order to take advantage of its excellent durability and color characteristics, this study tried to improve its dispersibility. For this purpose, a dispersion synergist was introduced to the dispersion of the di-substituted Pc.

Previous work in our laboratory has shown the dispersibility of the Pc pigment can be improved by the Pc derivative containing the anchoring group, which acts as a dispersion synergist [26]. The mechanism of the dispersion synergist can be explained as follows. When the pigment is mixed with this particular dispersion synergist, the synergist molecules can adsorb to the pigment particles via π-π interaction with the pigment [9, 59]. The adsorbed synergist interacts with the dispersant, resulting in stabilization of the pigment particles. As a result, its dispersion properties are enhanced. Therefore, the introduction of the dispersion synergist was thought to be effective in improving the dispersibility of the di-

substituted Pc. Since the di-substituted Pc is soluble, unlike the pigment, it is well suited for use with dispersing synergists. Hence, it was expected that a more dramatic dispersibility improvement would be possible with excellent mixing property than that of the pigment. However, mixing any dye randomly does not always produce a dispersion synergist effect. For the dispersion synergist effect, the synergist should be miscible with the target colorant and have good intermolecular interaction with the dispersant [36, 60]. The tetra-substituted Pc in this work can be appropriate for a dispersion synergist. The tetra-substituted Pc shows excellent dispersibility in the dispersion evaluation and can exhibit superior miscibility with di-substituted Pc owing to its structural similarity with the di-substituted Pc.

Therefore, tetra-substituted Pc was adopted as dispersion synergist to improve dispersion properties of di-substituted Pc. The di-substituted Pc and tetra-substituted Pc were mixed in DMF in a weight ratio of 7:3, 5:5, and 3:7, respectively, and then solvent was removed to prepare the mixture powders. These mixtures were respectively dispersed into nanosized particles, following blending with the dispersant in PGMEA.

As shown in Table 5.5, all mixtures of the di-substituted Pc and the tetra-substituted Pc have the average particle size of less than 100 nm. The re-agglomeration size of all dispersions is also less than 15 nm, showing excellent

dispersion stability. Besides, there seems to be no significant difference in dispersion properties between the mixtures of a weight ratio of 5:5 and 3:7. These results are in agreement with the impact of the dispersion synergist shown in our previous study. These facts demonstrate that the tetra-substituted Pc works well as a synergist in the dispersion of the di-substituted Pc.

Table 5.5. Dispersion properties of the dispersions of tetra-substituted ZnPC and di-substituted ZnPC mixtures (weight ratios of 7:3, 5:5, and 3:7, respectively).

Dye	Average Particle size	PDI[a]	Average Particle size after 168hr	Increment of particle size
3b/3c (3:7)	75 nm	0.151	87 nm	12 nm
3b/3c (5:5)	86 nm	0.165	99 nm	13 nm
3b/3c (7:3)	84 nm	0.164	99 nm	15 nm

[a]Polydispersity index

Consequently, as tetra-substituted Pc exhibits excellent dispersion synergistic ability, the dispersibility of di-substituted Pc can be increased by using the dispersion synergist. This finding documented that our method is useful in improving dispersibility of the di-substituted Pc.

5.3.7. Characterization of the spin-coated films

5.3.7.1. Spectral properties of the spin-coated films

Except for mono-substituted Pc with poor dispersion properties, the color filters were prepared using the dispersions of mixtures of di-substituted Pc and tetra-substituted Pc, tetra-substituted Pc, and di-substituted Pc, respectively. Fig. 5.8 and Table 5.6 show the spectral properties of the manufactured the color filters. The pigment-based color filter was produced using C.I pigment green 7.

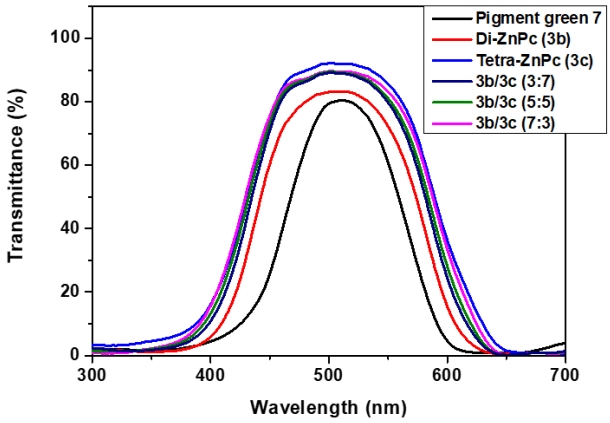

Figure 5.8. Transmittance spectra of the prepared color filters.

For the green color filter, the color filter should have high transmittance in the 500-540 nm range. All color filters manufactured using dye dispersions display a transmittance of over 80% in the 470-540 nm range, which is broader and

higher than that of C.I. pigment green 7. This difference in color properties of the color filters could have some explanations. First, the dyes indicate better dispersion properties than C.I. pigment green 7, so the dye dispersions exhibit stronger color strength than that of the pigment [51]. Second, the dyes are basically brighter and have a sharper absorption band than the pigment. The pigment has a variety of electron transition excited states because it exists in high stacking-state owing to its crystallinity and strong intermolecular forces. These features of the pigment result in broad absorption band and dimness in color [7]. However, unless the agglomeration of the dye particles in the solid-state is suppressed, the dye-based color filter also may show comparable color properties to the pigment-based one. This is why it is important to properly adjust the aggregation ability and particle stability of the dye.

In this work, it appears that the applied dyes show superior dispersion properties than the pigment, and thus provide excellent spectral properties of the color filter. Therefore, the color filter with the dyes can display wider and stronger transmittance, whereas that of the pigment shades visible light, resulting in the reduction of transmittance [12].

Among the dye-based color filters, tetra-substituted Pc shows the highest transmittance at 500-540 nm., and di-substituted Pc exhibits lower transmittance than the tetra-substituted Pc. The smallest particle size of tetra-substituted Pc is

postulated as the reason of this phenomenon. The difference in particle size in the films can be determined by SEM images of the color filters in Fig. 5.9.

Table 5.6. Characterization of the prepared color filters.

Dye	Wavelength of T_{max}[b]	Transmittance	Thermal stability (ΔEab)	Light stability (ΔEab)	Thickness (μm)
Pigment[a]	512 nm	80.4%	1.02	0.97	2.51
3b	512 nm	83.3%	1.66	1.61	2.20
3c	512 nm	92.0%	2.07	1.98	2.10
3c/3b (3:7)	512 nm	89.5%	2.04	1.96	2.11
3c/3b (5:5)	512 nm	89.1%	1.91	1.88	2.09
3c/3b (7:3)	512 nm	88.8%	1.85	1.80	2.09

[a]C.I pigment green 7
[b]Wavelength of maximum transmittance

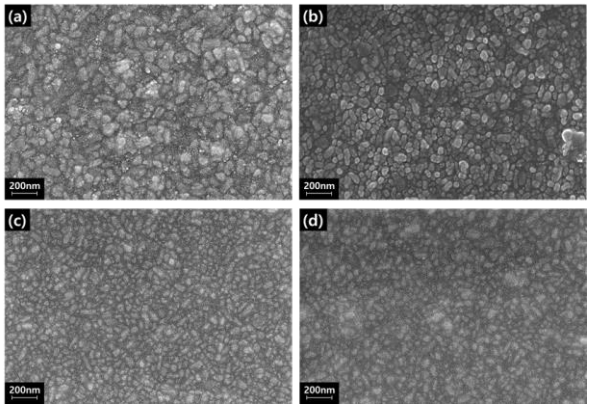

Figure 5.9. SEM images of the color filters. (a) C.I pigment green 7; (b) di-substituted Pc; (c) tetra-substituted Pc; (d) a mixture of di-substituted Pc and tetra-substituted Pc (7:3).

This difference could be attributed to dissimilarity in aggregation ability and dispersion stability. It appears that the aggregate behavior in the films is promoted as the bulkiness and the number of anchoring groups of the dyes declines [52]. Thus, it can be said that this factor leads to a drop-in optical characteristic. It is inferred that as particle size decreases, the color strength and color purity of the colorant increases, which maintains the high transmittance of the non-absorbing region observed in the dye solution. As described above, the growth of aggregate can lower the transmittance in the visible region, causing unnecessary absorption. The result of the spectral properties of the dye aggregates solution ascertained this phenomenon. In Fig. 5.5, as the aggregation of di-substituted Pc rises, unnecessary absorption in the 450-550 nm region and Q-band broadness enhances in the UV-Vis spectra. As a result, the color filter with di-substituted Pc indicates inferior optical properties to that of tetra-substituted Pc. Therefore, these results emphasize that to improve the optical property of the color filter, it is important to suppress the agglomeration of particles in the film.

In the color filters of the dispersion of dye mixtures, the color filter with the weight ratio of 7: 3 shows the highest transmittance in 480-540 nm, and the color filter with the weight ratio of 3: 7 has the broadest absorption in the 600-700 nm region. Taken together, the transmittance diminishes little by little as the particle

size of the dispersions being larger. However, the color filters of all dispersions of the mixtures exhibit the maximum transmittance difference of less than 1%. The optical properties of the color filters based on the mixtures are superior to that of di-substituted Pc. This fact suggests that in the case of the dispersion of the mixtures in this work, the difference of about 10 nm in the particle size does not have a significant effect on the color properties. Hence, it seems likely that the difference in color characteristics is due to changing the content of the di-substituted Pc.

For the green color filter, it is advantageous to have high absorption in the region of 600-700 nm. The color filter with tetra-substituted Pc has the best performance in terms of transmittance. However, it shows relatively high transmissions in the 600-700 nm region. Therefore, among the manufactured color filters, the color filter with the mixture dispersion of the weight ratio of 3: 7 is believed to be most suitable for the green color filter. This result supports that the dispersion of di-substituted Pc, which exhibits the broad Q-band, prepared by mixing with the dispersion synergist can be effective in development of the color filter for the green color filter.

5.3.7.2. Thermal and light stability and thickness of the spin-coated films

To determine the thermal stability of the color filters, baking was further performed at 230 ° C. for 60 min and color differential (ΔEab) was measured. Furthermore, to characterize the light stability, color differential (ΔEab) was obtained following exposure of the prepared color filters under a xenon lamp (350 W) for 30 h. All color differentials (ΔEab) must be less than 3 for the color filter. The measurement results are shown in Table 5.6.

For the thermal stability, the color filters with individual colorants show the similar trend to the TGA results. The thermal stability of the color filter increases in order of tetra-substituted Pc < di-substituted Pc < C.I. pigment green 7. All dispersed-dye-based color filters with individual dyes also indicate superior thermal stability of less than 2.1 of ΔEab. This fact can be interpreted to be as reduced bulkiness leading to improved durability.

The results of the light stability analysis of the color filters with individual colorants coincide with the above result. Similar to the tendency of the thermal stability, all dye-based color filters display excellent light resistance (ΔEab < 2.0). The color differential decreases in the order of tetra-substituted Pc > di-substituted Pc > C.I. pigment green 7. Hence, it could be hypothesized that as the bulky substituents are removed, the π-πstacking of Pc dyes can increase, which

in turn can improve the stability in the film [35]. In addition, reducing the substituents also can lead to a reduction of defect sites that can be destroyed by heat and light. Thus, it is estimated that the stability of color filters could be improved by combining these factors.

For the color filters with the dispersions of mixtures, both thermal and light stability enhance in the order of the weight ratio 7:3, 5:5, and 3:7. In other words, the stability rises as the content of di-substituted Pc increases in mixtures. Furthermore, all color filters with the mixture dispersions have better stability than that of tetra-substituted Pc. It is inferred that the incorporation of a di-substituted Pc can be effective in increasing the durability.

These findings suggest that the thermal and light stability in the solid-state can improve by a simple approach of inducing a moderate aggregation ability owing to reducing the number of functional groups of Pc. As a result, the color filter with the mixture dispersion (3:7) shows excellent durability of less than 1.9 of ΔEab for both heat and light resistance. This stability is superior to the durability of the dispersion-dye-based color filter developed in our previous study.

Overall, these results provide crucial insights into the possibility that asymmetry in polychloro Pc can be suitable in colorants for the development of durable dye-based color filters.

The surface profiler (Alpha-step) was used to confirm the thickness of the prepared color filters. The result is shown in Table 5.6. For the color filters with individual dyes, the thickness increases in the order of tetra-substituted Pc < di-substituted Pc < C.I. pigment green 7. This result corresponds exactly with the tendency of the average particle size of the dispersion of colorants. It is possible that as the dispersed particle size decreases, the volume of the films can decline, which can lead to diminishing the thickness of the color filter. Hence, it could be demonstrated that the formation of well-dispersed fine particles can lower the thickness of the film.

In the case of the color filters with the mixture dispersions, no significant difference in thickness is observed. The previous study has concluded that the dye, which has a low molar mass with high color strength, can lower the thickness of the color filter [26]. Based on this finding, it was predicted that as the amount of di-substituted Pc increases in the color filter, the film thickness may decrease. Contrary to expectations, although di-substituted Pc have relatively small bulkiness and molar mass, the thickness of the color filters did not change significantly. This unanticipated finding can be interpreted as follows. The drop-in bulkiness of di-substituted Pc can elevate the aggregation ability, so that the particle size can grow. Hence, although di-substituted Pc has lower molar mass than tetra-substituted Pc, color strength can be inferior due to the relatively higher

aggregate order and dispersed particle size [7, 18]. In other words, the reduced bulkiness of the molecule can offer a negative effect on the thickness of the color filter. Therefore, it is assumed that due to the fall in color strength, the thickness of the color filter with the mixture dispersions could not be reduced as intended. These facts suggest that the diminution of the bulkiness of the colorant may have a positive effect on its durability but may have a negative effect on the color properties and thickness of the color filter. That is, the stability of the color filter can be in a trade-off relationship with the color properties and film thickness.

5.4 Conclusion

In this study, the goal was to develop a green colorant for the dispersed-dye-based color filter to improve the durability and the color properties of the color filter. For this purpose, mono-substituted, di-substituted, and tetra-substituted polychoral zinc Pc containing benzoic acid derivatives as a dispersant anchoring group were synthesized for the development of the green color filter.

In the results of geometry optimization, the synthesized dyes had a saddle-shaped deformed molecular structure, and it was confirmed that as the number of benzoic acid substituents decreases, the bulkiness of the molecules decreases. The results of ESP surface mapping ascertained that the substituted chlorines of polychloro Pc act as an electron-withdrawing group (EWG) and induce an

inductive effect on the π-electron cloud of the whole Pc core. The TD-DFT calculation and UV-Vis spectrometry showed that this inductive effect of chlorine could cause a fall in oscillator strength and extinction coefficient of dyes. All dyes displayed superior thermal stability in the TGA analysis. The thermal stability decreased in the order of mono-substituted, di-substituted, tetra-substituted Pc.

These results demonstrated that the decrease in bulkiness of the Pc dyes could increase the π-π stacking of the molecule, leading to an increase in the Q-band broadness and thermal stability of the dyes. It was inferred that as the aggregation forces of Pc dyes are promoted, the stability can improve but the color properties diminish.

The analysis of dispersion characterization of the dyes proposed that the strong intermolecular interactions could also reduce the dispersibility of the dyes. As a result, mono-substituted Pc showed inferior dispersion properties, and tetra-substituted Pc had superior dispersion properties.

However, the dispersibility of di-substituted Pc could be improved by incorporation of tetra-substituted Pc as the dispersion synergist, and dispersions of this mixtures could be applied to the color filter to improve the durability and the optical properties. As a result, the color filter with the mixture dispersion of

the weight ratio 3: 7 showed the appropriate spectral properties and the superior stability for the green color filter.

However, even though di-substituted Pcs with the low bulkiness and molar mass were mixed, the thickness of the color filter indicated no significant decrease. The reduced color strength owing to the high aggregate order of the di-substituted Pc is assumed as a cause for this result.

This study clearly demonstrated that varying the number of substituents in tetra-benzoic acid-substituted polychloro zinc Pc could fine-tune the bulkiness and the structure of the molecule. This approach could alter the color properties and durability of the Pc. It was also shown that the lack of dispersibility of the di-benzoic acid-substituted polychloro Pc can be significantly increased by the introduction of tetra-benzoic acid-substituted polychloro Pc as a synergist, without complicated treatment.

Through this work, it was presented that a simple method to control the aggregation ability and color characteristics of polychloro Pc without complex change of substituents.

In conclusion, a color filter with excellent color properties and thermal and light stability was produced by incorporation of di-substituted polychloro Pc dispersion with the dispersion synergist tetra-substituted polychloro Pc. This investigation resulted in the development of dispersed-dye-based color filters that

avoided the disadvantages of the inferior stability and dye migration of the soluble-dye-based color filter.

However, further research is needed to increase the color strength and decrease the film thickness of dispersed dyes. Therefore, future studies will be required to design functional groups and molecular structures that can have small bulkiness and high color strength while maintaining low aggregate order.

5.5 References

[1] Sabnis RW. Color filter technology for liquid crystal displays. Displays. 1999;20(3):119-29.

[2] Freeman HS, Peters AT. Colorants for Non-Textile Applications: Elsevier Science, 2000.

[3] Herbst W, Hunger K. Industrial Organic Pigments: Production, Properties, Applications: Wiley, 2006.

[4] Sugiura T. A History of CFs Development for Color LCD. Journal of Printing Science and Technology. 1996;33(6):356-68.

[5] Kim YD, Kim JP, Kwon OS, Cho IH. The synthesis and application of thermally stable dyes for ink-jet printed LCD color filters. Dyes and Pigments. 2009;81(1):45-52.

[6] Kim YD, Cho JH, Park CR, Choi J-H, Yoon C, Kim JP. Synthesis, application

and investigation of structure–thermal stability relationships of thermally stable water-soluble azo naphthalene dyes for LCD red color filters. Dyes and Pigments. 2011;89(1):1-8.

[7] Sakong C, Kim YD, Choi J-H, Yoon C, Kim JP. The synthesis of thermally-stable red dyes for LCD color filters and analysis of their aggregation and spectral properties. Dyes and Pigments. 2011;88(2):166-73.

[8] Choi J, Sakong C, Choi J-H, Yoon C, Kim JP. Synthesis and characterization of some perylene dyes for dye-based LCD color filters. Dyes and Pigments. 2011;90(1):82-8.

[9] Choi J, Kim SH, Lee W, Yoon C, Kim JP. Synthesis and characterization of thermally stable dyes with improved optical properties for dye-based LCD color filters. New Journal of Chemistry. 2012;36(3):812.

[10] Choi J, Lee W, Sakong C, Yuk SB, Park JS, Kim JP. Facile synthesis and characterization of novel coronene chromophores and their application to LCD color filters. Dyes and Pigments. 2012;94(1):34-9.

[11] Choi J, Lee W, Namgoong JW, Kim T-M, Kim JP. Synthesis and characterization of novel triazatetrabenzcorrole dyes for LCD color filter and black matrix. Dyes and Pigments. 2013;99(2):357-65.

[12] Lee J-Y, Kim J-H, Bae J-H, Yoon C, Kim J-P, Choi J-H. The Synthesis and Characterizations of Thermally-Stable Yellow Metal Complex Dyes for LCD

Color Filters. Molecular Crystals and Liquid Crystals. 2013;583(1):60-9.

[13] Choi J, Kim SH, Lee W, Chang JB, Namgoong JW, Kim YH, et al. The influence of aggregation behavior of novel quinophthalone dyes on optical and thermal properties of LCD color filters. Dyes and Pigments. 2014;101:186-95.

[14] Kim JY, Choi J, Namgoong JW, Kim SH, Sakong C, Yuk SB, et al. Synthesis and characterization of novel perylene dyes with new substituents at terminal-position as colorants for LCD color filter. Journal of Inclusion Phenomena and Macrocyclic Chemistry. 2015;82(1-2):203-12.

[15] Kim SH, Namgoong JW, Yuk SB, Kim JY, Lee W, Yoon C, et al. Synthesis and characteristics of metal-phthalocyanines tetra-substituted at non-peripheral (α) or peripheral (β) positions, and their applications in LCD color filters. Journal of Inclusion Phenomena and Macrocyclic Chemistry. 2015;82(1-2):195-202.

[16] Park S, Park J, Lee S, Park J. New Dyes Based on Anthraquinone Derivatives for Color Filter Colorants. Journal of Nanoscience and Nanotechnology. 2014;14(8):6435-7.

[17] Muthukumar P, Kim H-S, Jeong JW, Son Y-A. Synthesis and characterization of tetra phenoxy-substituted halogen-rich metallophthalocyanine derivatives: A study on their LCD color filter requirements. Journal of Molecular Structure. 2016;1119:325-31.

[18] Kim IJ, Palanisamy M, Jeong J, Son Y-A. Synthesis of octa-phenoxy

substituted metallophthalocyanines and their green color filter application in liquid crystal display. Molecular Crystals and Liquid Crystals. 2017;644(1):88-97.

[19] Kim JY, Hwang TG, Kim SH, Namgoong JW, Kim JE, Sakong C, et al. Synthesis of high-soluble and non-fluorescent perylene derivatives and their effect on the contrast ratio of LCD color filters. Dyes and Pigments. 2017;136:836-45.

[20] Kong NS, Jung H, Kim B, Lee CK, Kong H, Jun K, et al. Development of dimeric triarylmethine derivatives with improved thermal and photo stability for color filters. Dyes and Pigments. 2017;144:242-8.

[21] Namgoong JW, Chung S-W, Jang H, Kim YH, Kwak MS, Kim JP. Improving nanoparticle dispersions of pigment and its application to a color filter: New phthalocyanine derivatives as synergist. Journal of Industrial and Engineering Chemistry. 2018;58:266-77.

[22] Namgoong JW, Kim SH, Chung S-W, Kim YH, Kwak MS, Kim JP. Aryloxy- and chloro-substituted zinc(II) phthalocyanine dyes: Synthesis, characterization, and application for reducing the thickness of color filters. Dyes and Pigments. 2018;154:128-36.

[23] Sugiura T. Dyed color filters for liquid-crystal displays. Journal of the Society for Information Display. 1993;1(2):177.

[24] Kalugasalam P, Ganesan S. Surface morphology of annealed lead phthalocyanine thin films. International journal of engineering science and technology. 2010;2(6):1773-9.

[25] Löbbert G. Phthalocyanines. Ullmann's Encyclopedia of Industrial Chemistry: Wiley-VCH Verlag GmbH & Co. KGaA; 2012. p. 181-213.

[26] Kobak RZU, Arı MU, Tekin A, Gül A. Aggregation behavior in unsymmetrically substituted metal-free phthalocyanines. Chemical Physics. 2015;448:91-7.

[27] Gueli AM, Bonfiglio G, Pasquale S, Troja SO. Effect of particle size on pigments colour. Color Research & Application. 2017;42(2):236-43.

[28] Müller M, Dinnebier RE, Jansen M, Wiedemann S, Plüg C. The influence of temperature, additives and polymorphic form on the kinetics of the phase transformations of copper phthalocyanine. Dyes and Pigments. 2010;85(3):152-61.

[29] Müller F, Peukert W, Polke R, Stenger F. Dispersing nanoparticles in liquids. International Journal of Mineral Processing. 2004;74:S31-S41.

[30] Kim JP, Kim JS, Park JS, Jang SS, Lee JJ. Synthesis of temporarily solubilised azo disperse dyes containing a β-sulphatoethylsulphonyl group and dispersant-free dyeing of polyethylene terephthalate fabric. Coloration Technology. 2016;132(5):368-75.

[31] Yoon C, Kwon H-S, Yoo J-S, Lee H-Y, Bae J-H, Choi J-H. Preparation of thermally stable dyes derived from diketopyrrolopyrrole pigment by polymerisation with polyisocyanate binder. Coloration Technology. 2015;131(1):2-8.

[32] McDowell R. Particle size reduction of phthalocyanine blue pigment. Electronic Theses and Dissertations. 2006.

[33] Özçeşmeci İ, Tekin A, Gül A. Synthesis and aggregation behavior of zinc phthalocyanines substituted with bulky naphthoxy and phenylazonaphthoxy groups: An experimental and theoretical study. Synthetic Metals. 2014;189:100-10.

[34] Naito M, Yokoyama T, Hosokawa K, Nogi K. Characteristics and Behavior of Nanoparticles and Its Dispersion Systems. Nanoparticle Technology Handbook (Third Edition): Elsevier; 2018. p. 109-68.

[35] Auschra C, Eckstein E, Mühlebach A, Zink M-O, Rime F. Design of new pigment dispersants by controlled radical polymerization. Progress in Organic Coatings. 2002;45(2–3):83-93.

[36] Verdree VT, Pakhomov S, Su G, Allen MW, Countryman AC, Hammer RP, et al. Water soluble metallo-phthalocyanines: the role of the functional groups on the spectral and photophysical properties. J Fluoresc. 2007;17(5):547-63.

[37] Gregory P. Industrial applications of phthalocyanines. Journal of Porphyrins

and Phthalocyanines. 2000;04(04):432-7.

[38] Frisch MJ, Trucks GW, Schlegel HB, Scuseria GE, Robb MA, Cheeseman JR, et al. Gaussian 09, Revision E.01. Wallingford CT2009.

[39] Zeng W, Gong S, Zhong C, Yang C. Prediction of Oscillator Strength and Transition Dipole Moments with the Nuclear Ensemble Approach for Thermally Activated Delayed Fluorescence Emitters. The Journal of Physical Chemistry C. 2019;123(15):10081-6.

[40] Irie M, Yokoyama Y, Seki T. New Frontiers in Photochromism: Springer Japan, 2013.

[41] Corsini NR, Hine ND, Haynes PD, Molteni C. Unravelling the Roles of Size, Ligands, and Pressure in the Piezochromic Properties of CdS Nanocrystals. Nano Lett. 2017;17(2):1042-8.

[42] Egli M, Sarkhel S. Lone Pair−Aromatic Interactions: To Stabilize or Not to Stabilize. Accounts of Chemical Research. 2007;40(3):197-205.

[43] Liu JJ, Guan YF, Chen Y, Lin MJ, Huang CC, Dai WX. The impact of lone pair-pi interactions on photochromic properties in 1-D naphthalene diimide coordination networks. Dalton Trans. 2015;44(39):17312-7.

[44] Klyamer D, Sukhikh A, Gromilov S, Krasnov P, Basova T. Fluorinated Metal Phthalocyanines: Interplay between Fluorination Degree, Films Orientation, and Ammonia Sensing Properties. Sensors (Basel). 2018;18(7).

[45] Bayda M, Dumoulin F, Hug GL, Koput J, Gorniak R, Wojcik A. Fluorescent H-aggregates of an asymmetrically substituted mono-amino Zn(ii) phthalocyanine. Dalton Trans. 2017;46(6):1914-26.

[46] Bächle F, Maichle-Mössmer C, Ziegler T. Helical Self-Assembly of Optically Active Glycoconjugated Phthalocyanine J-Aggregates. ChemPlusChem. 2019;84(8):1081-93.

[47] Bıyıklıoğlu Z, Çakır V, Çakır D, Kantekin H. Crown ether-substituted water soluble phthalocyanines and their aggregation, electrochemical studies. Journal of Organometallic Chemistry. 2014;749:18-25.

[48] Hughes DFK, Robb ID, Dowding PJ. Stability of Copper Phthalocyanine Dispersions in Organic Media. Langmuir. 1999;15(16):5227-31.

[49] Squires AD, Lewis RA. Terahertz Analysis of Phthalocyanine Pigments. Journal of Infrared, Millimeter, and Terahertz Waves. 2019;40(7):738-51.

[50] Denekamp IM, Veenstra FLP, Jungbacker P, Rothenberg G. A simple synthesis of symmetric phthalocyanines and their respective perfluoro and transition-metal complexes. Applied Organometallic Chemistry. 2019;33(5).

[51] Schofield JD. Extending the boundaries of dispersant technology. Progress in Organic Coatings. 2002;45(2-3):249-57.

[52] Ridhi R, Saini GSS, Tripathi SK. Study of interaction mechanism of metal phthalocyanines dispersed sol-gel glasses with chemical vapours. Sensors and

Actuators B: Chemical. 2018;255:1849-68.

[53] Mooibroek TJ, Gamez P, Reedijk J. Lone pair–π interactions: a new supramolecular bond? CrystEngComm. 2008;10(11):1501-15.

[54] Wheeler SE, Seguin TJ, Guan Y, Doney AC. Noncovalent Interactions in Organocatalysis and the Prospect of Computational Catalyst Design. Acc Chem Res. 2016;49(5):1061-9.

[55] Jones FN, Nichols ME, Pappas SP. Effect of Pigments on Coating Properties. Organic Coatings: John Wiley & Sons, Inc.; 2017. p. 323-30.

Summary

Highly durable phthalocyanine dyes for green color filters were developed and the color filters with those dyes were prepared. It involved the synthesis of metal phthalocyanine derivatives with bulky benzoate and benzoic acid moieties, and their molecular properties, spectral properties, thermal stability, dispersion properties, and crystal structures were measured by computational method, UV-Vis spectrometry, thermalgravimetric analysis, dynamic light scattering, and powder-XRD. The optical properties, heat and light resistances, film thickness, and surface properties of the color filters with the dyes were analyzed by spectrophotometer, surface profiler (Alphastep), atomic force microscopy, and electron microscopy.

In this investigation, polychloro-zinc phthalocyanine with bulky benzoate moiety was found to have high solubility caused by deformed core structure. It was also revealed that the substituent induces high bulkiness of the molecule. It was ascertained that the dye indicated superior color strength in contrast to the pigment due to its high solubility. The result indicates that either the thickness of the color filter can be reduced and better color characteristics than the pigment-based color filter can be exhibited due to this fact. However, its durability has still needed to be improved.

In order to address the shortcomings of the soluble dye-based color filter, phthalocyanine dyes applicable in dispersion systems were designed. The zinc phthalocyanine derivatives containing dispersion anchoring groups was synthesized, and these dyes were introduced into the dispersion of C.I. pigment green 7 as a dispersion synergist. As a result, it was ascertained that the zinc phthalocyanine with the carboxylic acid group can be effective for the dispersion synergist, and the color filter was prepared with this. The results showed that the incorporation of the prepared dispersion synergist could improve the contrast ratio and transmittance of the color filter. However, this method still retained the disadvantages of pigment-based color filters because the pigment was incorporated into the colorant.

Therefore, the dye dispersions were prepared to develop colorants that could express both the merits of dye and pigment. To this end, metal phthalocyanine containing a carboxylic acid group as a dispersion anchoring group was synthesized. Among the synthesized dyes, polychloro-zinc phthalocyanine indicated superior dispersion properties thanks to its molecular properties and dispersion anchoring group. Furthermore, the durability of the color filter with the dye dispersion was higher than that of the soluble dye-based color filter, and its color characteristics were similar to those of the latter. These results demonstrate that the proposed dye-dispersion method can be useful for

improving the color filter characteristics. However, there was room for improvement with respect to its durability and color characteristics.

For this reason, polychloro-zinc phthalocyanine with different numbers of bulky anchoring groups was designed. As a result, mono-substituted, di-substituted, and tetra-substituted polychloro-zinc phthalocyanine dyes were synthesized. It was determined that the durability can be improved as the bulkiness of the phthalocyanine molecule is reduced. The di-substituted phthalocyanine showed the most appropriate durability and spectral characteristics but indicated insufficient dispersibility. However, the dispersibility of di-substituted phthalocyanine could be improved by introducing tetra-substituted phthalocyanine as a dispersion synergist. It was possible to enhance the durability and color characteristics of the disperse dye-based color filter using this approach. This study presented a simple method to improve on the durability and color properties of phthalocyanine dye dispersion for the green color filter.

In conclusion, this study demonstrated that either phthalocyanine dye or disperse dye-based color filters is highly durable for green color filters, and has the potential to be a highly durable high-transmit color filter, respectively. However, there is room for improvement on issues relating to film thickness and color characteristics. Further research is needed to investigate dye systems that

can improve color characteristics, while simultaneously reducing the thickness of disperse dye-based color filters.

초 록

현재, 세계는 정보화 사회를 뛰어 넘어 첨단기술 사회로 도래하고 있다. 이러한 첨단 기술 사회에서는 시각 정보의 활용이 높아지면서 카메라 및 디스플레이 장치의 성능 향상에 대한 필요성이 날로 상승하고 있다. 이러한 흐름에 따라 이미지 센서와 디스플레이 장치의 성능에 직접적인 영향을 미치는 컬러필터의 기술 발전에 대한 요구 또한 높아지고 있다.

따라서 본 논문에서는 적색, 녹색, 청색 컬러필터 중 기존 녹색 안료형 컬러필터의 문제점을 개선하고 성능을 향상시킬 수 있는 녹색의 염료형 컬러필터를 개발하기 위한 다양한 연구를 수행하였다. 종합적으로, 녹색 컬러필터에 적용 가능한 프탈로시아닌계 염료를 개발하고 이를 통해 궁극적으로 분광특성과 내구성이 향상된 녹색 염료형 컬러필터를 제시해 보고자 하였다.

이를 위해서 본 논문에서는 다양한 작용기가 도입된 프탈로시아닌 유도체를 합성하고 이들의 최적구조, 분광특성 및 내열성 등을 살펴보았다. 그리고 합성된 염료 중 일부 염료는 용해법이 아닌 분산법을 통해 적용하여 고 내구성의 컬러필터용 잉크를 제조하였다.

이 과정을 통해 합성된 염료들을 이용하여 다양한 녹색 컬러필터를 제조하였다.

먼저, 용해형으로 적용가능한 염료 개발을 위해, 부피가 큰 벤조에이트 작용기가 4 개 혹은 8 개가 도입된 프탈로시아닌 염료를 합성하였으며, 또한 4 치환 프탈로시아닌의 경우 분광특성의 조절을 위해 염소원자를 프탈로시아닌의 말단 혹은 말단과 비말단 위치 모두에 추가로 도입하였다. 합성된 염료들은 분자 시뮬레이션, UV-Vis 분광법, 열중량분석법 등을 통해 분석하였으며, 이들을 이용해 컬러필터를 제조하여 색차계, 표면분석법등을 통해 색특성 및 박막두께 등을 관찰하였다. 이를 통해 합성된 염료가 안료에 비해 컬러필터의 박막 두께를 낮추고 우수한 분광특성을 가질 수 있는지 확인하였다.

또한, 내구성 향상을 위한 분산법 도입을 위해 프탈로시아닌 염료에 각각 1 차아민, 3 차아민, 에스터 및 카복실산이 도입된 작용기를 치환하여, 4 종의 안료용 분산 시너지스트들을 합성하였으며, 이 염료들을 C.I pigment green 7 과 혼합하여 분산하였다. 그리고 분산체들의 분산특성은 광산란영동법을 이용하여 분석하였다. 그리고

분산체들을 컬러필터에 적용하여 그들의 특성을 분석하였다. 이 과정을 통해 프탈로시아닌계 염료의 유기계분산에서 효과적인 작용기를 확인하고자 하였다.

이 조사를 바탕으로 부피가 큰 벤조산을 분산제 고정 작용기로 도입하고, 염소원자를 조색단으로 도입한, 구리프탈로시아닌과 아연프탈로시아닌을 합성하여 염료 단독 분산시스템에 적용하였다. 이를 통해 미세하고 균일하게 분산된 염료 분산체를 제조하고, 염료형 컬러필터의 내구성과 분광특성을 동시에 향상시켜보고자 하였다. 합성된 염료들은 분자시뮬레이션, UV-Vis 분광법, 열중량분석법 등을 통해 분자 최적 구조, 정전기적 표면 전위, 분광특성, 열안정성 등을 분석하였으며, 광산란영동법을 이용하여 분산체의 분산특성을 분석하였다. 또한 분산특성이 우수한 분산체들을 이용하여 컬러필터를 제조하고 이들의 특성을 비교해 보았다. 이 과정에서 분산법에 적용하기에 유리한 프탈로시아닌 염료의 구조 정보를 확인하고, 분산형 염료가 도입된 컬러필터의 내구성과 용해형 염료가 도입된 컬러필터의 내구성을 비교해 보고자 하였다.

추가적으로 같은 벤조산 작용기와 말단과 비말단 위치 모두에 염소가 추가적으로 도입된 비대칭형 프탈로시아닌을 도입하여, 분산형 염료의 컬러필터의 분광특성을 녹색에 최적화하고자 하였다. 이를 위해 벤조산 작용기가 한 개, 두 개, 네 개가 도입된 아연 프탈로시아닌 염료를 합성하였으며, 앞선 연구와 동일하게 이들의 특성을 분석하고, 분산하여 컬러필터에 도입해 보았다. 이 과정에서 부피가 큰 작용기가 감소할수록 내구성은 향상될 수 있음을 확인할 수 있었으며, 작용기가 두개 치환된 프탈로시아닌 염료가 녹색 컬러필터에는 가장 적절한 분광특성을 가짐을 확인할 수 있었다. 다만 작용기가 감소함에 따라 분산특성이 급격히 감소하기 때문에 이 연구에서는 분산성 향상을 위해서 염료 혼합물의 도입을 추가적으로 시도하였다.

이 연구들을 통해 본 논문에서는 프탈로시아닌계 염료를 도입한 컬러필터가 안료형 컬러필터에 비해 낮은 막두께와 함께 우수한 분광특성을 가질 수 있음을 확인해 보고자 하였고, 또한 기존의 용해성 염료형 컬러필터의 단점을 극복할 수 있는 방법으로 분산형 염료가 도입된 컬러필터를 제안해 보았다. 이를 위해 용해형 염료

시스템에 적절한 염료뿐만 아니라 분산형 시스템에 유리한 프탈로시아닌 염료의 구조와, 분산제 고정기로 적절한 작용기를 조사해 보았으며, 이 과정에서 말단 및 비말단 위치에 염소가 풍부한 프탈로시아닌 유도체가 용해형 및 분산형 시스템에 적절함을 확인하였다. 최종적으로 본 연구에서는 부피가 큰 벤조산 작용기가 도입되고, 염소가 풍부한 아연 프탈로시아닌 유도체가 녹색 염료형 컬러필터에 적절할 수 있음을 보여주었다.

List of Publications

Original Papers

1. Sim Bum Yuk, Jae Moon Lee, **Jin Woong Namgoong**, Chun Sakong, Tae Gyu Hwang, Se Hun Kim, Woosung Lee, Jae Pil Kim, 'Synthesis of bay-linked perylene dimers with enhanced solubility for high optical density black matrix material.', Dyes and Pigments, 2019, 171, 107-695

2. Sol Choi, Kwan Hyun Cho, **Jin Woong Namgoong**, Jeong Yun Kim, Eui Sang Yoo, Woosung Lee, Jae Woong Jung, Jun Choi, 'The synthesis and characterisation of the perylene acid dye inks for digital textile printing.', Dyes and Pigments, 2019, 163, 381-392

3. Tae Gyu Hwang, Jeong Yun Kim, **Jin Woong Namgoong**, Jae Moon Lee, Sim Bum Yuk, Se Hun Kim, Jae Pil Kim, 'Aggregation induced emission of diketopyrrolopyrrole (DPP) derivatives for highly fluorescent red films.', Photochemical & Photobiological Sciences, 2019, 18, 1064-1074

4. Jong Hyuk Bae, Seung Ju Lim, Jun Choi, Sim Bum Yuk, **Jin Woong Namgoong**, Jae Hoon Ko, Woosung Lee, Jae Pil Kim, 'Effects of introducing functional groups on the performance of phenoxazine-based dye-sensitized solar cells.', Dyes and Pigments, 2019, 162, 905-915

5. Sung Wun Woo, Jeong Yun Kim, Tae Gyu Hwang, Jae Moon Lee, Hong Mo Kim, **Jin Woong Namgoong**, Sim Bum Yuk, Jae Pil Kim, 'Effect of weakly coordinating anions on photo-stability enhancement of basic dyes in organic solvents.', Dyes and Pigments, 2019, 160, 765-771

6. **Jin Woong Namgoong,** Sei-Won Chung, Hyeyoun Jang, Young Hoon Kim, Moo Sun Kwak, Jae Pil Kim, 'Improving nanoparticle dispersions of pigment and its application to a color filter: New phthalocyanine derivatives as synergist.', Journal of Industrial and Engineering Chemistry, 2018, 58, 266-277

7. **Jin Woong Namgoong,** Se Hun Kim, Sei-WonChung, Young Hoon Kim, Moo Sun Kwak, Jae Pil Kim, 'Aryloxy- and chloro-substituted zinc(II) phthalocyanine dyes: Synthesis, characterization, and application for reducing the thickness of color filters', Dyes and Pigments, 2018, 154, 128-136

8. **Jin Woong Namgoong, Hyeyoun Jang**, Min-Gyu Sung, Yongkeun Chang, Jae Pil Kim, 'Synthesis and characterization of fluorescent dyes and their applications for the enhancement of growth rate of Chlorella vulgaris.', Dyes and Pigments, 2018, 158, 142-150

9. Sim Bum Yuk, Woosung Lee, Se Hun Kim, **Jin Woong Namgoong**, Jae Moon Lee, Jae Pil Kim, 'Application of perylene dyes for low dielectric hybrid-type black matrices.', Journal of Industrial and Engineering Chemistry, 2018, 64, 237-244

10. Jeong Yun Kim, Sung Wun Woo, **Jin Woong Namgoong**, Jae Pil Kim, 'A study on the fluorescence property of the perylene derivatives with methoxy groups', Dyes and Pigments, 2018, 148, 196-205

11. Sivalingam Suganya, **Jin Woong Namgoong**, Anil Kumar Mutyala, Sivan Velmathi, Jae Pil Kim, Jong S.Park, 'A new perylenediimide with NH functionality as a colorimetric and fluorescent probe for the selective

detection of trivalent Fe^{3+} and Al^{3+} ions.', Journal of Photochemistry and Photobiology A: Chemistry, 2017, 344, 36-41

12. Anil Kumar Mutyala, Sun-Mi Hong, **Jin Woong Namgoong**, Jae Pil Kim, Jong S.Park, 'Low bandgap poly(fluorinated metallophthalocyanine-alt-diketopyrrolopyrrole)s with outstanding thermal stability.', Dyes and Pigments, 2017, 142, 237-242

13. Jeong Yun Kim, Tae Gyu Hwang, Se Hun Kim, **Jin Woong Namgoong**, Ji Eon Kim, Chun Sakong, Jun Choi, Woosung Lee, Jae Pil Kim, 'Synthesis of high-soluble and non-fluorescent perylene derivatives and their effect on the contrast ratio of LCD color filters', Dyes and Pigments, 2017, 136, 836-845

14. Jeong Yun Kim, Tae Gye Hwang, Sung Wun Woo, Jae Moon Lee, **Jin Woong Namgoong**, Sim Bum Yuk, Sei-won Chung, Jae Pil Kim, 'Simple modification of basic dyes with bulky & symmetric WCAs for improving their solubilities in organic solvents without color change', Scientific Reports, 2017, 7, 46178

15. Jae Bok Chang, **Jin Woong Namgoong**, Chun Sakong, Jun Choi, Su Hyun Park, Byoung Har Hwang, Jae Pil Kim, 'Optimized molecular structures of guest–host system for highly efficient coatable polarizer.', Dyes and Pigments, 2015, 121, 265-275

16. Jae Bok Chang, **Jin Woong Namgoong**, Se Hun Kim, Su Hyun Park, Byoung Har Hwang, Jae Pil Kim, 'Effect of dye structure on orientational behavior and transition dipole moments in coatable guest–host polarizers.', Dyes and Pigments, 2015, 121, 30-37

17. Se Hun Kim, **Jin Woong Namgoong**, Sim Bum Yuk, Jeong Yun Kim, Woosung Lee, Chun Yoon, Jae Pil Kim, 'Synthesis and characteristics of metal-phthalocyanines tetra-substituted at non-peripheral (α) or peripheral (β) positions, and their applications in LCD color filters', Journal of Inclusion Phenomena and Macrocyclic Chemistry, 2015, 82, 195-202

18. Jeong Yun Kim, Jun Choi, **Jin Woong Namgoong**, Se Hun Kim, Chun Sakong, Sim Bum Yuk, Sang-a Choi, Woosung Lee, Jae Pil Kim, 'Synthesis and characterization of novel perylene dyes with new substituents at terminal-position as colorants for LCD color filter', Journal of Inclusion Phenomena and Macrocyclic Chemistry, 2015, 82, 203-212

19. Sim Bum Yuk, Woosung Lee, **Jin Woong Namgoong**, Jun Choi, Jae Bok Chang, Se Hun Kim, Jeong Yun Kim, Jae Pil Kim, 'Synthesis and characterization of bay-substituted perylene dyes for LCD black matrix of low dielectric constant', Journal of Inclusion Phenomena and Macrocyclic Chemistry, 2015, 82, 187-194

20. Se Hun Kim, Jun Choi, Chun Sakong, **Jin Woong Namgoong**, Woosung Lee, Dong Hoe Kim, Boeun Kim, Min Jae Ko, Jae Pil Kim, 'The effect of the number, position, and shape of methoxy groups in triphenylamine donors on the performance of dye-sensitized solar cells.', Dyes and Pigments, 2015, 113, 390-401

21. Se Woong Park; **Jin Woong Namgoong**; Il Keun Kwon, Jae Pil Kim, 'Comparison Between Organic Sensitizers Containing Stilbene and Azo Group as Bridging Unit for Dye Sensitized Solar Cells.', Journal of Nanoscience and Nanotechnology, 2014, 14, 7502-7507

22. Woosung Lee, Jun Choi, **Jin Woong Namgoong**, Se Hun Kim, Kyung Chul Sun, Sung Hoon Jeong, Kicheon Yoo, Min Jae Ko, Jae Pil Kim, 'The effect of five-membered heterocyclic bridges and ethoxyphenyl substitution on the performance of phenoxazine-based dye-sensitized solar cells.', Dyes and Pigments, 2014, 104, 185-193

23. Jun Choi, Se Hun Kim, Woosung Lee, Jae Bok Chang, **Jin Woong Namgoong**, Young Hoon Kim, Sang Hun Han, Jae Pil Kim, 'The influence of aggregation behavior of novel quinophthalone dyes on optical and thermal properties of LCD color filters.', Dyes and Pigments, 2014, 101, 186-195

24. Jun Choi, Woosung Lee, **Jin Woong Namgoong**, Tae-Min Kim, Jae Pil Kim, 'Synthesis and characterization of novel triazatetrabenzcorrole dyes for LCD color filter and black matrix.', Dyes and Pigments, 2013, 99, 357-365

25. Chun Sakong, Hae Joong Kim, Se Hun Kim, **Jin Woong Namgoong**, Jong Ho Park, Jang-Hyun Ryu, Boeun Kim, Min Jae Ko, Jae Pil Kim, 'Synthesis and applications of new triphenylamine dyes with donor–donor–(bridge)–acceptor structure for organic dye-sensitized solar cells.', New Journal of Chemistry, 2012, 36, 2025-2032

26. Chun Sakong, Se Hun Kim, Sim Bum Yuk, **Jin Woong Namgoong**, Se Woong Park, Min Jae Ko, Dong Hoe Kim, Kug Sun Hong, Jae Pil Kim, 'Influence of Solvent and Bridge Structure in Alkylthio-Substituted Triphenylamine Dyes on the Photovoltaic Properties of Dye-Sensitized Solar Cells.', Chemistry an Asian journal, 2012, 7, 1817-1826

27. Se Hun Kim, Hyun Woo Kim, Chun Sakong, **Jin woong Namgoong**, Se Woong Park, Min Jae Ko, Choong Hyuk Lee, Wan In Lee, Jae Pil Kim,

‘Effect of Five-Membered Heteroaromatic Linkers to the Performance of Phenothiazine-Based Dye-Sensitized Solar Cells.’, Organic Letter, 2011, 13, 5784-5787

List of Presentations

International

1. **Jin Woong Namgoong**, Hyeyoun Jang, Minkyu Sung, Yongkeun Chang, Jae Pil Kim, ‘Synthesis and characterization of fluorescent dyes and their applications for the enhancement of growth rate of Chlorella vulgaris’, The 3rd International Caparica Conference on Chromogenic and Emissive Materials, Lisbon, Portugal, 2018, Poster

2. Hong Mo Kim, **Jin Woong Namgoong**, Jae Pil Kim, ‘Synthesis of phthalocyanine-based synergists for improving contrast ratio of green color filter’, International Conference on Porphyrins and Phthalocyanines, Munich, Germany, 2018, Poster

3. **Jin Woong Namgoong**, Hong Mo Kim, Jae Pil Kim, ‘Synthesis and characterization of halogenated phthalocyanine dyes, and their application on dye-based color filter’, International Conference on Porphyrins and Phthalocyanines, Munich, Germany, 2018, Poster

4. **Jin Woong Namgoong**, Tae Gyu Hwang, Jeong Youn Kim, Jae Pil Kim, ‘Synthesis of perylene-based wavelength shifting dyes and their application to a light converting agricultural film’, The 7th Advanced Functional Materials and Devices, Havana, Cuba, 2017, Poster

5. **Jin woong Namgoong**, Sei-won Chung, Jae Pil Kim, ‘Synthesis of Phthalocyanine Derivatives as Synergists for Improving Contrast Ratio of Liquid Crystal Displays’, International Conference on Porphyrins and

Phthalocyanines, Nanjing, China, 2016, Poster

6. **Jin Woong Namgoong**, Se Hun Kim, Jae Pil Kim, ‘The Synthesis and Application of Thermally-stable Deep Green Phthalocyanine Dyes for Dye-based LCD Colorfilter’, IUPAC-2015, Busan, Korea, 2015, Poster

7. **Jin Woong Namgoong**, Sei-won Chung, Jae Pil Kim, ‘The synthesis and application of thermally-stable deep green phthalocyanine dyes for dye-based LCD color filter’, 27th International Conference on Photochemistry, Jeju, Korea, 2015, Poster

8. **Jin Woong Namgoong**, Jae Pil Kim, ‘The synthesis and application of thermally-stable green phthalocyanine dyes for dye-based LCD color filters’, International Symposium on Nano and Supramolecular Chemistry, Bali, Indonesia, 2014, Oral

Domestic

1. **Jin Woong Namgoong**, Tae Gyu Hwang, Jeong Youn Kim, Jae Pil Kim, ‘Synthesis of perylene-based wavelength shifting dyes and their application to a light converting agricultural film’, Korean Chemical Society, 2018, Poster

2. **Jin Woong Namgoong**, Tae Gyu Hwang, Jae Pil Kim, ‘Synthesis of perylene-based wavelength shifting dyes and their application for the enhancement of growth rate of microalgae’, The Korean Society of Industrial and Engineering Chemistry, 2018, Poster

3. **Jin Woong Namgoong**, Jung Woo Roh, Jae Pil Kim, ‘Synthesis,

characterization, and application for reducing thickness of the color filter', Korean Chemical Society, 2017, Poster

4. **Jin Woong Namgoong**, Jung Woo Roh, Sei-won Chung, Jae Pil Kim, 'Improving contrast ratio of LCD by enhancing dispersion performance: new phthalocyanine derivatives as synergist', Korean Chemical Society, 2017, Poster

5. **Jin Woong Namgoong**, Hyeyoun Jang, Jae Pil Kim, 'Synthesis and characterization of phthalocyanine derivatives as synergists for improving contrast ratio of LCD', The Korean Society of Industrial and Engineering Chemistry, 2016, Poster

6. **Jin Woong Namgoong**, Hyeyoun Jang, Jae Pil Kim, 'Synthesis and application of green phthalocyanine dyes for decreasing thickness of LCD color filter', The Korean Society of Industrial and Engineering Chemistry, 2016, Poster

7. **Jin Woong Namgoong**, Sei-won Chung, Jae Pil Kim, 'The synthesis and application of green phthalocyanine dyes as synergists for improving contrast ratio of liquid crystal displays', The Korean Society of Industrial and Engineering Chemistry, 2015, Poster

8. **Jin Woong Namgoong**, Se Hun Kim, Jae Pil Kim, 'The synthesis and application of thermally-stable cyan dyes for six-color primary (RGBCMY) LCD color filters', The Korean Society of Industrial and Engineering Chemistry, 2013, Poster